北京大学
PEKING UNIVERSITY

Stony Brook University

Explore charm hadronic physics from BESIII to sPHENIX

Xudong Yu
Peking University

CFNS Seminar

Research Profile — Xudong Yu 余旭东

➔ Education

- Ph.D. candidate, **Peking University**, 2021-2026
- Bachelor of Science, **Sun Yat-Sen University**, 2017-2021

北京大學 PEKING UNIVERSITY

中山大學 SUN YAT-SEN UNIVERSITY

➔ Experiment participation

- **BESIII** (2018-Now): Charm baryon decay, and QCD studies
- **sPHENIX** (2023-Now): Tracking calibration, detector operation, heavy flavor/quarkonium

➔ Selected achievements

- 4 published papers + 1 under review
  - First observation / evidence in Λ_c^+ decay analyses
- 2025 RHIC & AGS Merit Award
- sPHENIX Hero
- 17 talks / posters + 6 proceedings
  - Lepton photon 2023, Quark Matter 2025, …

sPHENIX Hero: Xudong Yu

How long have you been working in sPHENIX and at what institution?

I joined sPHENIX in May 2023 as a second year Ph.D student at Peking University at the same time sPHENIX began taking data. Therefore, I am still a newbie in sPHENIX.

What is the focus of your work on the sPHENIX experiment?

My focus on sPHENIX experiment separates into two parts. One is heavy flavor physics including quarkonium and open heavy flavor. Another one is doing service work in MVTX group and tracking software group.

Where were you born and what is your educational background before your current position?

I was born in Japan, but I am a Chinese from Fujian province. I got my bachelor's degree in Sun Yat-sen University before I went to Peking University. I Join in BESIII experiment since I was a sophomore and do some physics analysis about Lambda_c decay. Therefore, I have some experience on physics analysis, but lack of experience on hardware. I hope I can learn some hardware knowledge in sPHENIX to be a true experimental physicist.

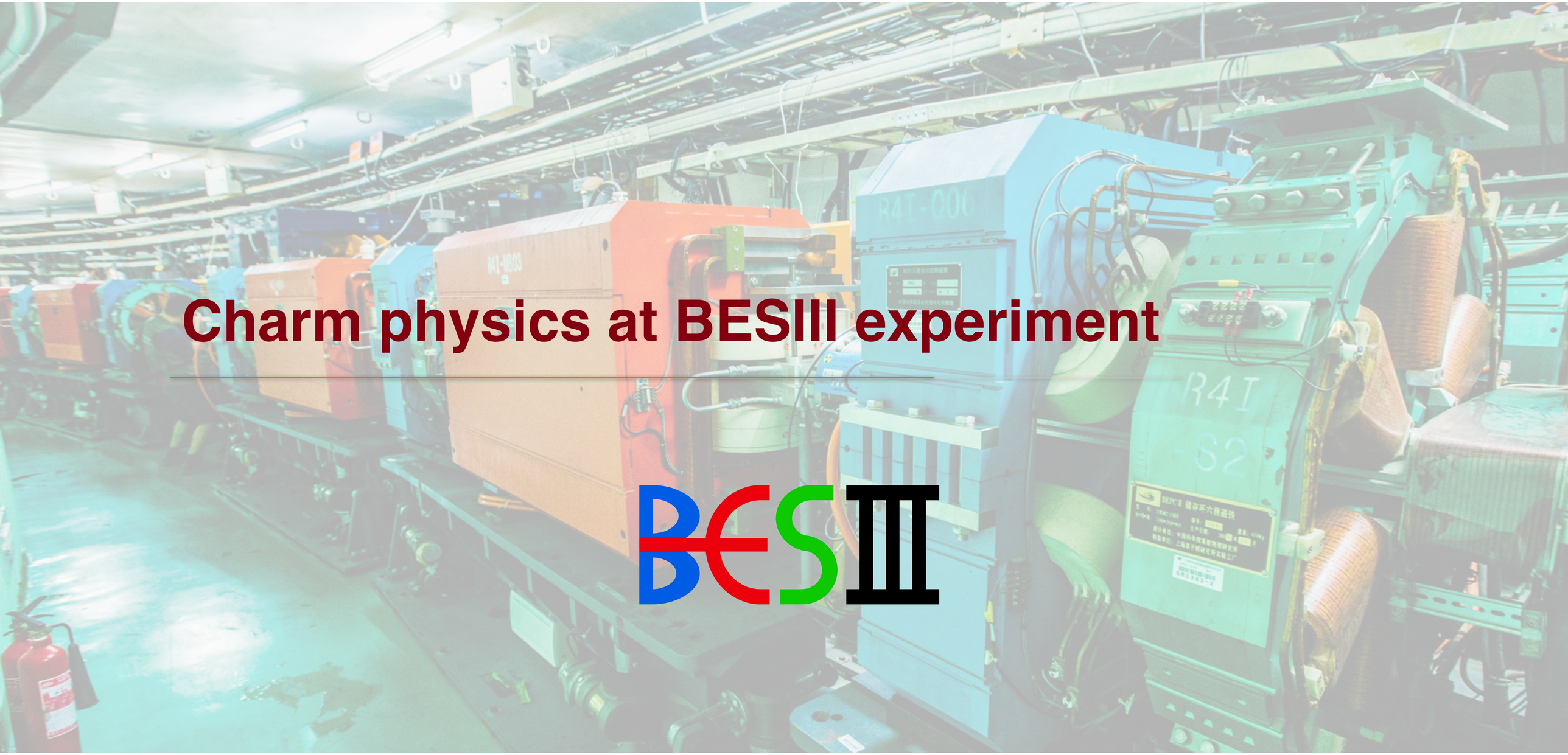

Charm physics at BESIII experiment

BEPCII & BESIII

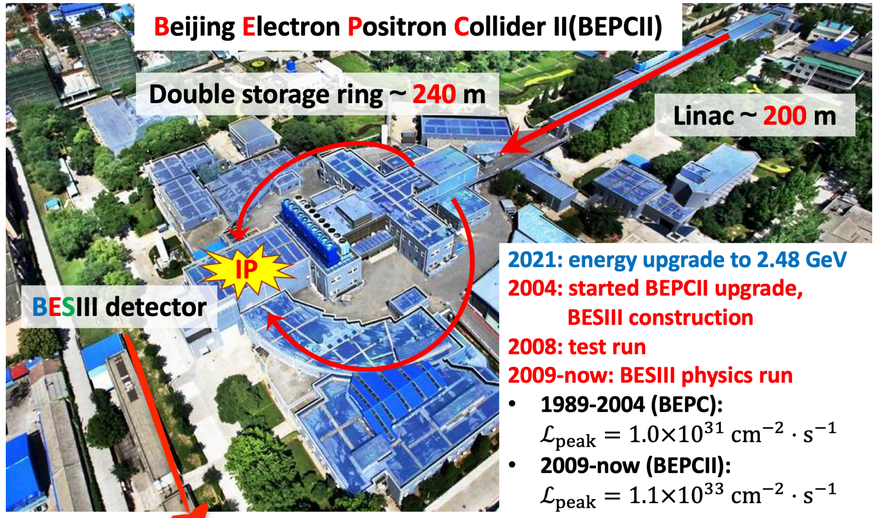

2021: energy upgrade to 2.48 GeV
2004: started BEPCII upgrade, BESIII construction
2008: test run
2009-now: BESIII physics run

- 1989-2004 (BEPC): $\mathcal{L}_{\rm peak} = 1.0\times10^{31}\ {\rm cm}^{-2}\cdot{\rm s}^{-1}$
- 2009-now (BEPCII): $\mathcal{L}_{\rm peak} = 1.1\times10^{33}\ {\rm cm}^{-2}\cdot{\rm s}^{-1}$

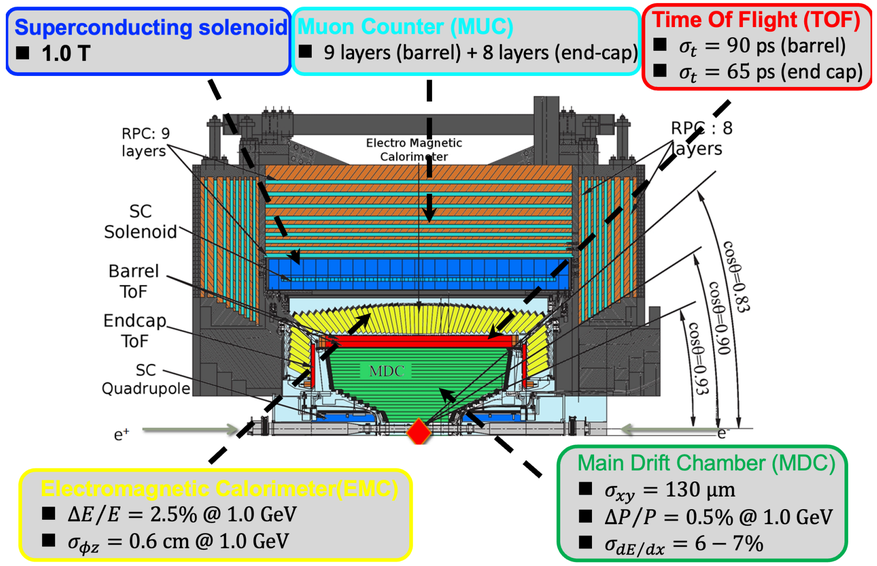

➔ BEPCII operates in the tau-charm region 1.84 - 4.95 GeV

➔ BESIII has accumulated > 50 fb^{-1} high-statistics, low-background, near-threshold unique data sample

➔ BESIII Collaboration has published > 700 physics papers, conducting high-precision measurements on charmonium, charm meson/baryons

BESIII main webpage: http://bes3.ihep.ac.cn/

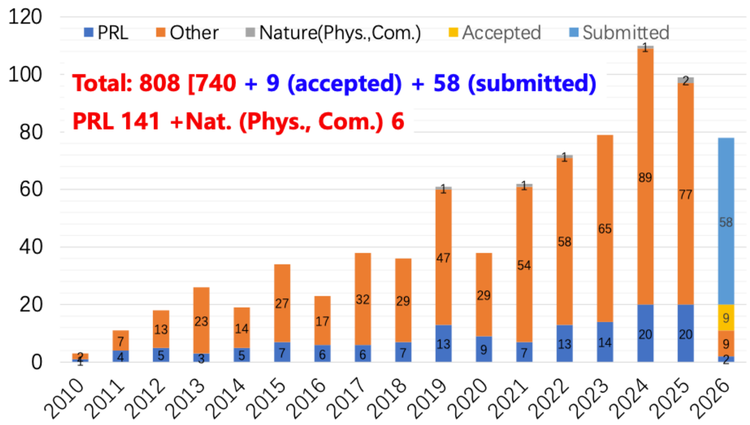

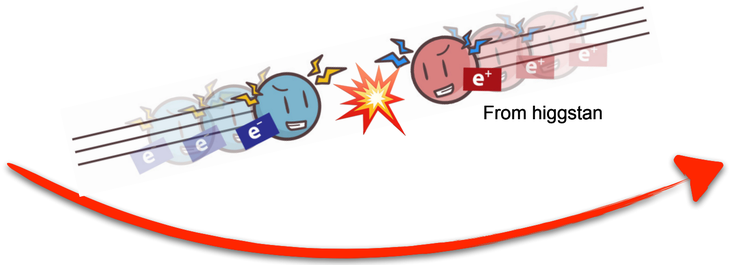

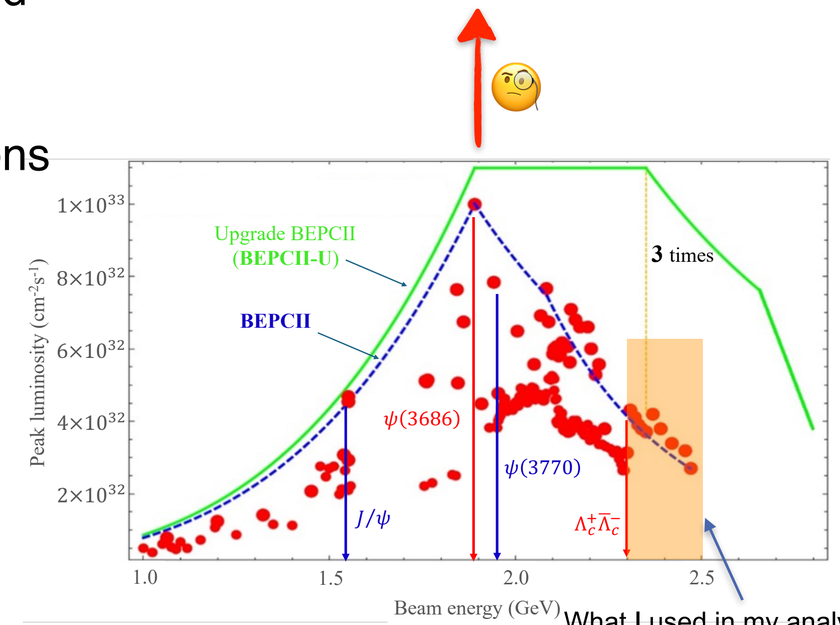

Charm decay and hadronization

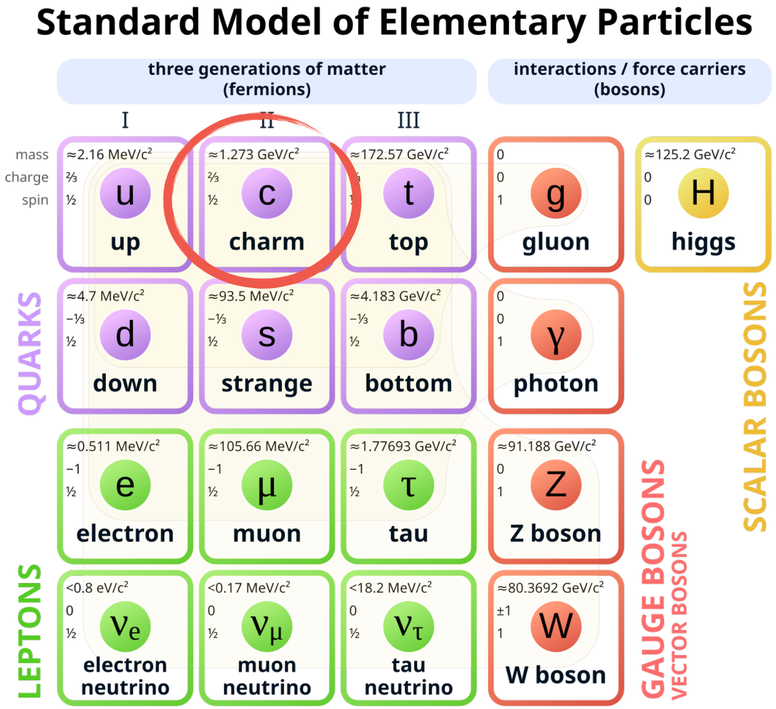

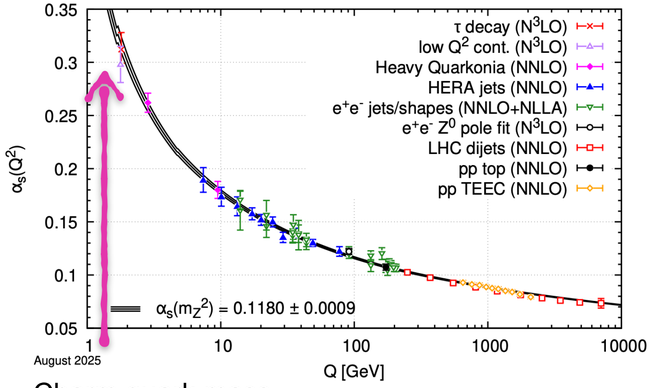

Charm quark mass

➔ Charm quark provides ideal platform for studying strong/weak interactions

- ❖ Charm quark in the transition region between perturbative and non-perturbative region

➔ Two main topics that I focus on at BESIII experiment

- ❖ How charm baryon (Λ_c^+) decays?
- ❖ How charm quarks combine to form bound state (J/ψ)?

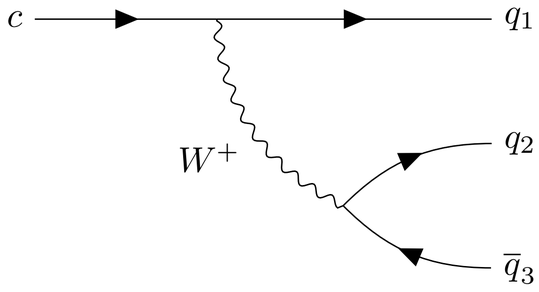

Charm decay

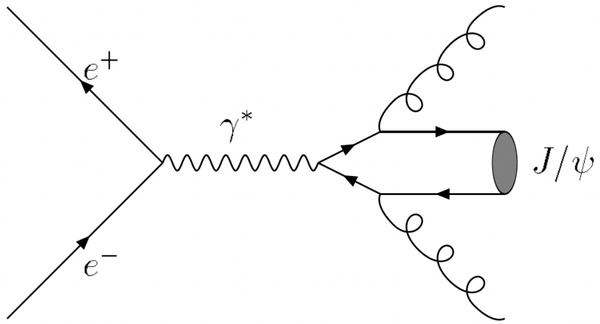

Charm hadronization

Charm baryon decays

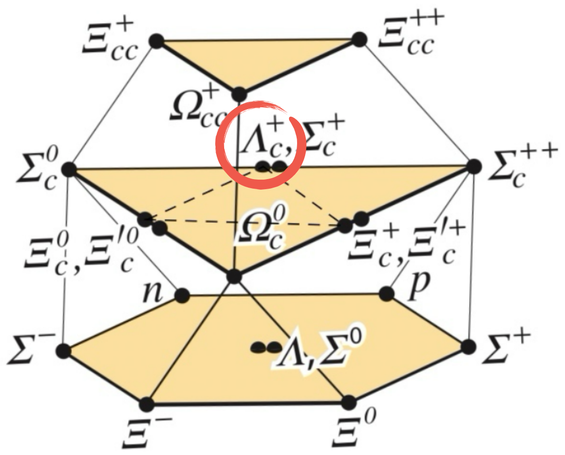

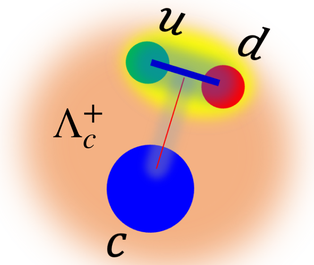

Naive quark model

$m_u, m_d \gg m_c \Rightarrow \text{diquark}(qq) + \text{quark}(Q)$

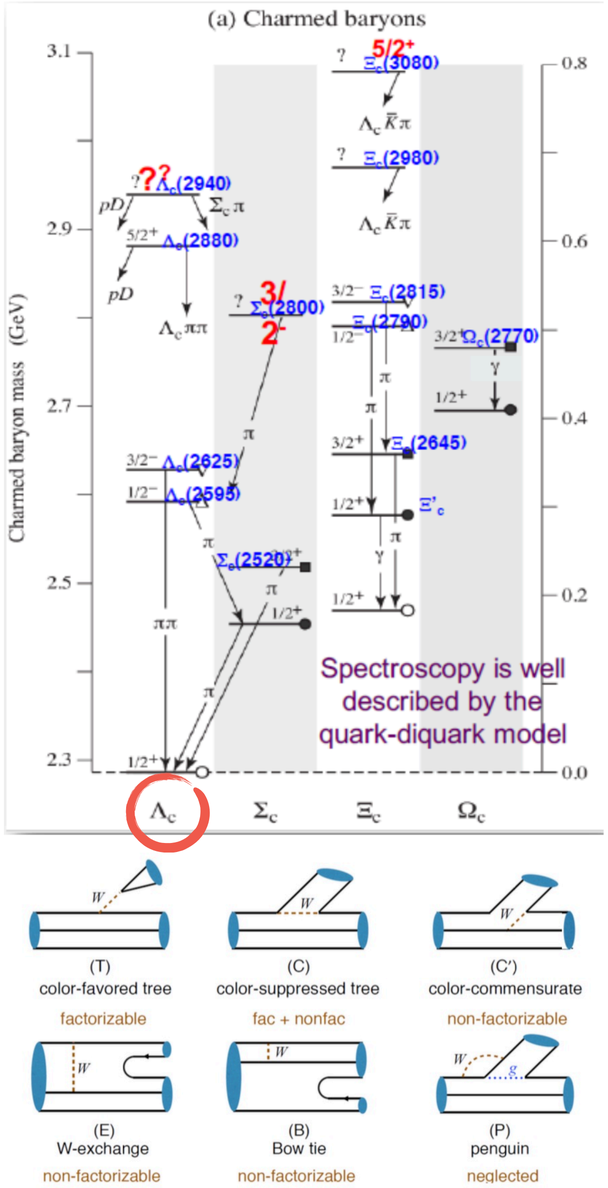

➔ Λ_c^+: the lightest charmed baryon

- ❖ First observation in MARK II experiment (1979)
- ❖ Complementary to $D_{(s)}$ in charm region
- ❖ Important tagging for excited charmed baryons and Bottom baryons

➔ Λ_c^+ decay classification

- ❖ Final state
  - ▸ Hadronic (two-body, three-body) & Semi-leptonic
- ❖ Strength
  - ▸ Cabibbo Favored, Singly Cabibbo Suppressed, Doubly Caibbbo Suppressed
- ❖ Topology
  - ▸ Factorizable, non-factorizable

➔ Theoretical methods

- ❖ Phenomenology models (quark model + current algebra)
- ❖ Model independent methods (TDA, IRA)
- ❖ Calculation from first principle (LQCD)

My work in Λ_c^+ decays

Λ_c^+ two-body decays

- Measurement of branching fractions (BF) of $\Lambda_c^+ \to \Sigma^0 K^+$ and $\Sigma^+ K_S^0$
  - Published in Phys. Rev. D **106** (2022), 052003

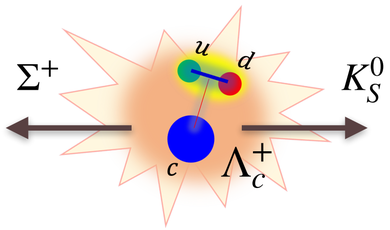

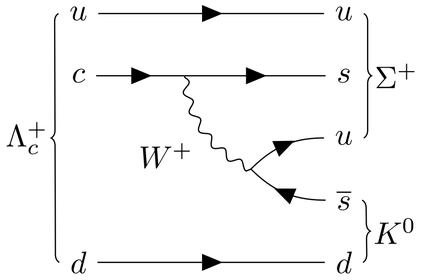

Highlight in this talk

Λ_c^+ three-body decays

- Partial wave analysis of $\Lambda_c^+ \to \Lambda \pi^+ \eta$
  - Published in Phys. Rev. Lett. **134**, (2025), 021901
- Observation of $\Lambda_c^+ \to n\pi^+\eta$ and search for $\Lambda_c^+ \to n a_0(980)^+$
  - arXiv:2603.28232, submitted to JHEP

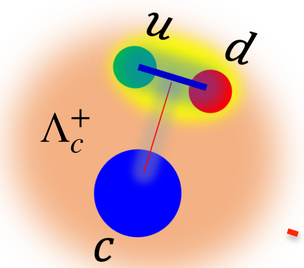

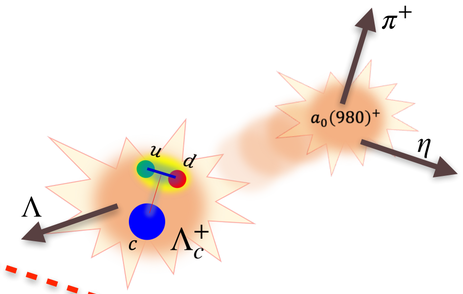

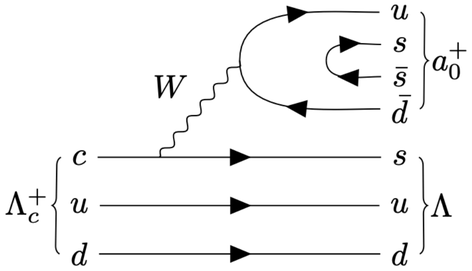

Λ_c^+ semi-leptonic decays

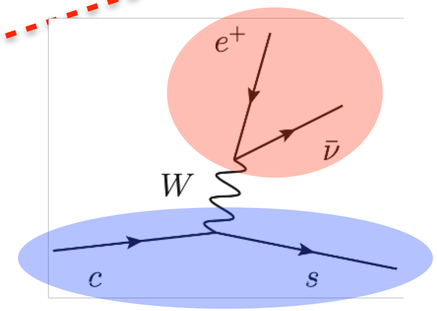

- Search for $\Lambda_c^+ \to \Lambda \pi^+ \pi^- e^+ \nu_e, p K_S^0 \pi^- e^+ \nu_e$
  - Published Phys. Lett. B **843**, (2023), 137993
- Measurement of BF of $\Lambda_c^+ \to p \pi^- e^+ \nu_e$
  - BAM-00736 (REV-830), currently in BESIII spokersperson review stage

Physics motivation for $\Lambda_c^+ \to \Lambda\pi^+\eta$

BESIII2019 $N_{\Lambda\pi^+\eta} = 154 \pm 17$

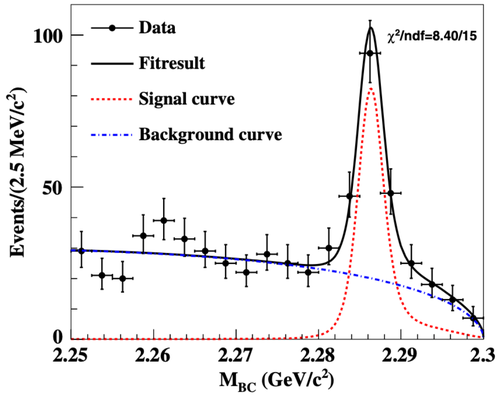

Belle2021

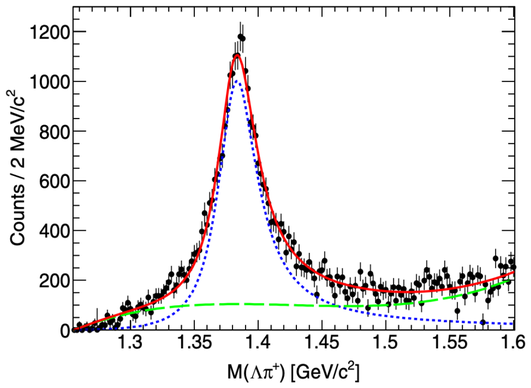

$N_{\Sigma^{*+}\eta} = 54 \pm 11$

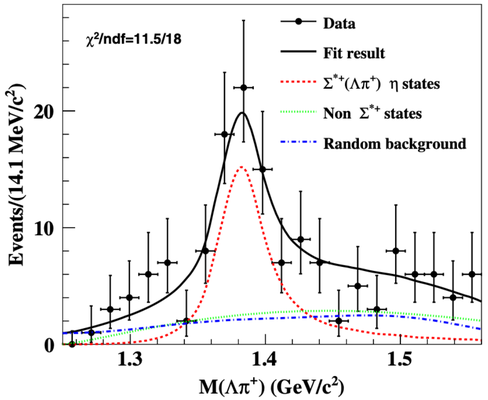

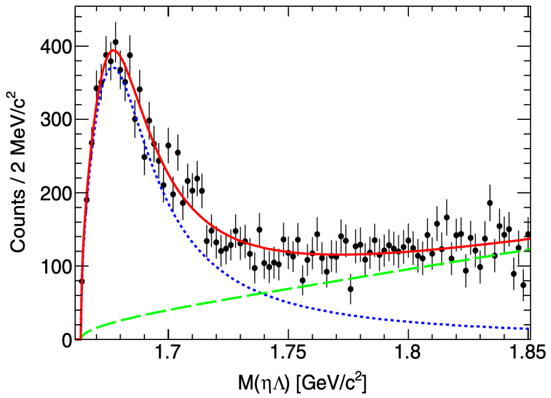

Early study on this channel by BESIII and Belle
- Three-body BF
- Intermediate resonances $\Sigma(1385)^+$ & $\Lambda(1670)$

Topological diagrams describing charm baryon decaying into decuplet baryon + pseudoscalar meson

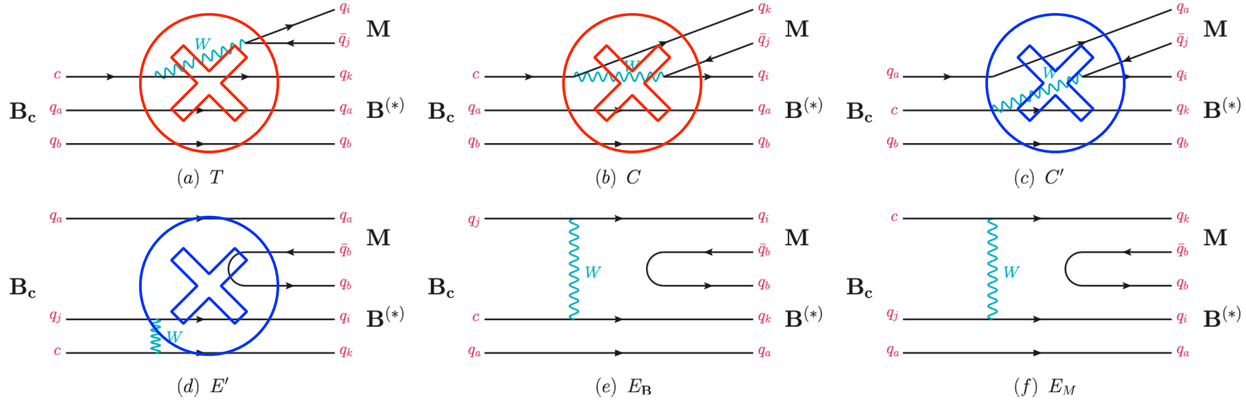

$\Lambda_c^+ \to \Sigma(1385)^+\eta$ only receives contributions from non-factorizable W-exchange diagram.
Decay asymmetry parameter predictions differ from different theoretical works.

方法	$\mathcal{B}$ ($\times 10^{-3}$)	α
SQM[205]	10.4	0
$SU(3)_F$ IRA[8]a	$2.1 \pm 1.1 (1.4 \pm 1.0)$	0
$SU(3)_F$ IRA[206]b	$6.2 \pm 0.5 (3.1 \pm 0.6)$	$-1.00^{+0.34}_{-0} (-0.97^{+0.43}_{-0.03})$
$SU(3)_F$ IRA[207]c	$4.67 \pm 0.76 / 9.27 \pm 1.24 / 7.00 \pm 0.55$	0.52 ± 0.17
$SU(3)_F$ TDA[204]	$5.3 \pm 0.8 (7.3 \pm 1.5)$	–

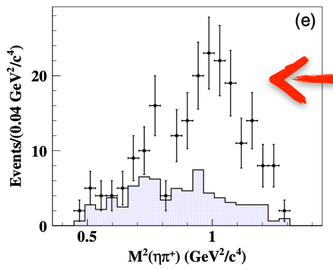

Any more resonances?
Like $a_0(980)^+$?

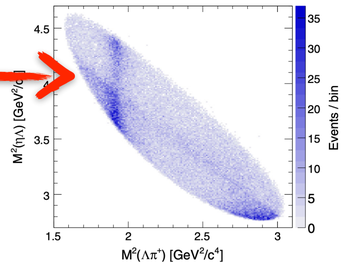

$a_0(980)^+$ & $\Sigma(1380)^+$ in $\Lambda_c^+ \to \Lambda\pi^+\eta$

Light scalar particle — $a_0(980)^+$

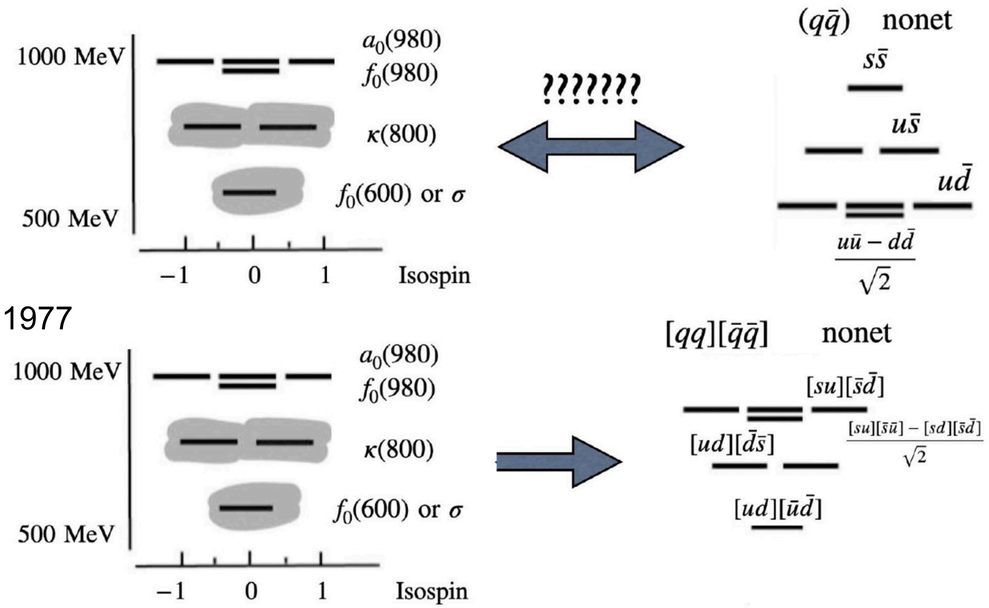

Jaffe 1977

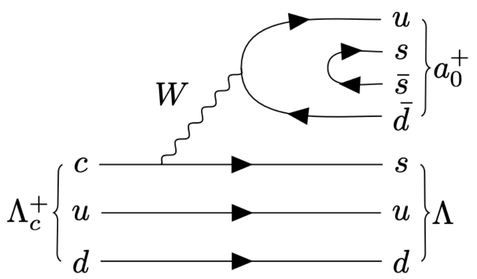

J. Phys. G ***36****, (2009), 075005*

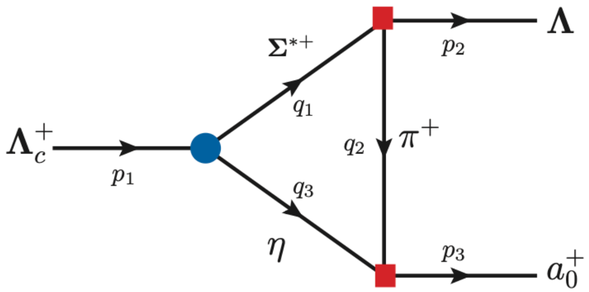

Phys. Lett. B ***820****, (2021), 136586*

$\mathcal{B}(\Lambda_c^+ \to \Lambda a_0(980)^+) = 1.9 \times 10^{-4}$

$\mathcal{B}(\Lambda_c^+ \to \Lambda a_0(980)^+) = (1.7^{+2.8}_{-1.0} \pm 0.3) \times 10^{-3}$

Predictions based on tetraquark state assumption and triangle rescattering mechanism are very different

"missing" $\Sigma_{1/2^-}$ hyperon — $\Sigma(1380)^+$

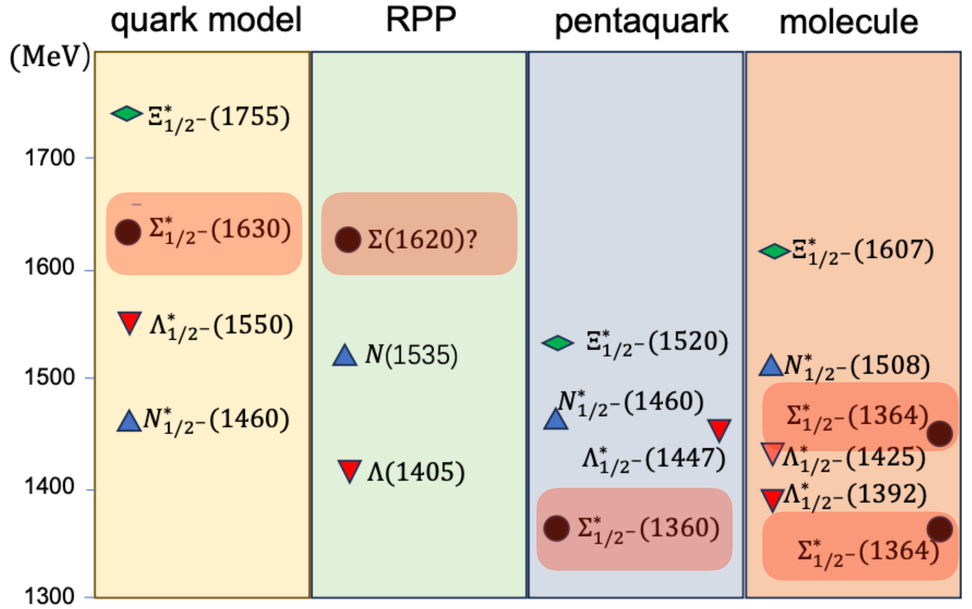

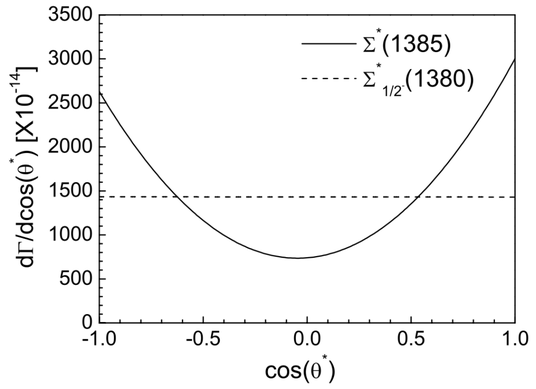

Phys. Rev. D ***95****, (2017), 074024*

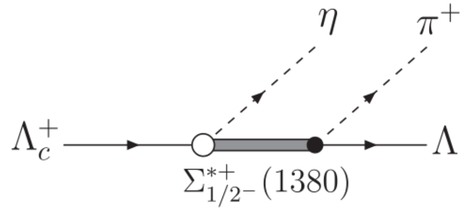

- Due to different spin-parity, $\Sigma(1385)^+$ and $\Sigma(1380)^+$ have different angular distributions
- Partial wave analysis is feasible to separate them from data

Signal reconstruction and PWA sample preparation

PWA requirement: high-purity sample
Adopt boosted decision tree (BDT) to suppress background

- $M_{p\pi^-}$: the invariant mass of $p\pi^-$ pair
- L/σ_L: the decay length of Λ over corresponding error
- $M_{\gamma\gamma}$: the invariant mass of $\gamma\gamma$ pair
- $M_{\pi^+\pi^-\pi^0}$: the invariant mass of $\pi^+\pi^-\pi^0$ (only for $\eta \to \pi^+\pi^-\pi^0$ channel)
- $\cos\theta_{\eta(\pi^0)}$: the helicity angle for $\eta(\pi^0) \to \gamma\gamma$
- $Lat(\gamma_{\rm High})$: the lateral moment of shower with relatively higher energy
- $Lat(\gamma_{\rm Low})$: the lateral moment of shower with relatively lower energy
- ΔE: the energy difference

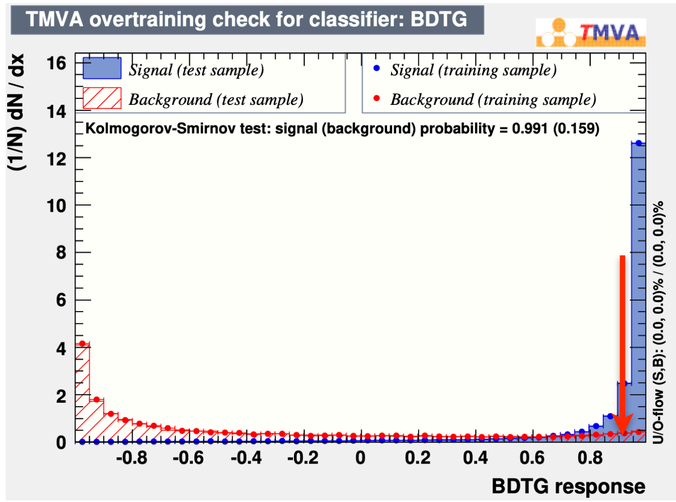

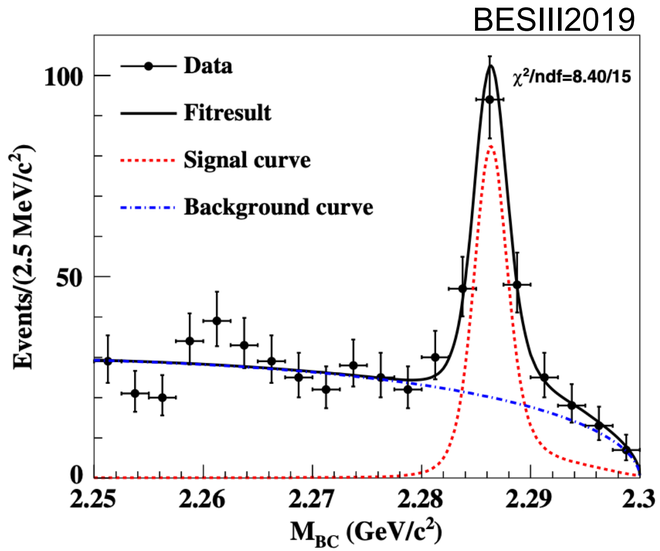

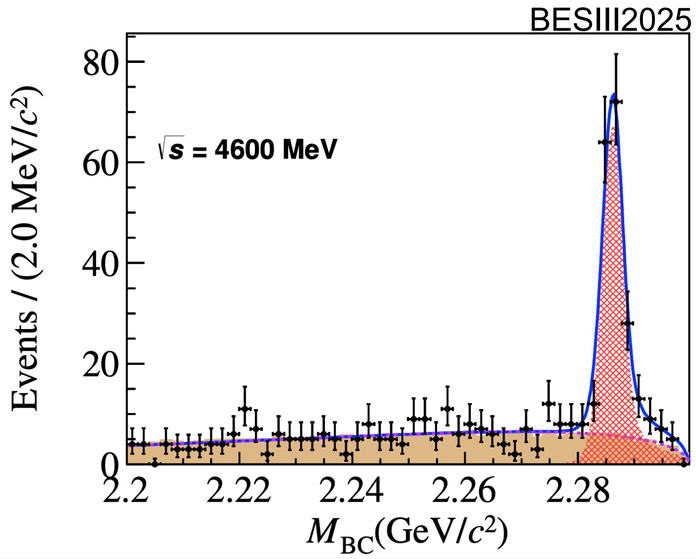

Purity ~ 80%
~ 1100 signals

Brief introduction to Partial Wave Analysis (PWA)

➔ 3C kinematic fit for improving momentum resolution

❖ Constrain signal $\Lambda\pi^+\eta$, recoiling $\bar{\Lambda}_c^-$ or $p\pi^-$ masses

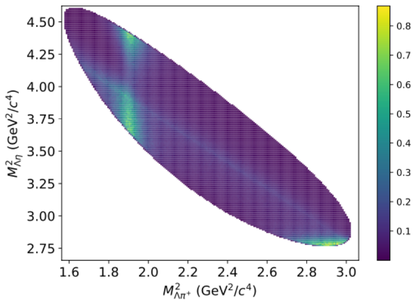

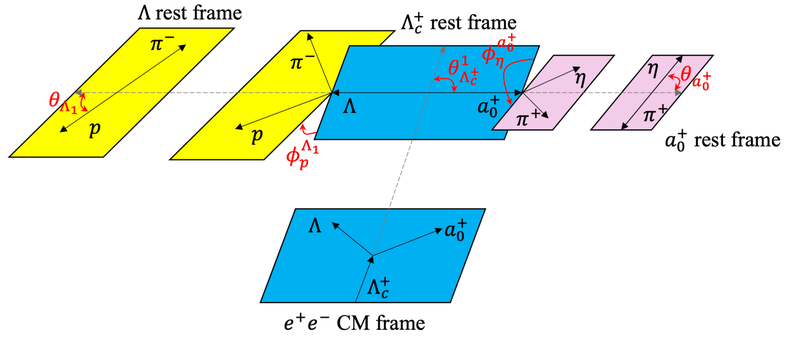

➔ Signal kinematic is described by helicity amplitude

$$A^{0\to1+2}_{\lambda_0,\lambda_1,\lambda_2} = H^{0\to1+2}_{\lambda_1,\lambda_2} D^{J_0*}_{\lambda_0,\lambda_1-\lambda_2}(\phi,\theta,0) \qquad H^{0\to1+2}_{\lambda_1,\lambda_2} = \sum_{ls} g_{ls} \sqrt{\frac{2l+1}{2J_0+1}} \langle l,0;s,\delta|J_0,\delta\rangle \langle J_1,\lambda_1;J_2,-\lambda_2|s,\delta\rangle \left(\frac{q}{q_0}\right)^l B'_l(q,q_0,d)$$

Helicity coupling | Wigner-D matrix | Partial wave amplitude | CG coefficient | Blatt-Weiskopf barrier factor

➔ Intermediate resonance modelling

❖ $a_0(980)^+$: Flatté; Λ^*/Σ^*: Breit-Wigner; Non-resonant: 1

➔ Background is considered by sWeight factor in the Negative Log Likelihood

$$-\ln L = -\alpha \sum_{i\in\text{data}} w_i \ln P(p^i)$$

➔ Physics observables: Fit fraction (FF) & decay asymmetry parameter (α)

$$\alpha = \frac{\sum_{i\in\text{data}} w_i}{\sum_{i\in\text{data}} w_i^2}$$

$$\text{FF}_i = \frac{\int |\mathscr{A}_i|^2 R_5(p)\mathrm{d}p}{\int |\sum_k \mathscr{A}_k|^2 R_5(p)\mathrm{d}p} \approx \frac{\sum_{j\in\text{PHSP}} |\mathscr{A}_i(p^j)|^2}{\sum_{j\in\text{PHSP}} |\sum_k \mathscr{A}_k(p^j)|^2}$$

$$\alpha_{\Lambda a_0(980)^+} = -\frac{2\Re\left(g^{\Lambda_c^+\to\Lambda a_0(980)^+}_{0,\frac{1}{2}} \cdot g^{\Lambda_c^+\to\Lambda a_0(980)^+ *}_{1,\frac{1}{2}}\right)}{\left|g^{\Lambda_c^+\to\Lambda a_0(980)^+}_{0,\frac{1}{2}}\right|^2 + \left|g^{\Lambda_c^+\to\Lambda a_0(980)^+}_{1,\frac{1}{2}}\right|^2}$$

Partial Wave Analysis — baseline solution

➔ Use open-source framework TF-PWA to do amplitude fitting TF-PWA

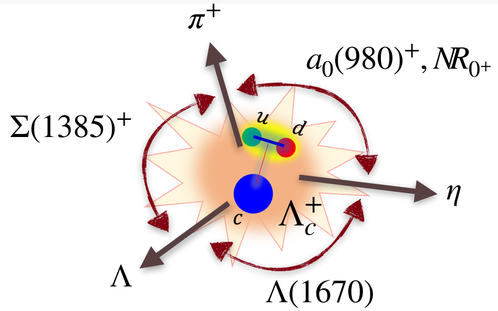

➔ Consider three res $\Sigma(1385)^+, \Lambda(1670), a_0(980)^+$ and $\pi^+\eta$ non-res

- ❖ Significance test: only consider components with significance > 5σ

➔ **First observation of $\Lambda_c^+ \to \Lambda a_0(980)^+$ process, FF ~ 54%**

➔ **First measurement of decay asymmetry parameters α**

Total FF 115.2%, total IF 15.2%

Process	FF (%)	$\mathcal{S}$	α
$\Lambda a_0(980)^+$	$54.0 \pm 8.4 \pm 2.6$	13.1σ	$-0.91^{+0.18}_{-0.09} \pm 0.08$
$\Sigma(1385)^+\eta$	$30.4 \pm 2.6 \pm 0.7$	22.5σ	$-0.61 \pm 0.15 \pm 0.04$
$\Lambda(1670)\pi^+$	$14.1 \pm 2.8 \pm 1.2$	11.7σ	$0.21 \pm 0.27 \pm 0.33$
ΛNR_{0^+}	15.4 ± 5.3	6.7σ	$\cdots$

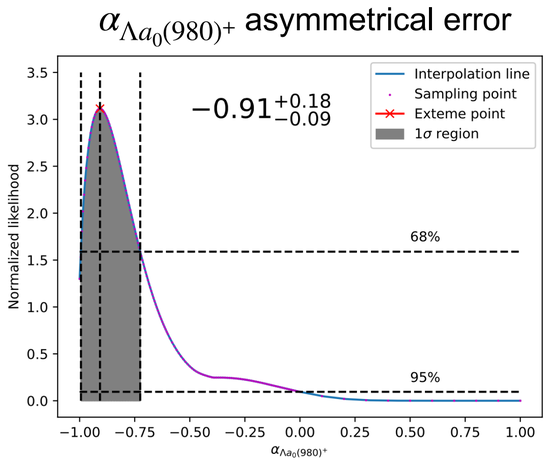

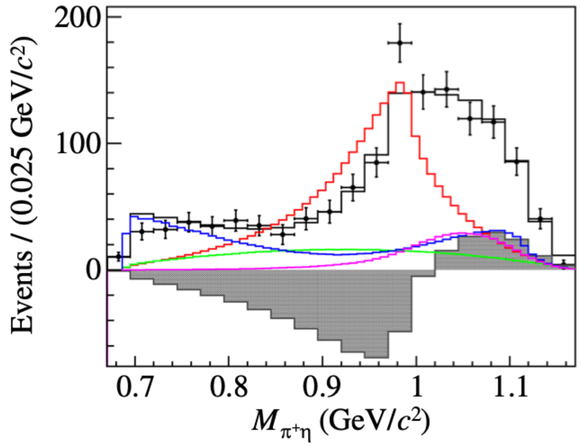

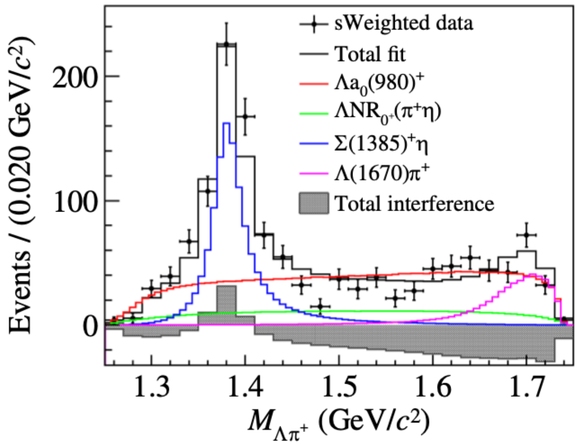

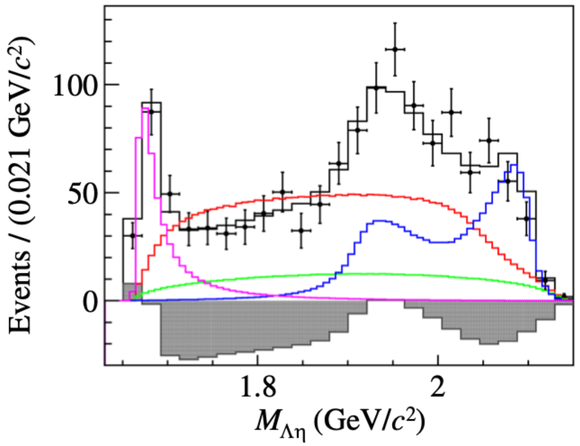

Partial Wave Analysis — test existence of $\Sigma(1380)^+$

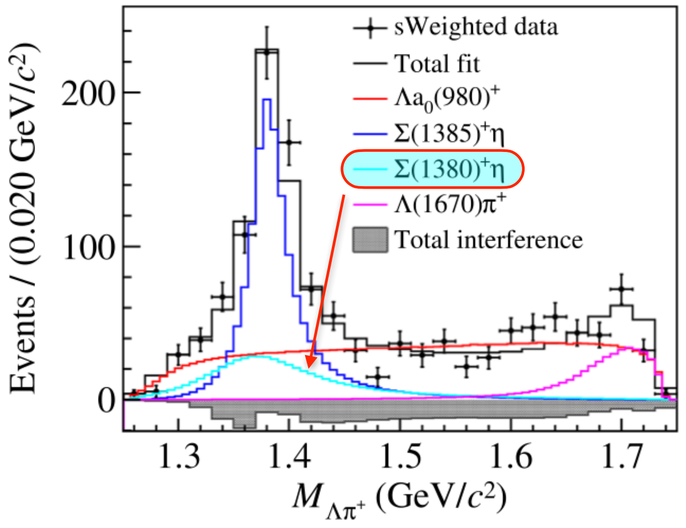

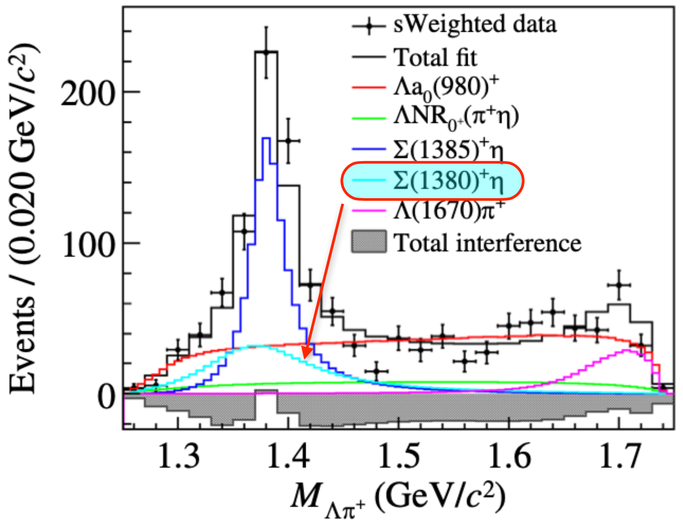

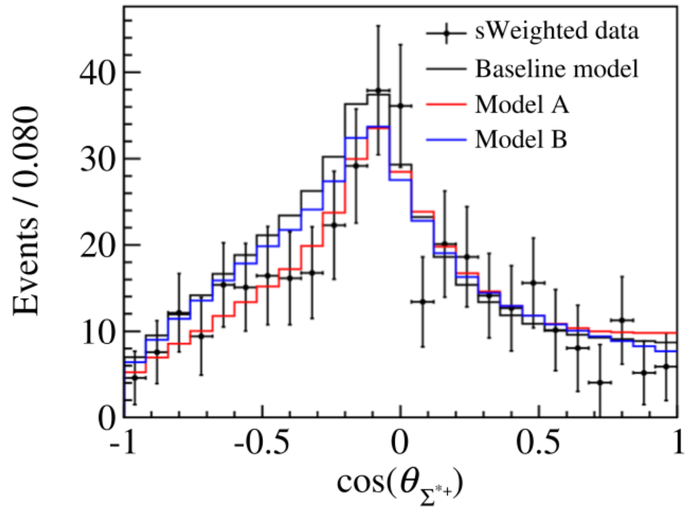

Process	Model A	Model B
$\Lambda a_0(980)^+$	$52.9 \pm 4.5(13.4\sigma)$	$50.6 \pm 8.0(11.1\sigma)$
$\Sigma(1385)^+\eta$	$36.6 \pm 2.6(15.8\sigma)$	$31.3 \pm 3.0(14.6\sigma)$
$\Lambda(1670)\pi^+$	$10.7 \pm 1.4(15.0\sigma)$	$9.0 \pm 1.6(11.9\sigma)$
$\Sigma(1380)^+\eta$	$15.5 \pm 4.4(6.1\sigma)$	$17.7 \pm 5.7(3.3\sigma)$
ΛNR_{0^+}	...	$11.3 \pm 4.4(4.2\sigma)$

➔ The existence of $\Sigma(1380)^+$ is tested in the alternative models

- Breit-Wigner lineshape ($m_0 = 1380\,\mathrm{MeV}/c^2$, $\Gamma = 120\,\mathrm{MeV}$)

➔ **In four-res models, the significance of $\Sigma(1380)^+$ (6.1σ) is slightly lower than NR_{0^+}(6.7σ)**

- In five-res model, the significance of $\Sigma(1380)^+$ is 3.3σ
- Σ^{*+} helicity angle distribution slightly favor model including $\Sigma(1380)^+$

➔ **Considering systematic uncertainty from Σ^{*+}, Λ^*, a_0^+, a_2^+ as well as mass/ width, significance always exceed 3σ**

➔ **First experimental evidence of $\Sigma(1380)^+$, but needs more experimental tests**

Systematic estimation

		$\mathrm{FF}_{a_0(980)^+}$	$\mathrm{FF}_{\Sigma(1385)^+}$	$\mathrm{FF}_{\Lambda(1670)^0}$	$\alpha_{\Lambda a_0(980)^+}$	$\alpha_{\Sigma(1385)^+\eta}$	$\alpha_{\Lambda(1670)^0\pi^+}$
Fixed parameters	I	0.09	0.10	0.32	0.08	0.05	0.11
Barrier factor	II	0.16	0.08	0.07	0.11	0.09	0.03
Fit component	III	0.21	0.21	0.25	0.14	0.12	1.19
Λ_c^+ polarization	IV	0.05	0.05	0.02	0.06	0.02	0.02
Fit bias	V	0.07	0.07	0.05	0.09	0.06	0.11
Data-MC difference	VI	0.09	0.01	0.15	0.04	0.08	0.09
Background description	VII	0.06	0.06	0.02	0.61	0.19	0.30
	Total	0.31	0.27	0.44	0.66	0.27	1.24

➔ Fixed parameters: vary the fixed parameters $\pm 1\sigma$

➔ Fit component: including the most significant unconsidered component

➔ Background description: sweight → data sideband distribution

Physics impact

➔ Main physics output, and comparison with earlier experimental results

	This work	BESIII2019[201]	Belle2021[202]
$\mathcal{B}(\Lambda_c^+ \to \Lambda\pi^+\eta)(\%)$	1.94 ± 0.13	1.84 ± 0.26	1.84 ± 0.13
$\mathcal{B}(\Lambda_c^+ \to \Lambda a_0(980)^+) \cdot \mathcal{B}(a_0(980)^+ \to \pi^+\eta)(\%)$	1.05 ± 0.18	—	—
$\mathcal{B}(\Lambda_c^+ \to \Sigma(1385)^+\eta)(\times 10^{-3})$	6.78 ± 0.76	9.1 ± 2.0	12.1 ± 1.5
$\mathcal{B}(\Lambda_c^+ \to \Lambda(1670)\pi^+) \cdot \mathcal{B}(\Lambda(1670) \to \Lambda\eta)(\times 10^{-3})$	2.74 ± 0.62	—	3.48 ± 0.53
$\alpha_{\Lambda a_0(980)^+}$	$-0.91^{+0.18}_{-0.09} \pm 0.08$	—	—
$\alpha_{\Sigma(1385)^+\eta}$	-0.61 ± 0.15	—	—
$\alpha_{\Lambda(1670)\pi^+}$	0.21 ± 0.43	—	—

Efficiency estimation based on PWA MC model

Difference between Belle's result
Absent consideration of $a_0(980)^+$ is a possible reason

➔ Comparing with theoretical predictions

- $\mathcal{B}(\Lambda_c^+ \to \Sigma(1385)^+\eta)$ consistent with recent calculations — global fit
- $\mathcal{B}(\Lambda_c^+ \to \Lambda a_0(980)^+)$ differs from theoretical predictions by 1-2 orders of magnitude
- Big difference of decay asymmetry parameters between EXP and THEO.

Decay Mode	Ref. [19]	Ref. [20]	Ref. [21]	Ref. [14]
$\Lambda_c^+ \to \Sigma(1385)^+\eta\,(\times 10^{-3})$	10.4	$2.1 \pm 1.1/1.4 \pm 1.0$	$6.2 \pm 0.5\,(3.1 \pm 0.6)$	$5.3 \pm 0.8\,(7.3 \pm 1.5)$

Decay Mode	Ref. [26]	Ref. [27]
$\Lambda_c^+ \to \Lambda a_0(980)^+$	1.9×10^{-4}	$(1.7^{+2.8}_{-1.0} \pm 0.3) \times 10^{-3}$

*Phys. Rev. D, **111**, (2025), 016004*

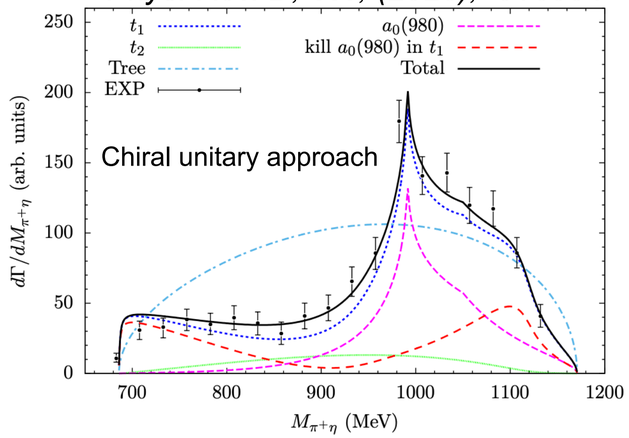

➔ Published in Phys. Rev. Lett. **134**, (2025), 021901

Physics motivation for $\Lambda_c^+ \to n\pi^+\eta$

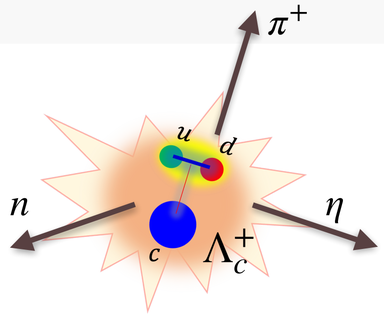

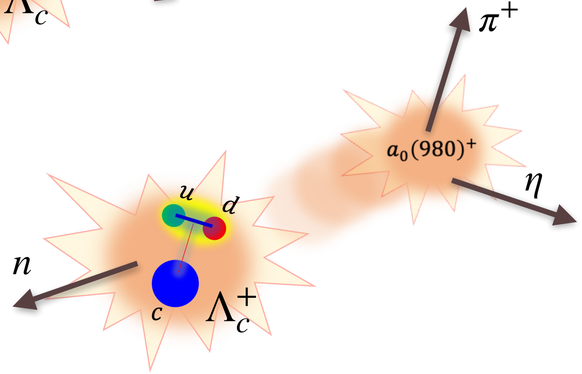

➔ Motivated by last analysis $\Lambda_c^+ \to \Lambda\pi^+\eta$

- Can we see SCS process involving $a_0(980)^+$?
- Three-body decay $\Lambda_c^+ \to n\pi^+\eta$ has never been measured yet

➔ Many theoretical calculations, needs experimental measurement

- **Pole model + tetraquark assumption**: $\mathcal{B}(\Lambda_c^+ \to n a_0(980)^+) = 7.1 \times 10^{-5}$
- $SU(3)_F$ **TDA**: $\mathcal{B}(\Lambda_c^+ \to n a_0(980)^+) = (1.4 \pm 1.0) \times 10^{-3}$ (two-quark)
  $(2.3 \pm 1.0) \times 10^{-3}$ (four-quark)
- **Chiral unitary approach**: $\mathcal{B}(\Lambda_c^+ \to n a_0(980)^+)/\mathcal{B}(\Lambda_c^+ \to n\pi^+\eta) \approx 0.313$
- $SU(3)_F$ **TDA**: $\mathcal{B}(\Lambda_c^+ \to n\pi^+\eta) = (4.52 \pm 1.21) \times 10^{-3}$

$\Lambda_c^+ \to n a_0(980)^+$ topological diagrams

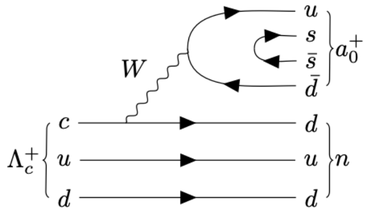

(a) factorizable W-emission

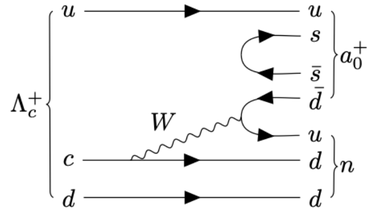

(a) non-factorizable W-emission

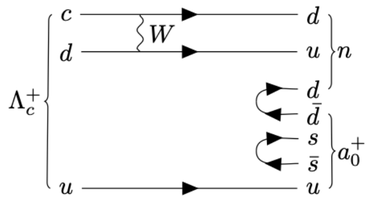

(a) non-factorizable W-exchange

$\Lambda_c^+ \to n\pi^+\eta$ topological diagrams

$H(\mathbf{6})$

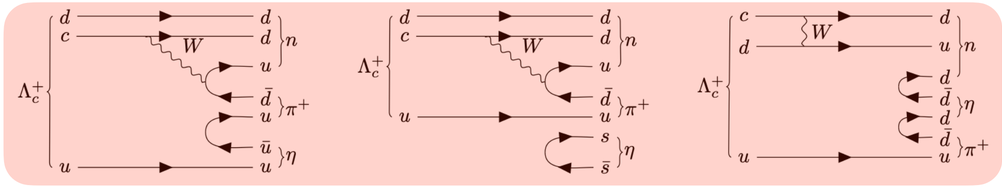

$H(\bar{\mathbf{15}})$

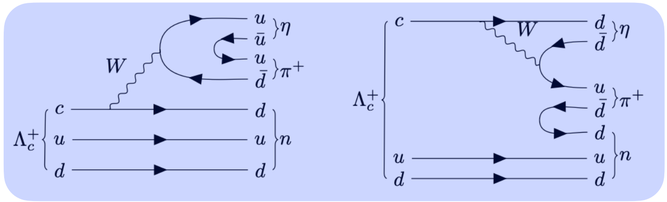

The dilemma of traditional methods

- ➔ Using double tag method, calculate recoiling neutron information based on four momentum conservation
  - ❖ Reconstruction neutron at BESIII is difficult with low efficiency
- ➔ Significant peaking background in $\eta \to \gamma\gamma$ & $\eta \to \pi^+\pi^-\pi^0$ tag modes
  - ❖ $\Sigma^+\eta[\eta \to \gamma, \eta \to \pi^+\pi^-\pi^0]$ & $\Lambda\pi^+\pi^-\pi^+$
- ➔ Abundant combinatorial background, fitting to $M_{\rm miss}$ spectrum yields 3.3σ significance 😖
  - ❖ $\mathcal{B}(\Lambda_c^+ \to n\pi^+\eta) = (2.37 \pm 0.77) \times 10^{-3}$
  - ❖ Tried tighter cuts or BDT method which produce very little improvement

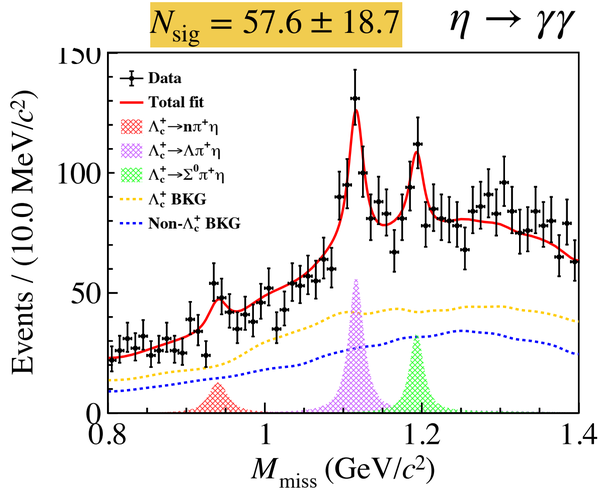

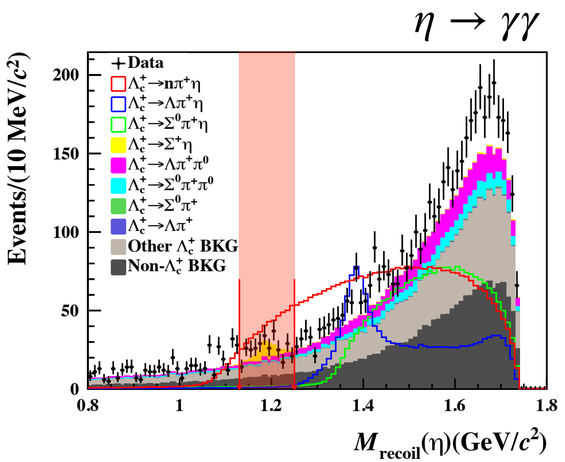

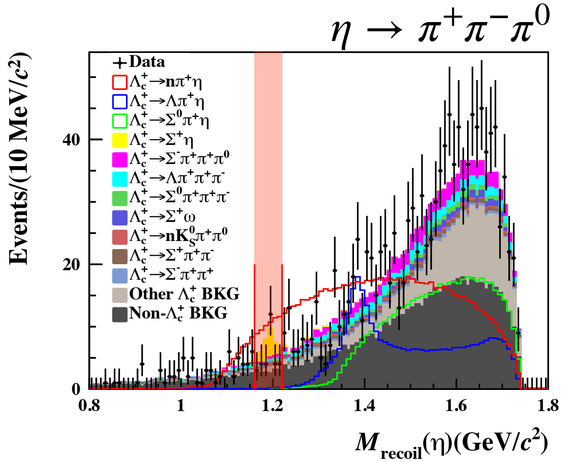

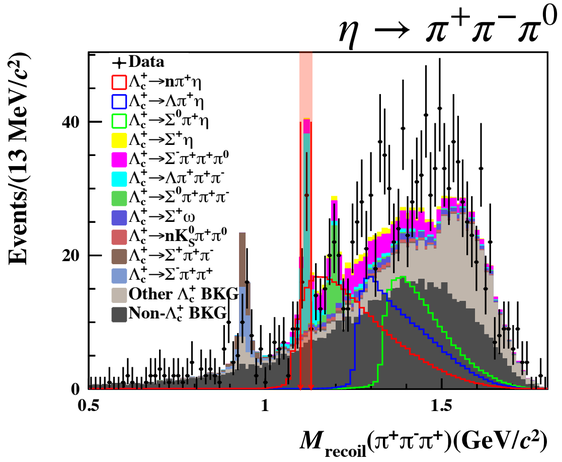

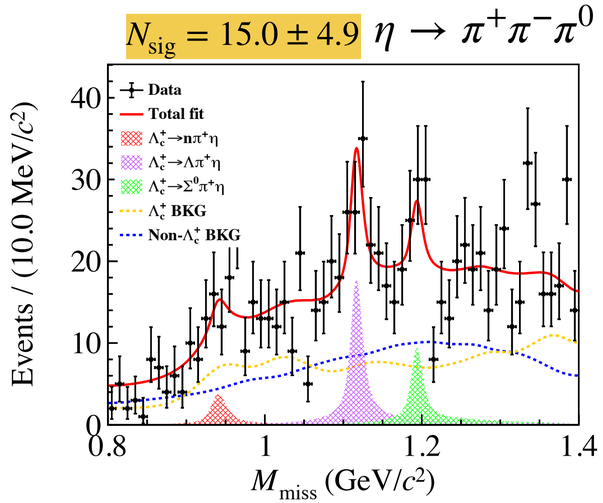

Deep-learning tools and model performance

Data representation for HEP: **Point Cloud**

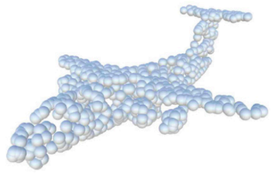

Point cloud of an aircraft generated by 3D scanning

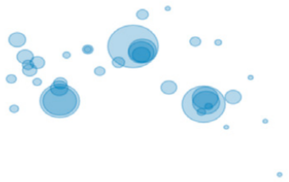

Point cloud of a HEP event

Input variable: low level detector information related to track/shower

- For charged tracks:
  - Azimuth angle θ & ϕ
  - Charge
  - Momentum
  - Helix parameters $d_\rho, d_z, \kappa, \phi_0, \lambda$
  - $\chi_{dE/dx}$ in $e/\pi/K$ hypotheses
  - χ_{TOF} in π/K hypotheses
  - Deposited energy on TOF
  - Velocity measured by TOF
  - Features for its related EMC shower ↗
- For neutral showers:
  - Azimuth angle θ & ϕ
  - Deposited energy: $E_{raw}, E_{seed}, E_{3\times3}, E_{5\times5}$
  - Hit number
  - Time
  - A_{20} moment & A_{42} moment
  - Secondary moment & lateral moment

$$\mathbf{U}' = \begin{cases} 1-\cos\theta_{a,b}, \\ \min\left(E_a,\ E_b\right)\left(1-\cos\theta_{a,b}\right), \\ \min\left(E_a,\ E_b\right)/\left(E_a+E_b\right), \\ \left(E_a+E_b\right)^2-\|\mathbf{p}_a+\mathbf{p}_b\|^2, \end{cases}$$

1. Reasonable data-MC agreement
2. Low level detector information as particle features
3. Four momentum to calculate pair-wise interaction features

Model architecture: **Transformer** **ParT**

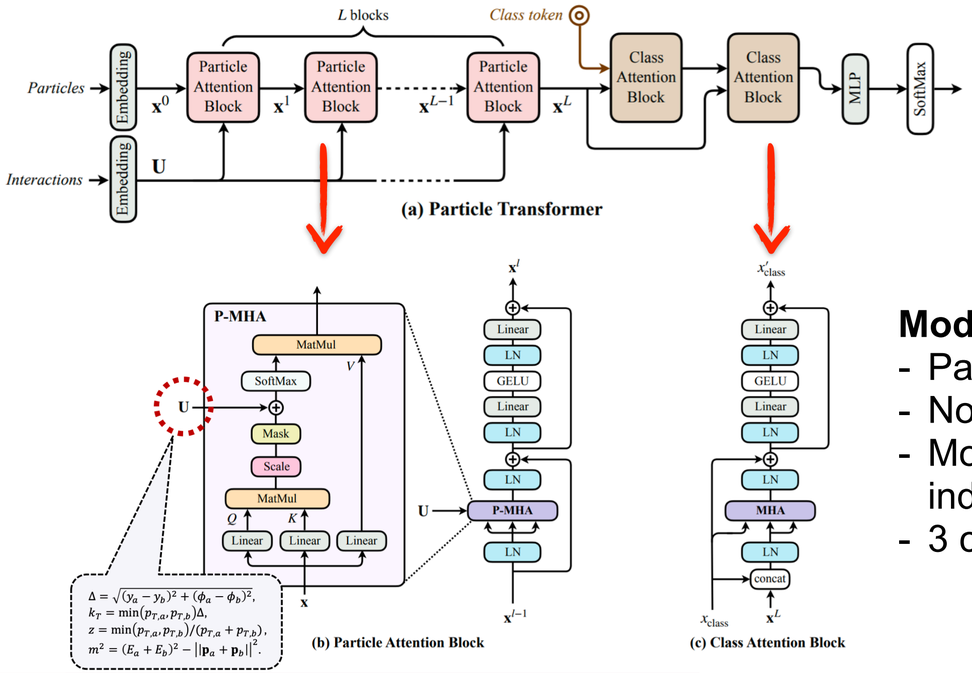

Train dataset: three-classifications Signal vs Other Λ_c^+ BKG vs Non-Λ_c^+ BKG

1. Larger dataset
2. Model generalization
3. Reference/control channel

$\Lambda_c^+ \to n\pi^+\eta, \Lambda\pi^+\eta, \Sigma^0\pi^+\eta$ signal MC
Including $\eta \to \gamma\gamma, \pi^+\pi^-\pi^0$

Inclusive $\Lambda_c^+\bar{\Lambda}_c^-$ MC

Inclusive non-Λ_c^+ MC

DNN relative efficiency: 35%~55%, BKG suppression ~ **1/20**

Model performance

- Parameters: 0.38Million
- No obvious overtraining
- Model ensemble: train 50 independent models and average
- 3 classification score normalized

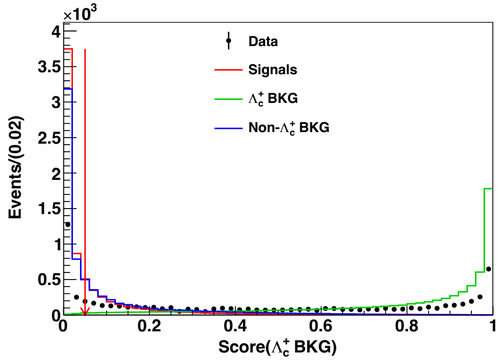

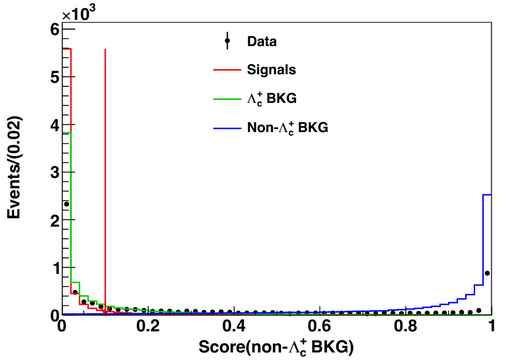

Signal extraction and systematic uncertainty

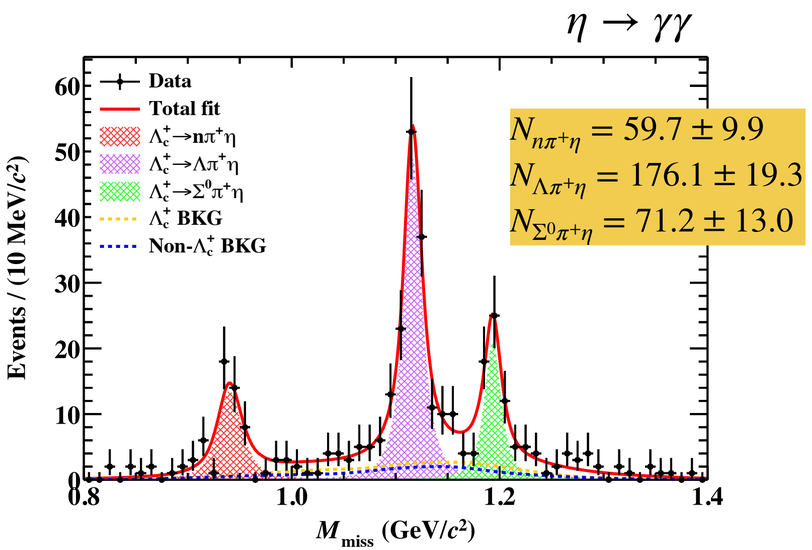

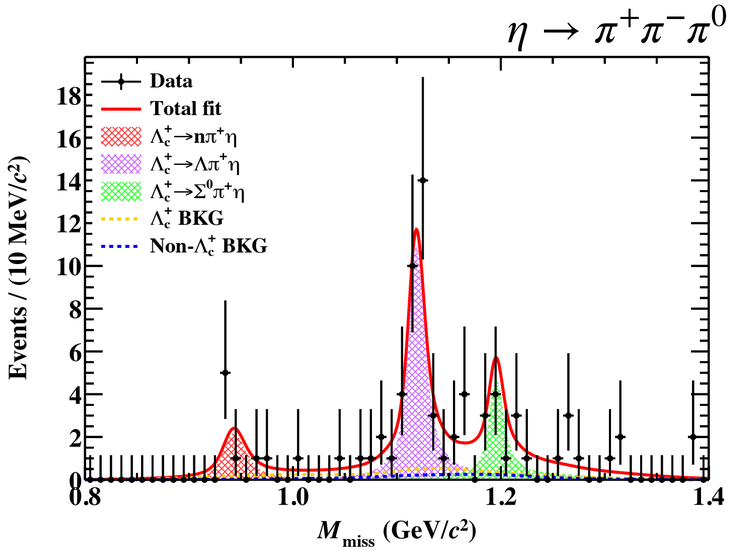

Absolute BF First observation!

$$\mathcal{B}(\Lambda_c^+ \to n\pi^+\eta) = (2.90 \pm 0.48_{\rm stat.}) \times 10^{-3}, \quad 9.5\sigma$$

$$\mathcal{B}(\Lambda_c^+ \to \Lambda\pi^+\eta) = (1.87 \pm 0.21_{\rm stat.}) \times 10^{-2},$$

$$\mathcal{B}(\Lambda_c^+ \to \Sigma^0\pi^+\eta) = (8.2 \pm 1.5_{\rm stat.}) \times 10^{-3}. \quad 7.3\sigma$$

Relative BF Final result to report

$$\mathcal{B}(\Lambda_c^+ \to n\pi^+\eta)/\mathcal{B}(\Lambda_c^+ \to \Lambda\pi^+\eta) = 0.155 \pm 0.031_{\rm stat.},$$

$$\mathcal{B}(\Lambda_c^+ \to \Sigma^0\pi^+\eta)/\mathcal{B}(\Lambda_c^+ \to \Lambda\pi^+\eta) = 0.436 \pm 0.093_{\rm stat.}.$$

Systematic uncertainty of relative BF

Sources	Size (%)
MC model	5.7
Peaking background vetoes	1.5
Deep learning vetoes	4.9
Simultaneous fit	0.9
Total	7.7

$\Lambda_c^+ \to n\pi^+\eta$: reweighting to data sweighted distribution

$\Lambda_c^+ \to \Lambda\pi^+\eta$: consider uncertainty of PWA model pars

Model uncertainty: hyper-pars, layers, pair-wise features

Domain shift: Data-MC difference is assessed using control channel $\Sigma^0\pi^+\eta$

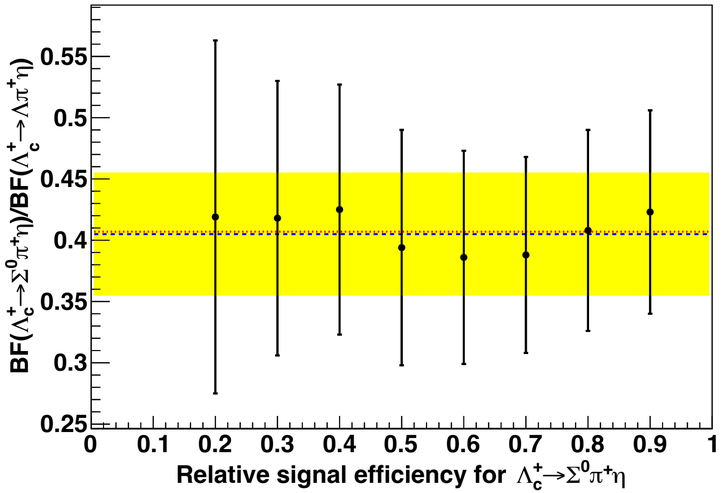

Search for $a_0(980)^+$

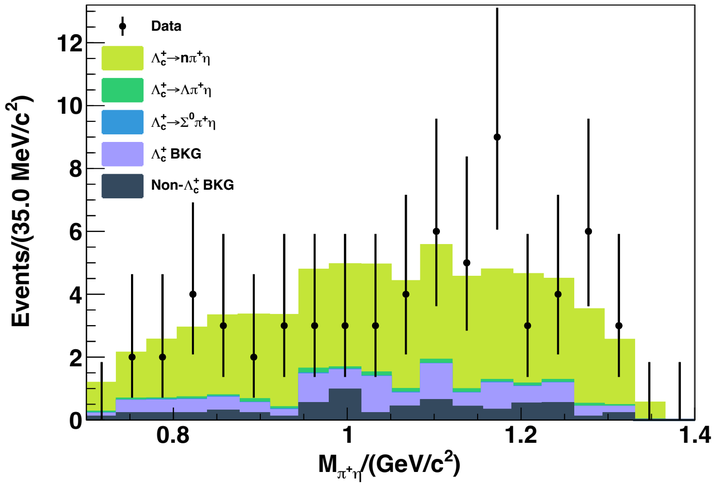

- After DNN requirement
- Within $M^2_{\rm miss}$ signal region
- Signal/background normalized to fit result
- No obvious $a_0(980)^+$ signal

Fitting model →

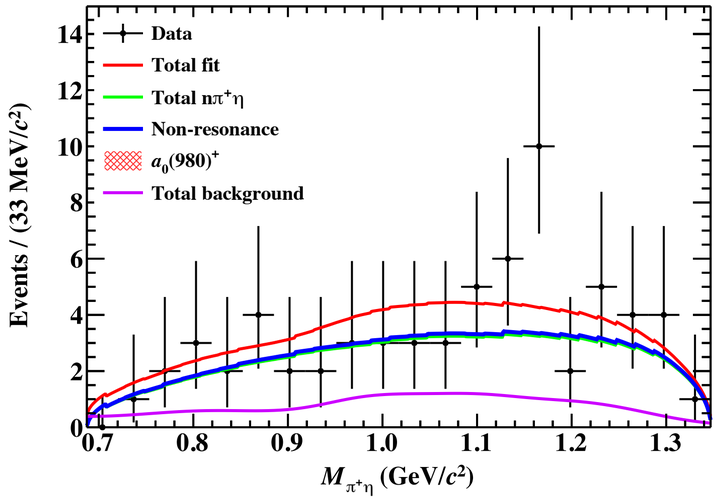

Efficiency curve

Data-MC resolution difference

$$\mathscr{PDF}_{\rm sig}(m) = [\varepsilon(m) \times \frac{{\rm d}\Gamma}{{\rm d}m}] \otimes \mathscr{G}(\mu,\sigma)$$

$$\frac{{\rm d}\Gamma}{{\rm d}m} = |\mathscr{A}(m)|^2 \cdot \frac{|\vec{P}_n(m)|}{m_{\Lambda_c^+}} \cdot \frac{|\vec{P}_{\pi^+}(m)|}{m} \cdot 2m$$

$$\mathscr{A}(m) = r \times \mathscr{R}_{a_0(980)^+}(m) + 1$$

$$\mathscr{R}_{a_0(980)^+}(m) = \frac{1}{m_0^2 - m^2 - i(g_1\rho_{\eta\pi}(m) + g_2\rho_{K\bar{K}}(m))}$$

Flatté lineshape

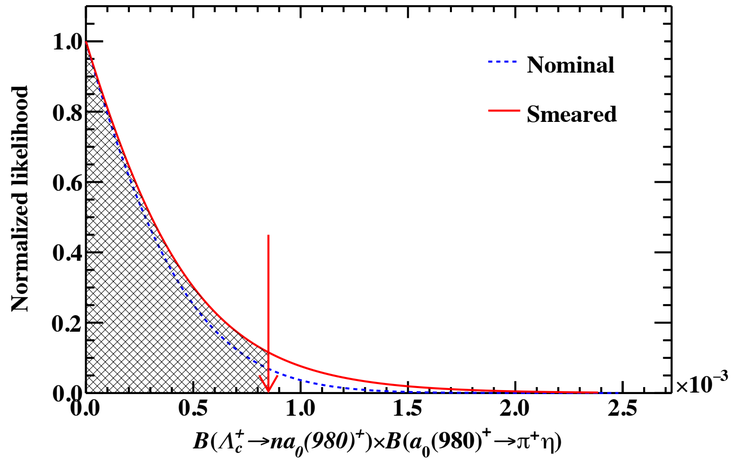

$$\mathscr{L}'(\mathscr{B}_{\rm 2body}) \propto \int_0^1 \mathscr{L}(\mathscr{B}_{\rm 2body} \cdot \frac{\hat{\mathscr{B}}_{\rm 3body}}{\mathscr{B}_{\rm 3body}}) e^{\frac{-(\mathscr{B}_{\rm 3body}-\hat{\mathscr{B}}_{\rm 3body})^2}{2\sigma_{\mathscr{B}_{\rm 3body}}}} d\mathscr{B}_{\rm 3body}$$

Consider additive and multiplicative systematic uncertainty
Additive systematic uncertainty includes:
- Signal description (shape, yields constrain)
- Background description (shape, yields constrain)

BF UL result:

$$\mathscr{B}(\Lambda_c^+ \to n a_0(980)^+) \times \mathscr{B}(a_0(980)^+ \to \pi^+\eta) < 8.5 \times 10^{-4}$$

Physics impact

- First observation of $\Lambda_c^+ \to n\pi^+\eta$ process with 9.5σ

$$\frac{\mathcal{B}(\Lambda_c^+ \to n\pi^+\eta)}{\mathcal{B}(\Lambda_c^+ \to \Lambda\pi^+\eta)} = 0.155 \pm 0.031_{\text{stat.}} \pm 0.012_{\text{syst.}}$$

- Absolute BF: $\mathcal{B}(\Lambda_c^+ \to n\pi^+\eta) = (2.89 \pm 0.60_{\text{stat.}} \pm 0.22_{\text{syst.}} \pm 0.17_{\text{ref.}}) \times 10^{-3}$
- Search for intermediate process $\Lambda_c^+ \to n a_0(980)^+$, set upper limit

$$\mathcal{B}(\Lambda_c^+ \to n a_0(980)^+) \times \mathcal{B}(a_0(980)^+ \to \pi^+\eta) < 8.5 \times 10^{-4}$$

- Submitted to JHEP, arXiv:2603.28232
- AI/ML technique boost physics observation!

Consistent with $SU(3)_F$ TDA theoretical predictions within 2σ

Smaller than $SU(3)_F$ TDA prediction
Consistent with pole model prediction

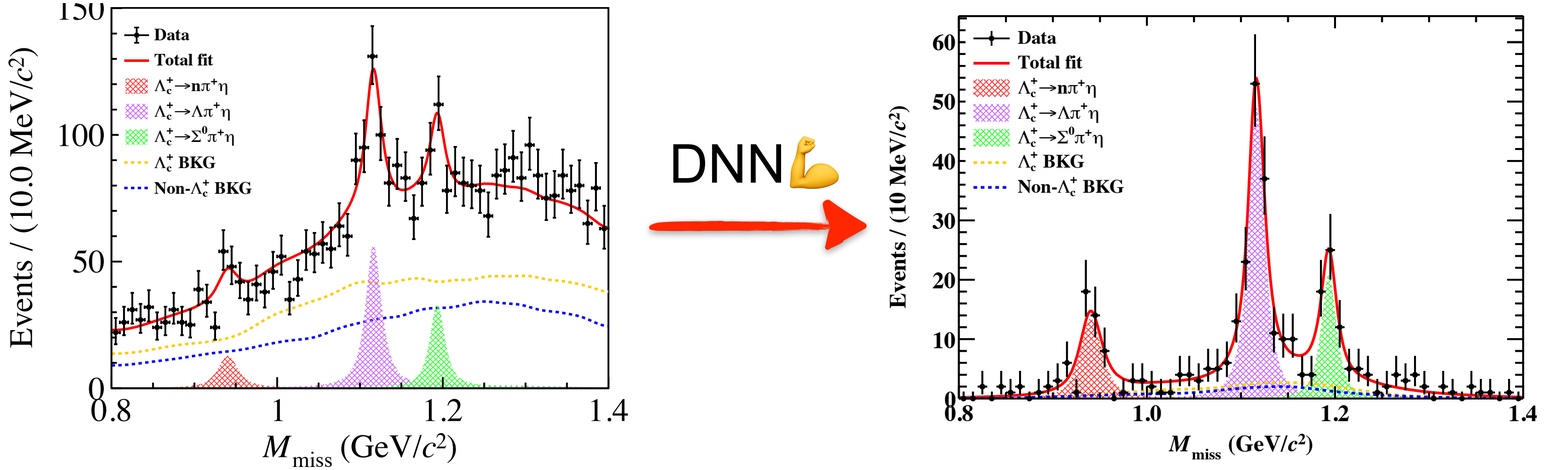

My work in Λ_c^+ decays

Λ_c^+ two-body decays

- Measurement of branching fractions (BF) of $\Lambda_c^+ \to \Sigma^0 K^+$ and $\Sigma^+ K_S^0$
  - Published in Phys. Rev. D **106** (2022), 052003

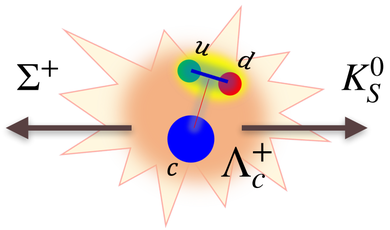

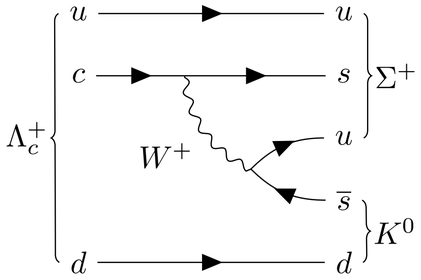

Highlight in this talk

Λ_c^+ three-body decays

- Partial wave analysis of $\Lambda_c^+ \to \Lambda \pi^+ \eta$
  - Published in Phys. Rev. Lett. **134**, (2025), 021901

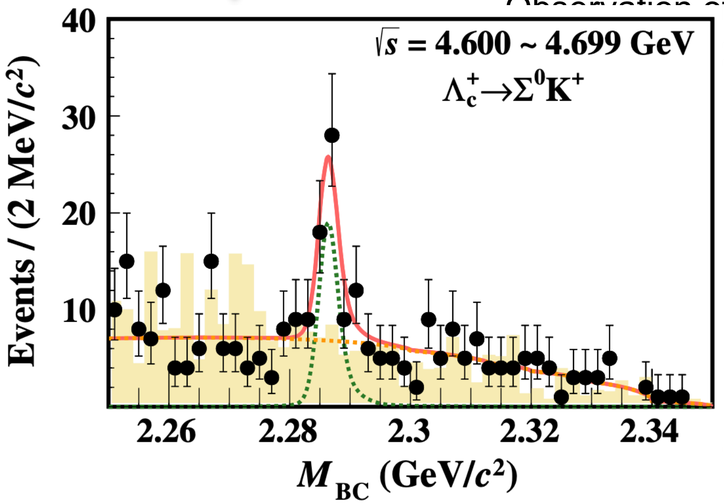

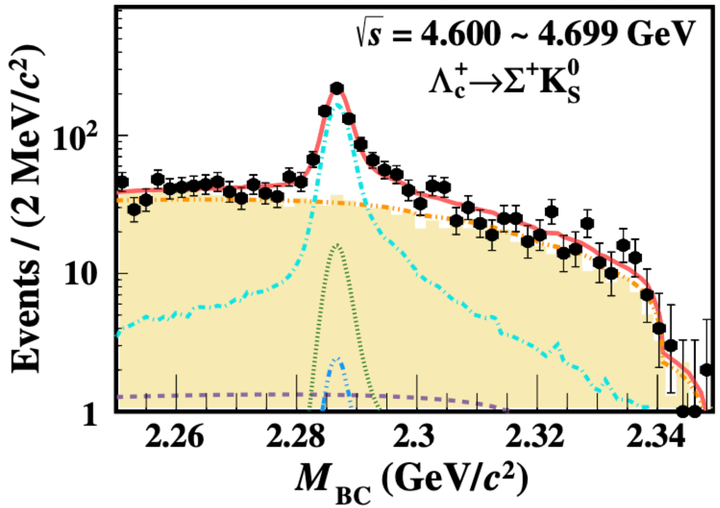

Λ_c^+ semi-leptonic decays

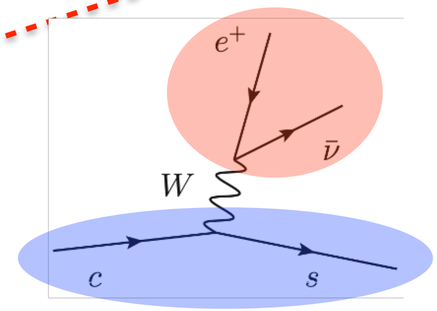

- Search for $\Lambda_c^+ \to \Lambda \pi^+ \pi^- e^+ \nu_e, p K_S^0 \pi^- e^+ \nu_e$
  - Published Phys. Lett. B **843**, (2023), 137993
- Measurement of BF of $\Lambda_c^+ \to p \pi^- e^+ \nu_e$
  - BAM-00736 (REV-830), currently in BESIII spokersperson review stage

My work in Λ_c^+ decays

Λ_c^+ two-body decays

- Measurement of branching fractions (BF) of $\Lambda_c^+ \to \Sigma^0 K^+$ and $\Sigma^+ K_S^0$
  - Published in Phys. Rev. D **106** (2022), 052003

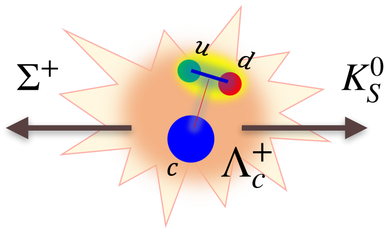

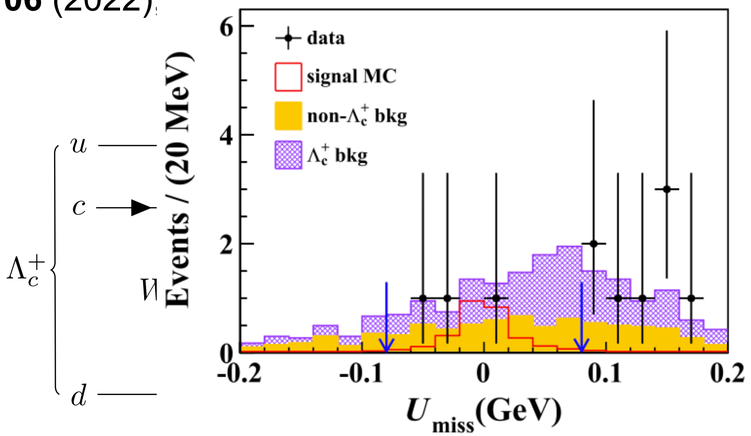

Highlight in this talk

Λ_c^+ three-body decays

- Partial wave analysis of $\Lambda_c^+ \to \Lambda\pi^+\eta$
  - Published in Phys. Rev. Lett. **134**, (2025), 021901

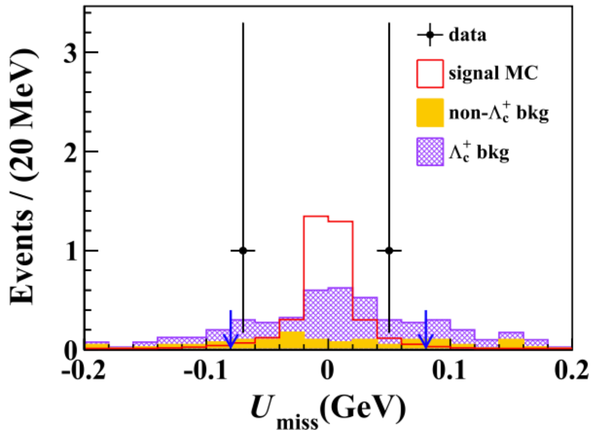

- $n\pi^+\eta$ and search for $\Lambda_c^+ \to n a_0(980)^+$ submitted to JHEP

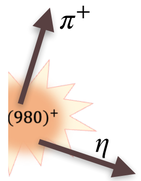

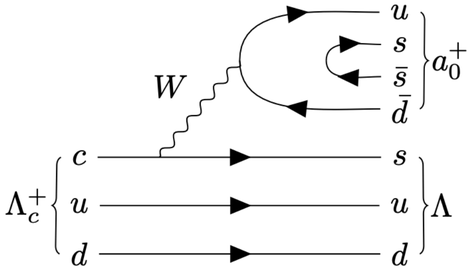

Λ_c^+ semi-leptonic decays

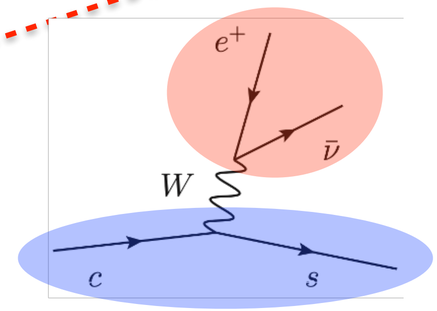

- Search for $\Lambda_c^+ \to \Lambda\pi^+\pi^- e^+\nu_e, pK_S^0\pi^- e^+\nu_e$
  - Published Phys. Lett. B **843**, (2023), 137993
- Measurement of BF of $\Lambda_c^+ \to p\pi^- e^+\nu_e$
  - BAM-00736 (REV-830), currently in BESIII spokersperson review stage

Physics motivation for J/ψ energy correlator

➔ Inclusive J/ψ production
- ❖ Ideal probe to study hadronization $c\bar{c} \to J/\psi$
- ❖ NRQCD factorization
- ❖ Long-standing tension between hadron collider and lepton collider as well as cross section and polarization

Long Distance Matrix Element (LDME): encode hadronization
Expand in order of quark velocity v, including color singlet and color octet

$$(2\pi)^2 2P_H^0 \frac{d\sigma_H}{d^3P_H} = \sum_n d\hat{\sigma}_n(P_H) \langle \mathcal{O}_n^H \rangle$$

Short Distance Coefficient (SDC): encode heavy quark production
Expand in order of α_s

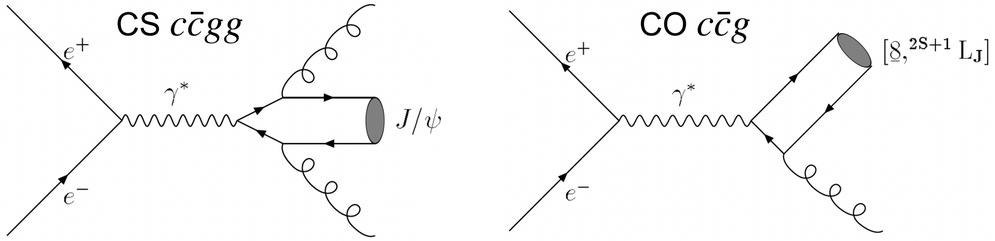

➔ **Quarkonium Energy Correlator (QEC)**: a new observable to study hadronization
- ❖ Cross section, momentum/energy distribution, polarization → energy flow pattern
- ❖ Distinguish CS and CO contribution, especially at large $\cos\chi$

➔ Advantage of BESIII
- ❖ Low energy (larger non-perturbative effects)
- ❖ Low background
- ❖ Constrain feed-down background

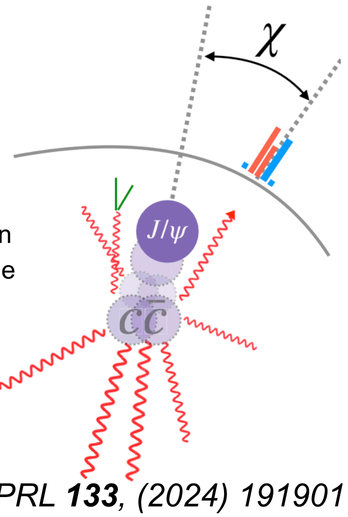

$$\Sigma(\cos\chi) = \int d\sigma \sum_i \frac{E_i}{M_{J/\psi}} \delta(\cos\chi - \cos\theta_i)$$

$d\sigma$: J/ψ production cross section
χ: helicity angle in J/ψ rest frame
E_i: particle energy along with θ_i
$M_{J/\psi}$: J/ψ mass

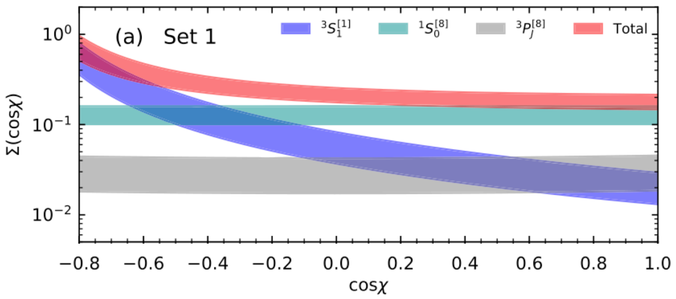

*PRL **133**, (2024) 191901*

BESIII Collaboration Service

➔ MC production and generator development

- ❖ Developed MC generator model for Λ_c^+ exclusive decay channels
- ❖ Coordinated dedicated MC production for physics analyses

➔ Internal review

- ❖ Served on BESIII Referee Committee
- ❖ Reviewed and supported **11 physics analyses** through internal approval

➔ Mentoring

- ❖ Guided **5+ junior PhD students** in BESIII physics analysis
- ❖ Provided support on whole analysis chain
  - ▸ physical concept, experimental principle, fitting, systematic evaluation, presentation, documentation and paper writing

➔ Detector operation and taking shift

- ❖ Completed 18 days of BESIII shifts

Heavy flavor and tracking study at sPHENIX experiment

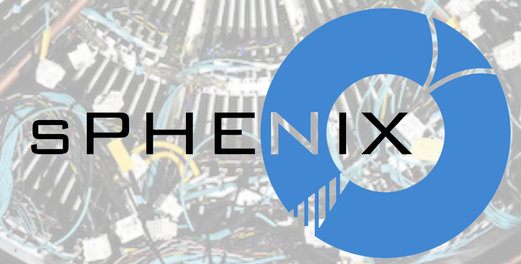

Transition from BESIII to sPHENIX

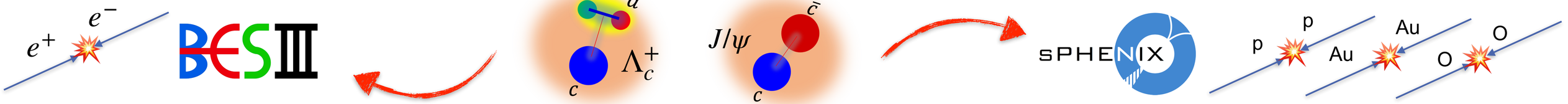

- **Motivation after BESIII analyses**

1. Completed multiple physics analyses at BESIII
2. Wanted to extend my skills beyond physics analysis and explore new experimental frontiers

- **Possible directions discussed with my advisor**

1. PKMUON dark matter experiment
   - A rapidly growing and highly active direction in particle physics
2. **sPHENIX** experiment at RHIC
   - Strong connection through my advisor's involvement in PHENIX/sPHENIX, especially the sPHENIX EMCal
   - New experiment about to start data taking
   - Many opportunities in detector, reconstruction, and physics

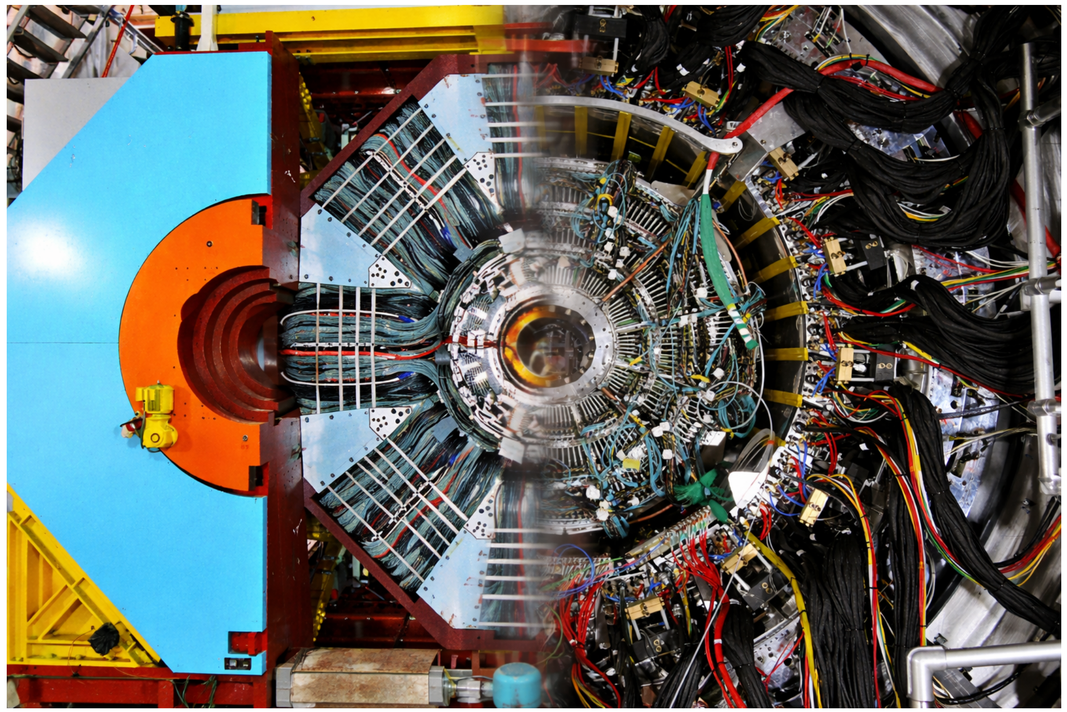

- **Why I chose sPHENIX**

1. To become a more complete experimental particle/nuclear physicist
   - Physics analysis is only the final step of a large experiment
   - Detector operation, calibration, reconstruction, and QA are equally essential
2. Strong interest in using heavy-flavor particles to study QCD matter and hadronization

- **Expected contributions in sPHENIX**

1. **Detector operation**
2. **Software & reconstruction**
3. **Physics analysis**

Cont

PKMUON

*Phys. Rev. D **110** (2024), 016017*

- ➔ A proposed PKU-Muon experiment for muon tomography and dark matter search
- ➔ **Geant4** simulation of GEM-based detector
- ➔ Dark matter (DM) and muon elastic scattering: model-independent method
- ➔ Three physics cases:
  - ❖ DM searches in a box
  - ❖ DM searches using muon beams
  - ❖ DM searches between mountain and sea level
- ➔ Use Higgscombine tool to obtain ULs on cross section for sub-GeV DM and muon scattering

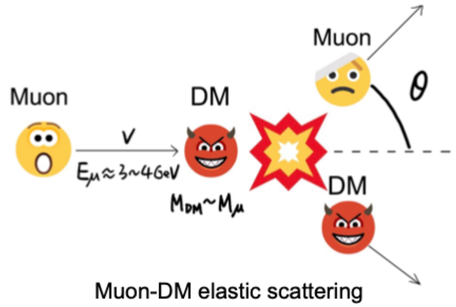

Muon-DM elastic scattering

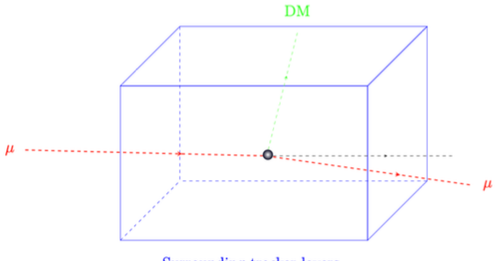

Phase I

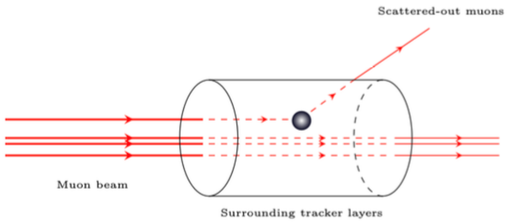

Phase II

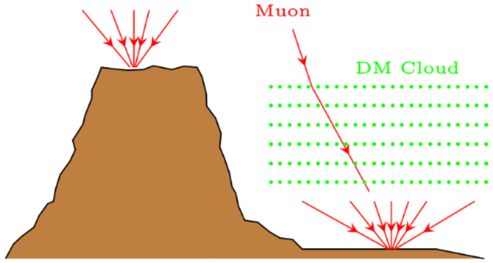

Phase III

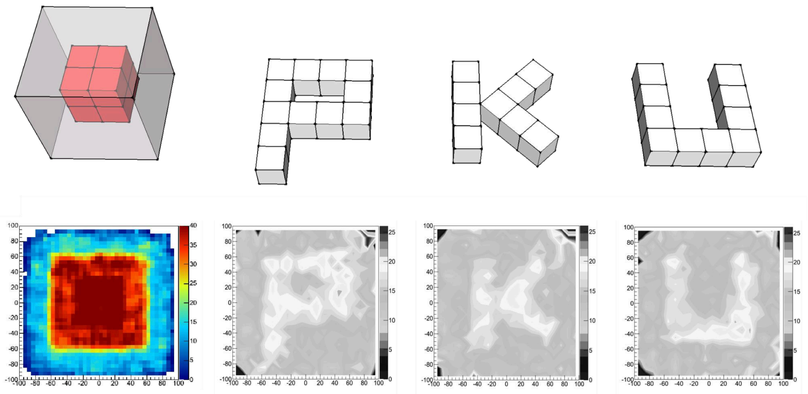

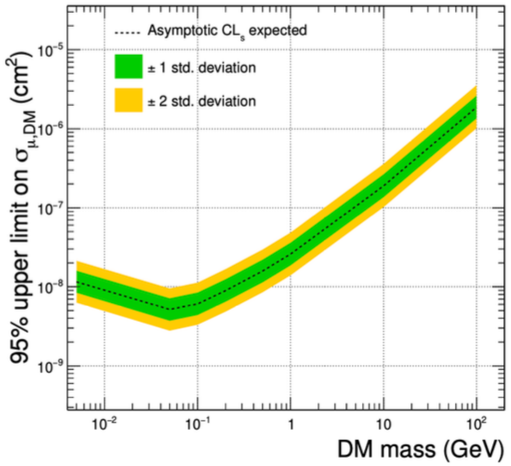

BACK

sPHENIX Experiment Overview

➔ sPHENIX: The first new major detector at RHIC in over 20 years

- ❖ A complete tear-down and rebuild of PHENIX reusing existing PHENIX equipment and support facilities, plus brand new detector subsystems and a completely upgraded experiment complex.

➔ Data taking from 2023-2025(6)

- ❖ 200 GeV Au+Au data taking commissioning in 2023
- ❖ 200 GeV p+p data taking in 2024
- ❖ 200 GeV Au+Au high-statistics data taking, additional p+p and O+O data taking in 2025 (end in Jan. 2026)

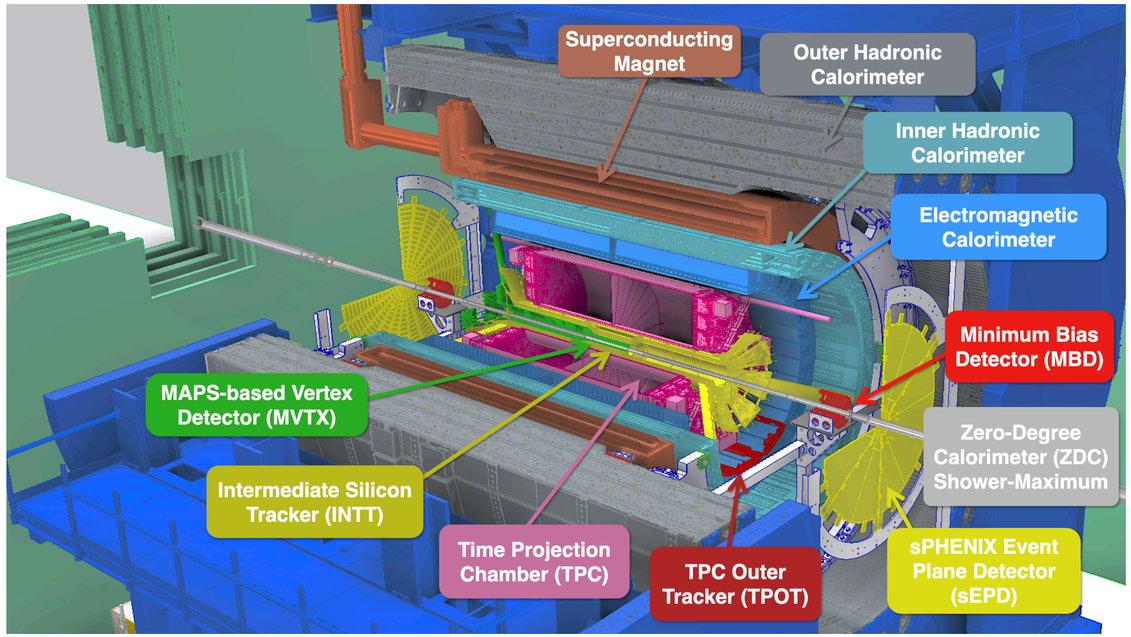

sPHENIX detector

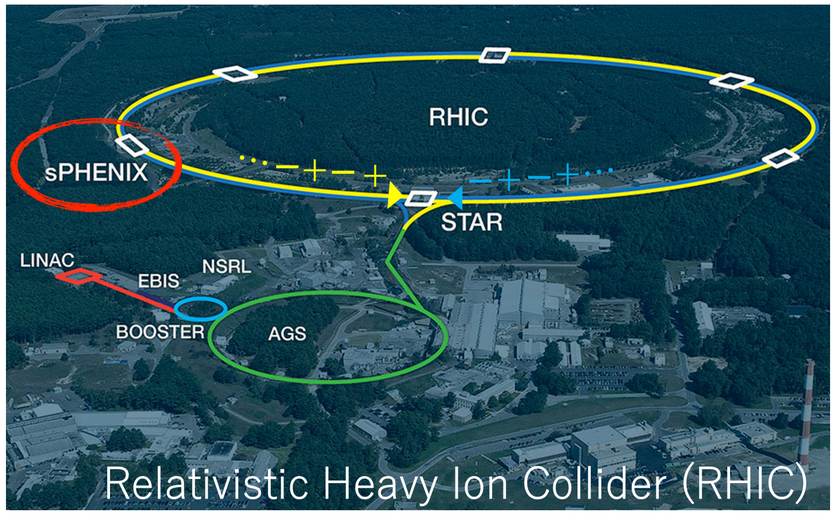

My sPHENIX Contributions

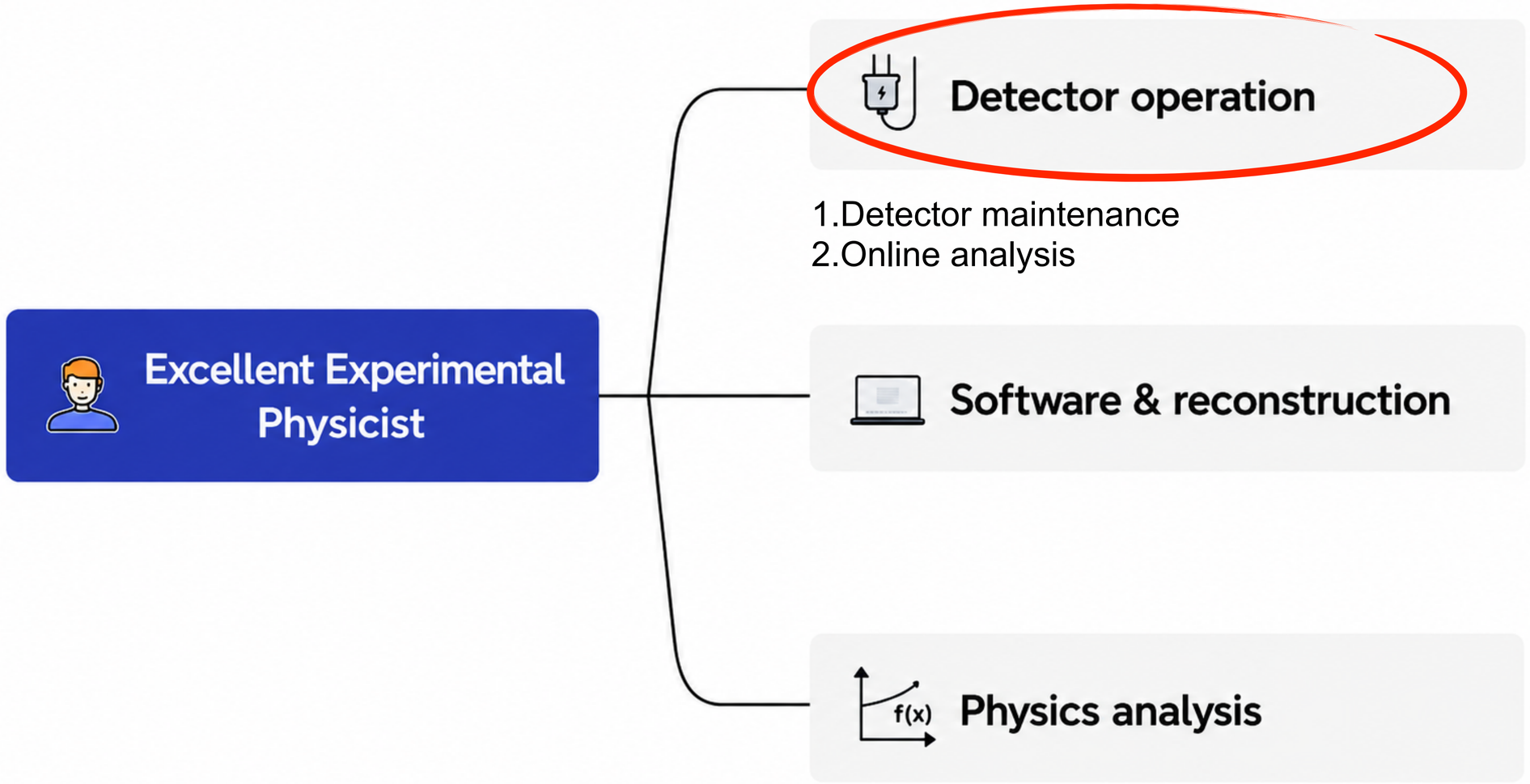

MVTX on-call expert

➔ Troubleshooting and maintenance according to MVTX expert note

- ❖ turn on/off detector, fix mixed states, clock error, flickering states, over temperature error etc.
- ❖ Adding algaecide, priming cooling system
- ❖ OnlMon improvement

➔ **Highlight**: on Oct. 13 2024, MVTX CAEN power supply module broken accidentally during the data taking. In SCM, this was identified as a high priority emergency, so I volunteered to replace CAEN. I unscrewed power supply from MVTX telescope then made a Control Access into Interaction region to swap power supply.

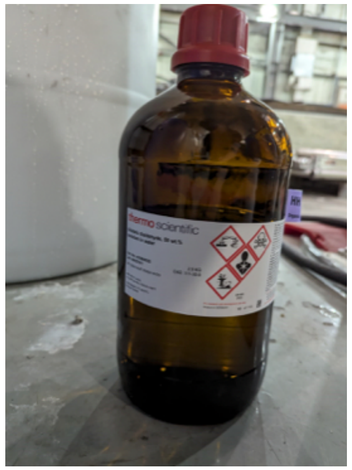

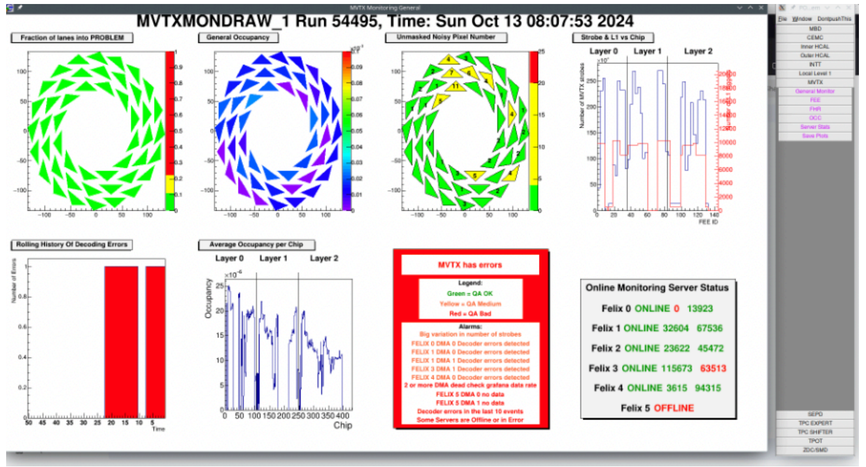

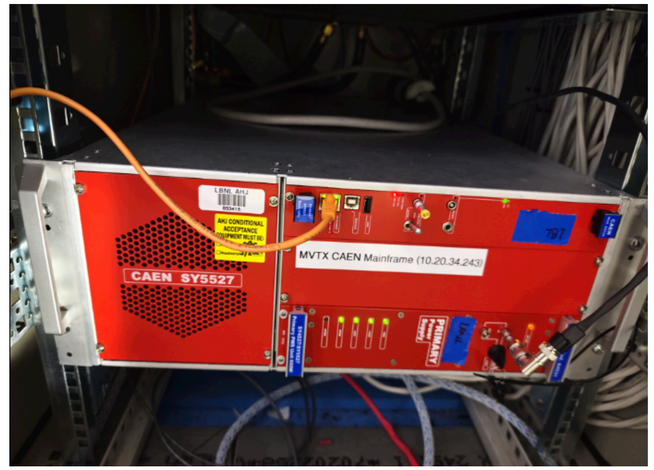

Online analysis — TPC gas contamination

- ➔ TPC dE/dx problem in Run 24 AuAu commisioning
  - ❖ dE/dx is suppressed near central membrane (CM)
- ➔ I setup dE/dx 1D/2D metric to quantify

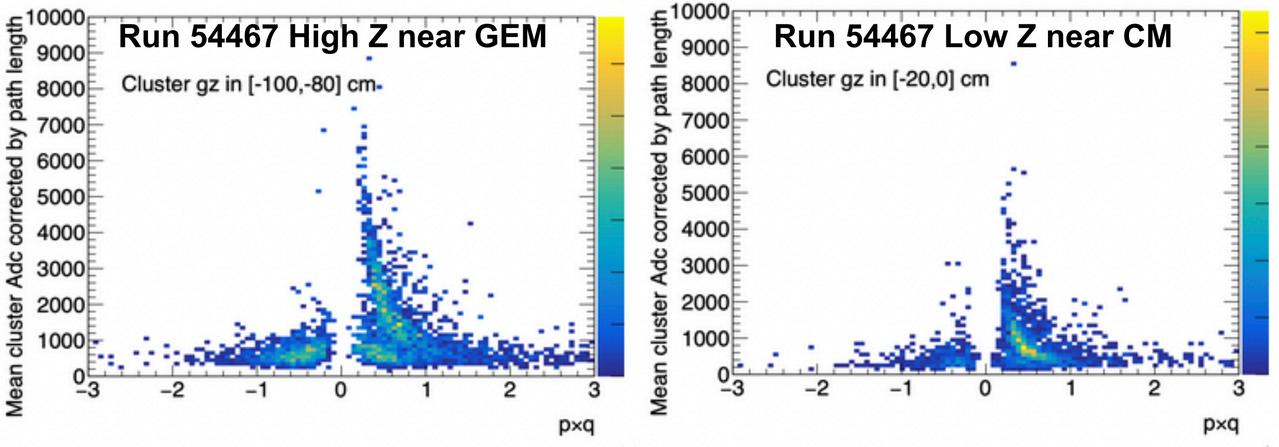

Y-axis:Sum of cluster ADC at R2 and R3 corrected by sin(theta) divided by number of clusters where theta is polar angle

- ➔ Two hypothesis
  - ❖ 1. GEM sagging within an AuAu event (centrality dependent)
  - ❖ 2. Electron attachment to form ions during drift due to gas contamination (centrality independent)

- ➔ Separate events into central collision event with high multiplicity and peripheral event with low multiplicity
  - ❖ Problem persists in low multiplicity events
  - ❖ Exclude hypothesis 1

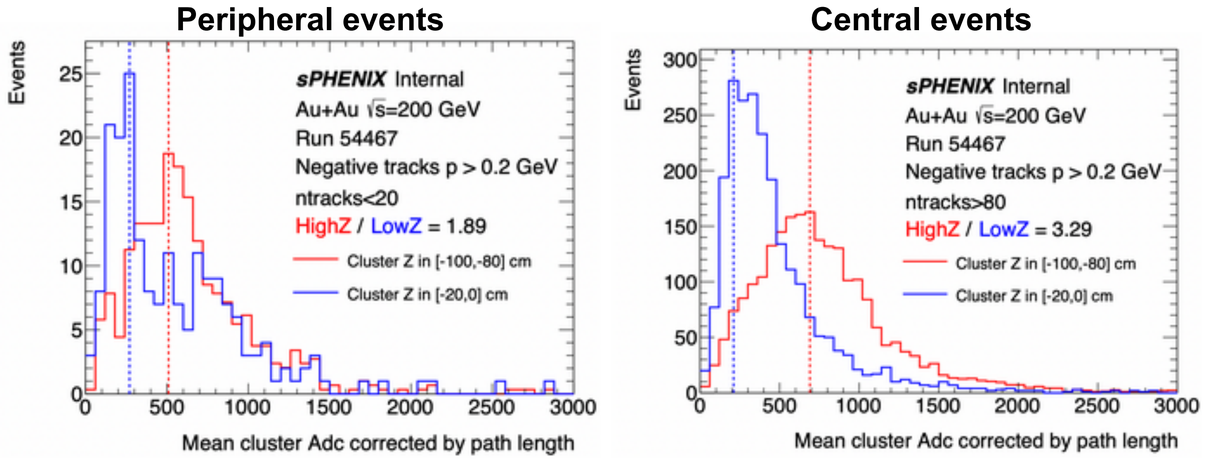

Online analysis — dE/dx vs z monitoring

➔ To exclude/confirm hypothesis 2, I did time series analysis of p+p and Au+Au runs

- There is a spike around 08/16, but in most of the time, dE/dx ratio is very stable

➔ TPC group finally solved dE/dx puzzle by swapping CF4 gas bottle

- Low quality CF4 gas bottle with more gas contamination
- This problem happened again in Run25, and my metric worked to help identify problem

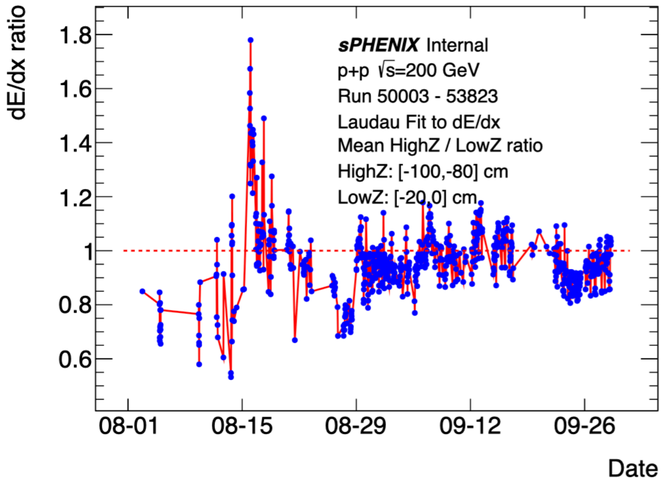

pp runs time series plot

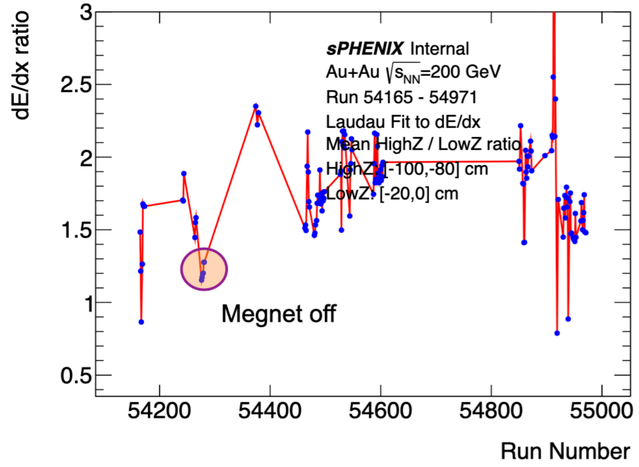

AuAu runs time series plot

Lesson #3

There is no future.
Tracking experts in person at BNL. No excuses.

Nothing focusses the mind better than staying at BNL and working round the clock in 1008 – fastest, most direct communication.

Example – most valuable player was Xudong (in 1008 all the time).
Great benefit when Tony and Joe were at BNL. Others are in denial.

Run coordinator Jamie Nagle's recognition in Run25 readiness review

Online analysis — resonance check

- ➔ 2025 Christmas holiday was in the critical period for p+p luminosity accumulation.
- ➔ Resonance check, e.g. K_S^0 reconstruction is important to ensure data we were taking is good
- ➔ Problem: K_S^0 yields η-dependence

Run24 with 40% dE/dx PID cut

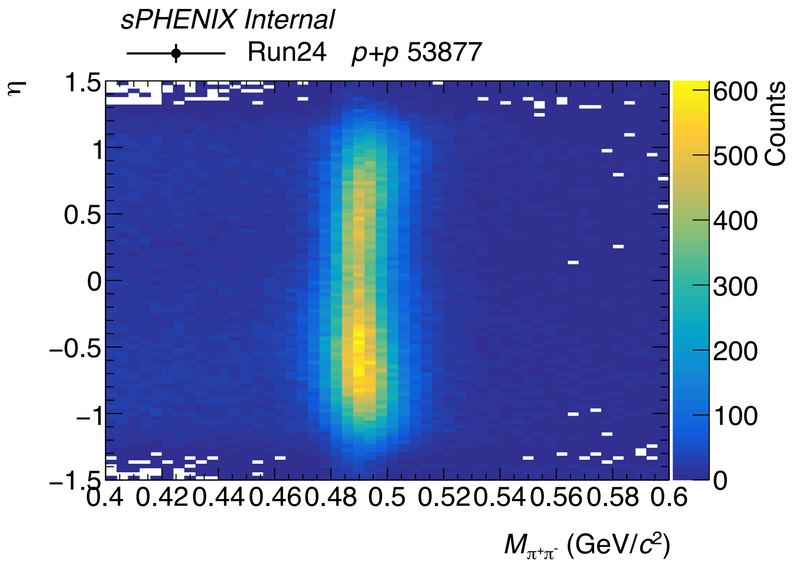

Run25 with 40% dE/dx PID cut

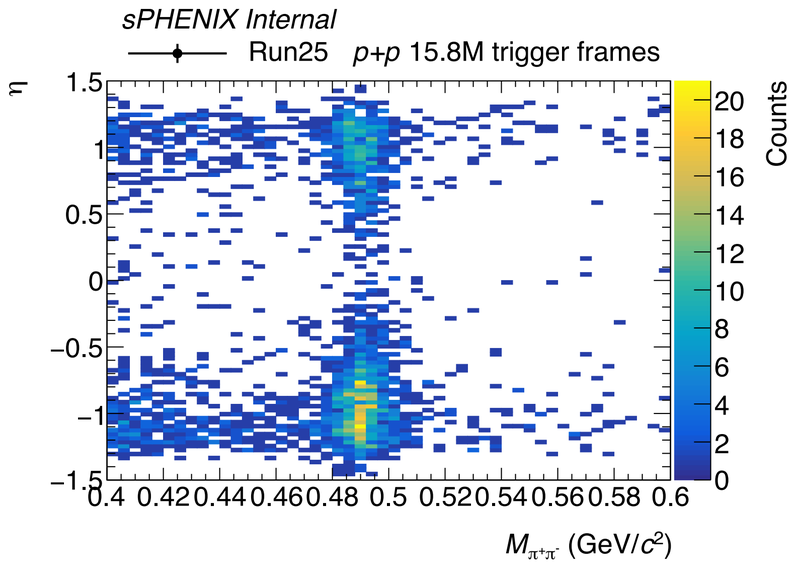

Run25 without dE/dx PID cut

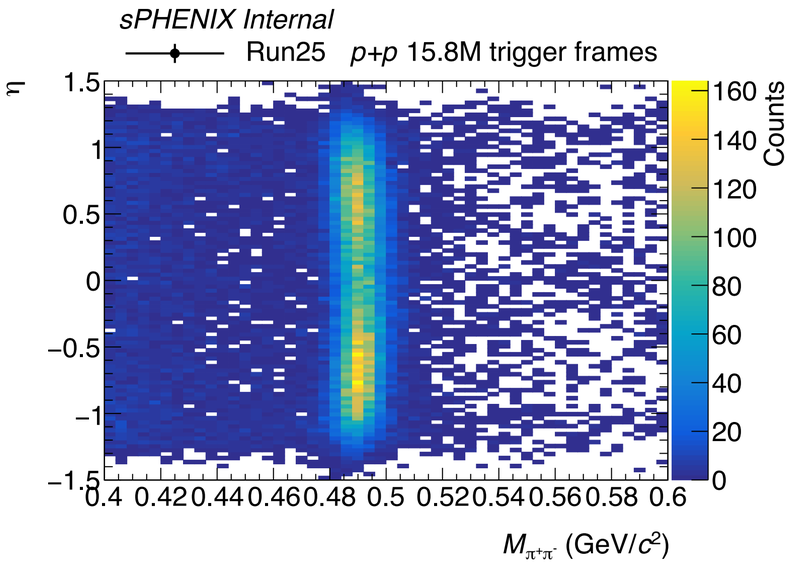

Joe's talk in GM: https://indico.bnl.gov/event/31016/contributions/118343/attachments/67319/115666/TrackingDataChecks.pdf

Online analysis — resonance check

➔ Observation: data is good but $\mathrm{d}E/\mathrm{d}x$ needs re-calibration from Run-24 to Run-25

- In Run-25, TPC is basically a new detector after the cascade HV power supplies
- $\mathrm{d}E/\mathrm{d}x$ band is narrower which is good!

Run24 dE/dx vs qp plot

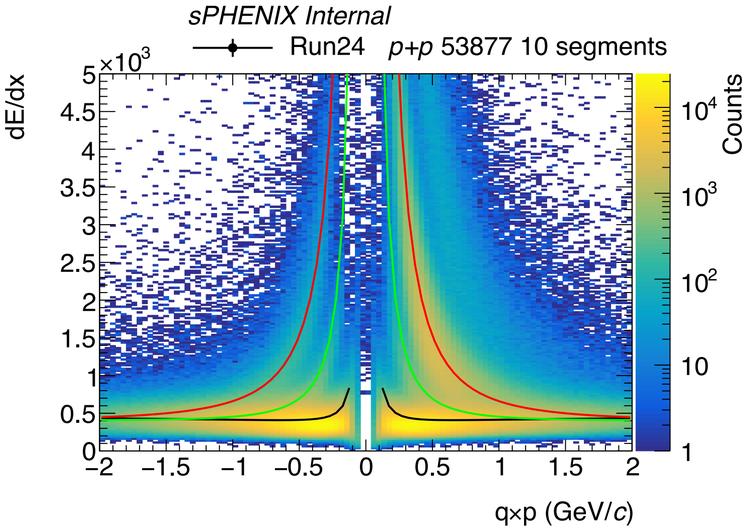

Run25 dE/dx vs qp plot

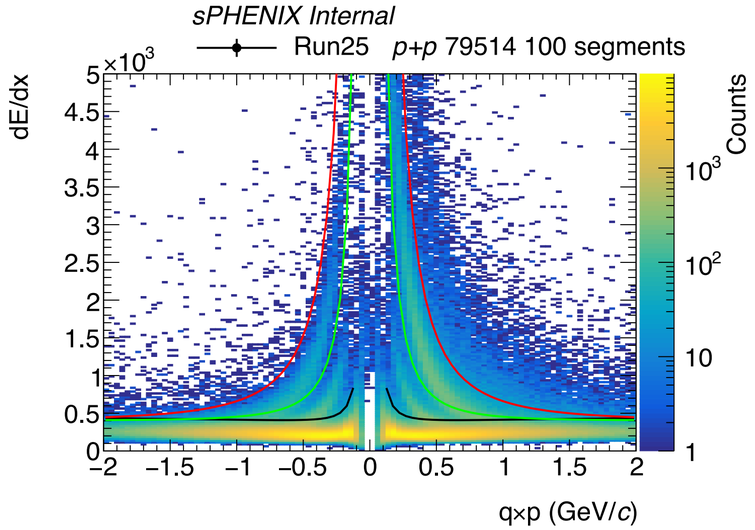

Run25 dE/dx vs qp plot with expectation scaled by 0.5

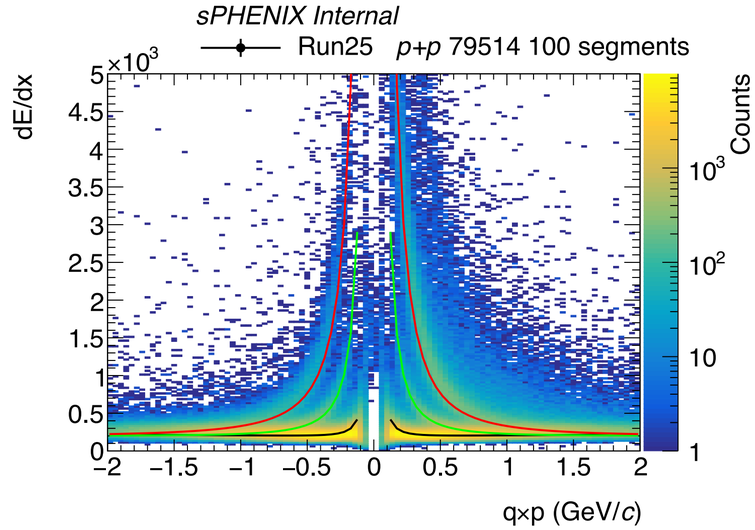

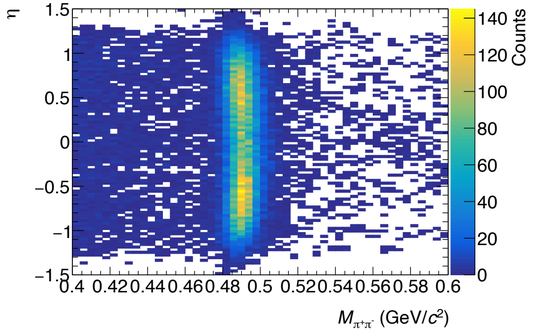

Red curve: proton dE/dx expectation
Green curve: kaon dE/dx expectation
Black curve: pion dE/dx expectation

Lesson learned:

- Rapid diagnostic and response during data taking
- Strong detector and QA awareness
- Close communication with run coordinators and detector experts
- Reliability under time pressure

My sPHENIX Contributions

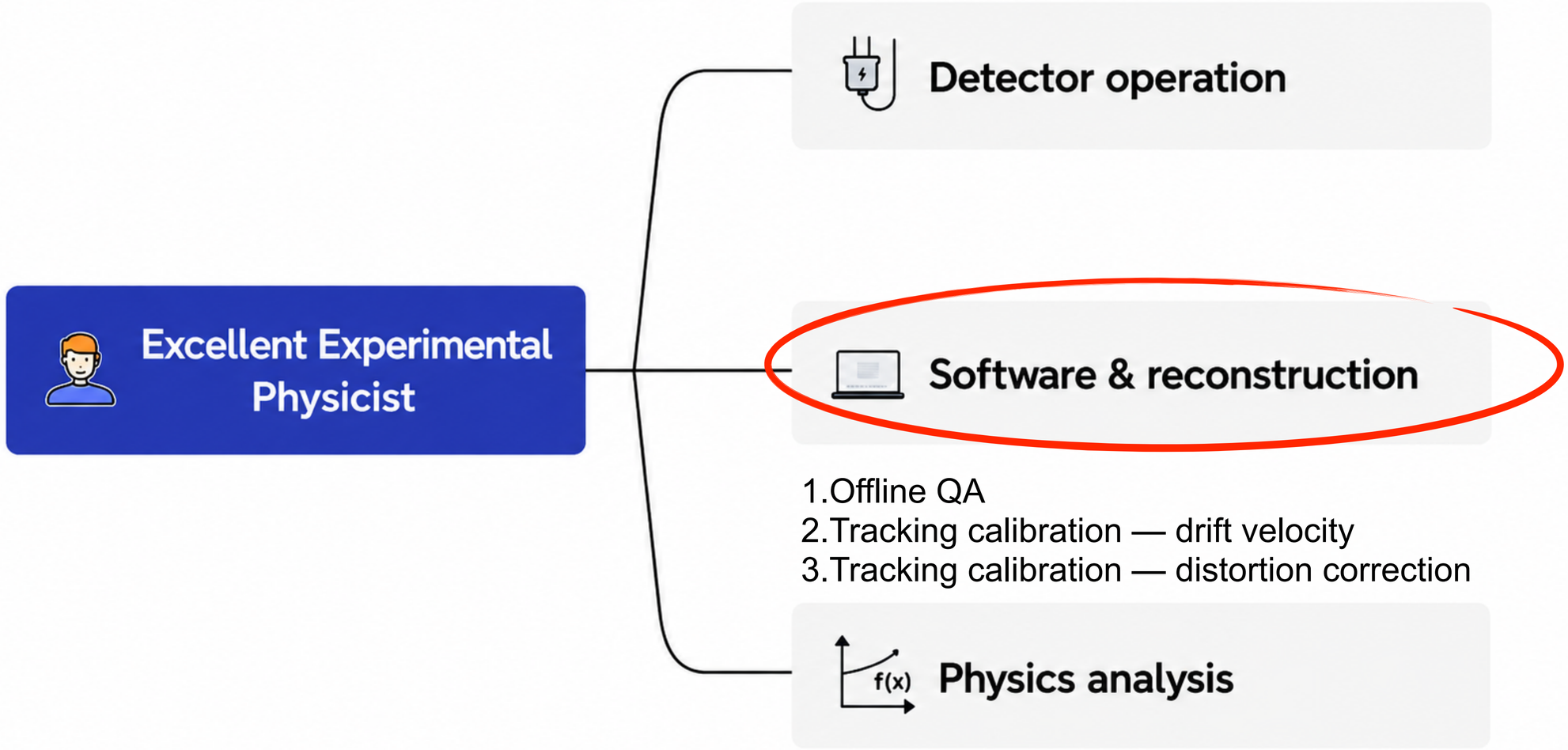

Offline QA

➔ Set up some QA modules in coresoftware for checking data from tracking detectors in different tracking reconstruction stages

- ❖ Mvtx Raw Hit QA (raw hit layer/stave 2D map, hit position map, Nhits, BCO…)
- ❖ Intt Raw Hit QA
- ❖ TPC seeds QA (Nclusters, Ntracks, pT/eta/phi, DCA, dE/dx)
- ❖ Vertex QA

➔ Write QAHtml code for implementing QA module into auto-production pipeline

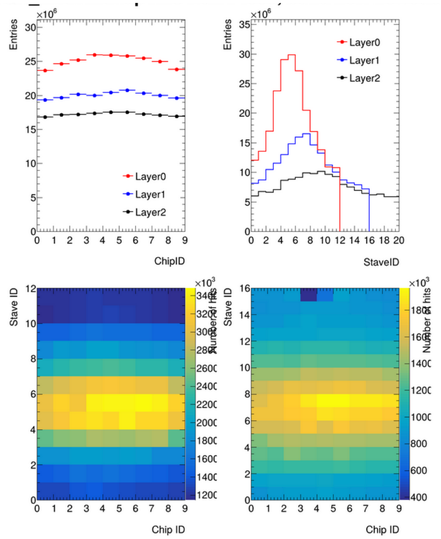

MVTX RawHit QA

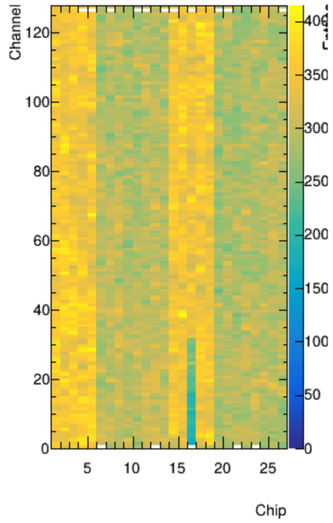

INTT RawHit QA

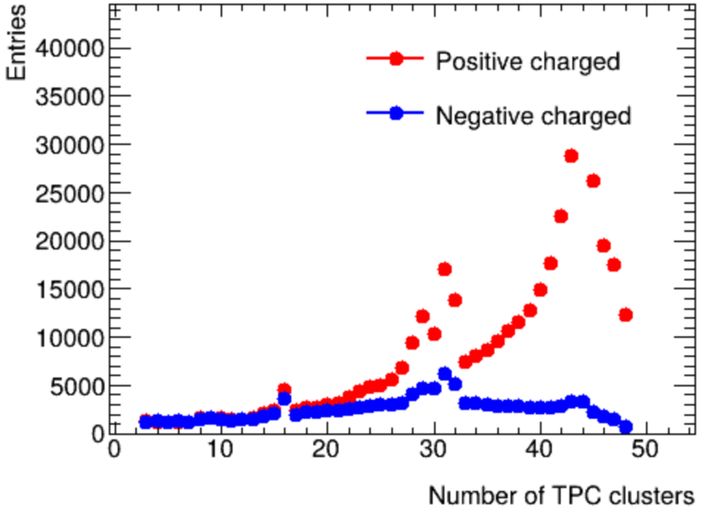

TPC seed QA — Nclus

Tracking calibration — drift velocity

- ➔ **Important TPC calibration parameters** in run-by-run basis
  - ❖ Vary with experiment conditions: electric field, gas mixture, weather (pressure, temperature)
- ➔ **Match TPC seeds with EMCal clusters** to provide sPHENIX first version of drift velocity (DV) calibration
  - ❖ Start with a initial drift velocity
  - ❖ Reconstruct TPC seeds, calculate projection position at EMCal surface
  - ❖ Plot the Δz vs z plot of each track and use linear function to fit distribution
  - ❖ The slope parameter is used to correct drift velocity
  - ❖ Iteration
- ➔ **Uploaded calibrated files to CDB**
  - ❖ Provided early TPC DV calibration for sPHENIX
  - ❖ Sensitive diagnostic for TPC gas-condition changes
- ➔ **Share my experience** with Zhenyu Ye and Bade Sayki who use similar method to calibrate drift velocity based on tracking detector

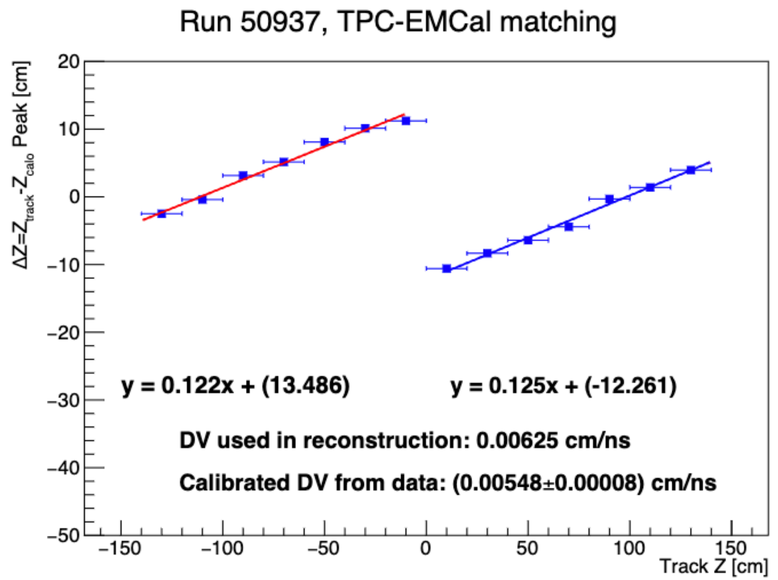

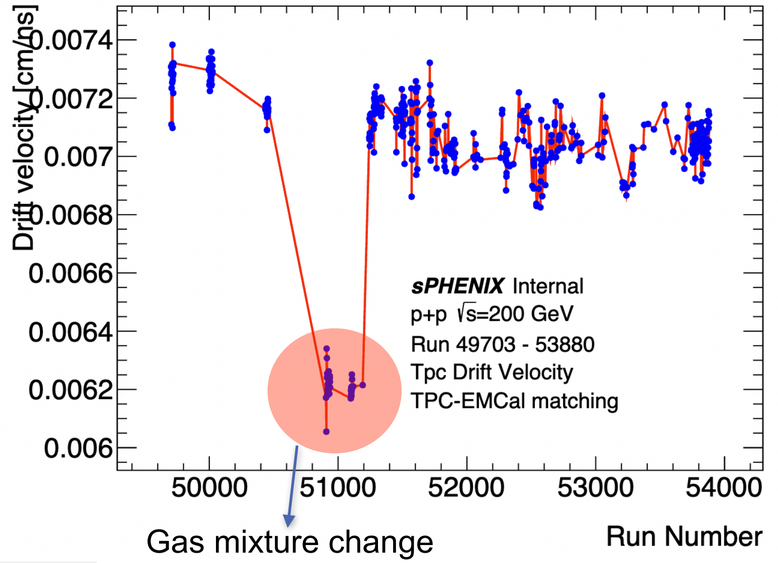

Tracking calibration — TPC distortion correction

➔ **Distortion correction** is the most complex calibration for TPC

- ❖ Static (ExB), Module edge, Space charge (time average), Fluctuation distortions
- ❖ The expected precision of tracking reconstruction can not be achieved without a good distortion correction!
- ❖ Precise tracking is essential for Λ_c^+, D^0 and quarkonia reconstruction

➔ Two complementary approaches for **space-charge distortion correction**: Diffuse lasers & track-based

- ❖ Need both methods: diffuse lasers for azimuthal and track-based for z + extrapolation
- ❖ Collaborated with Hugo, Ben and other folks in TF

Diffuse lasers

👍 Full azimuthal coverage

👎 No z dependence (only at CM)

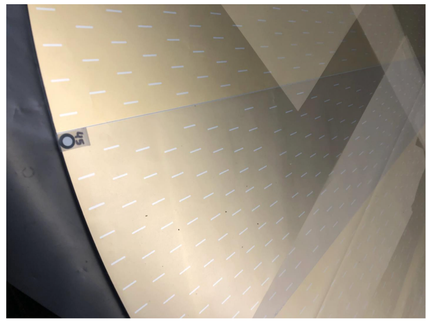

Contributing role

Track-based (TPOT)

👎 Only in TPOT sectors

👍 Provide z dependence

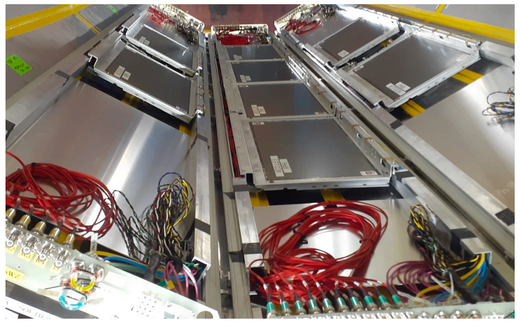

Leading role

Tracking calibration — Track-based distortion correction

➔ Big picture: construct Silicon-TPOT track, interpolate track parameters to TPC layers, correct TPC cluster position according to the residuals

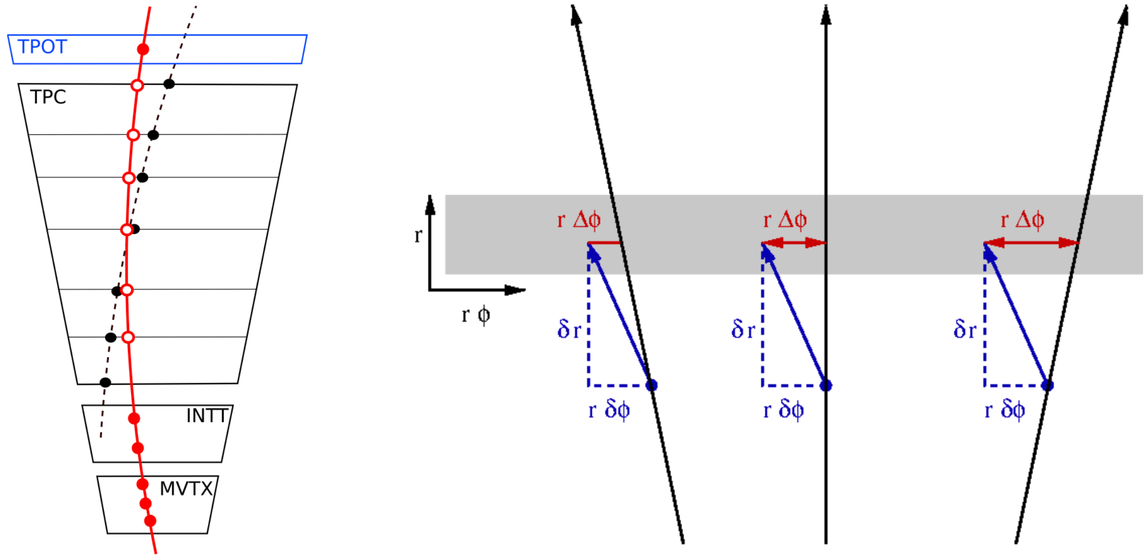

$$\chi^2 = \sum_{\text{tracks}} \sum_{\text{clusters}} \frac{[r\Delta\phi - (r\delta\phi + \delta r \tan\alpha)]^2}{\sigma^2_{r\phi}} + \frac{[\Delta z - (\delta z + \delta r \tan\beta)^2]^2}{\sigma^2_z}$$

$$\begin{pmatrix} \sum_{cl,tr} \frac{1}{\sigma^2_{r\phi}} & 0 & \sum_{cl,tr} \frac{\tan\alpha}{\sigma^2_{r\phi}} \\ 0 & \sum_{cl,tr} \frac{1}{\sigma^2_z} & \sum_{cl,tr} \frac{\tan\beta}{\sigma^2_z} \\ \sum_{cl,tr} \frac{\tan\alpha}{\sigma^2_{r\phi}} & \sum_{cl,tr} \frac{\tan\beta}{\sigma^2_z} & \sum_{cl,tr} \frac{\tan^2\alpha}{\sigma^2_{r\phi}} + \frac{\tan^2\beta}{\sigma^2_z} \end{pmatrix} \cdot \begin{pmatrix} r\delta\phi \\ \delta z \\ \delta r \end{pmatrix} = \begin{pmatrix} \sum_{cl,tr} \frac{r\Delta\phi}{\sigma^2_{r\phi}} \\ \sum_{cl,tr} \frac{\Delta z}{\sigma^2_z} \\ \sum_{cl,tr} \frac{r\Delta\phi\cdot\tan\alpha}{\sigma^2_{r\phi}} + \frac{\Delta z\cdot\tan\beta}{\sigma^2_z} \end{pmatrix}$$

➔ Distortions are 3D, but we can only measure $r\Delta\phi$ and Δz (only r info is layer number)

➔ Radial distortions affect how the residuals vary as a function of track angle

➔ In the (r, ϕ) plane, for a non zero δr distortion there is a linear relation between the measured residual $r\Delta\phi$ and the track angle α: $r\Delta\phi = r\delta\phi + \delta r \cdot \tan\alpha$

- ❖ The same in the (r, z) plane: $\Delta z = \delta z + \delta r \cdot \tan\beta$

➔ Construct matrix to transform true distortions to measured ones and invert

Difficulty: distortion is always correlated with alignment, drift velocity calibration, matching, … ***I will show two examples***

Track-based distortion correction — example 1

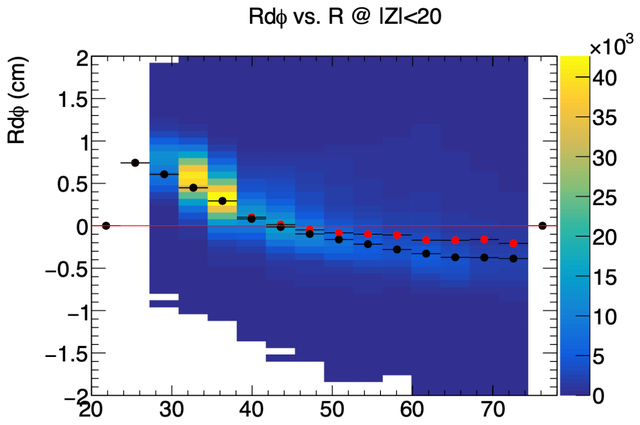

Black: fit to main peak
Red: fit to full region

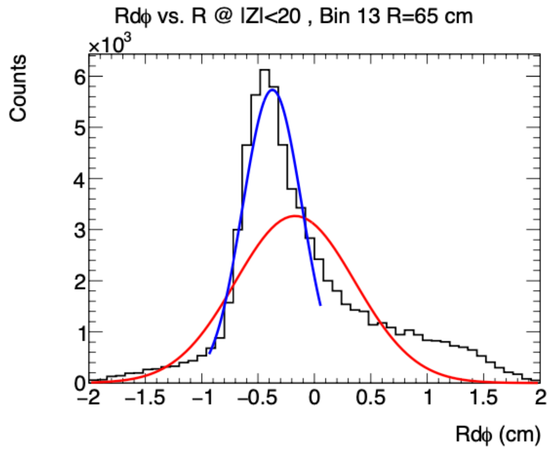

Tune Silicon-TPC window
Develop an iterative track fit strategy

- New workflow

1. Average distortion correction on (CDB)
2. Match Si-TPC with tighter window
3. Match TPC-TPOT with tighter window
4. Acts full track fit
5. Track cleaner choose best Si-TPC matches

1. Self-defined TrackPruner module: select good full tracks with pt/quality/nclusters/nstates cuts
2. Make a pruned SvtxTrackSeedContainer to contain SvtxTrackSeed of good full tracks

1. Perform Si-TPOT fit using Acts with pruned SvtxTrackSeedContainer
2. Disable average distortion correction in PHTpcResiduals module, propagate track parameters to TPC layers and calculate residuals

1. Disable distortion correction in QA module
2. Do QA evaluation

Some modifications on PHActsTrkFitter, TpcGlobalPositionWrapper and PHTpcResiduals modules needed, can make PR afterwards

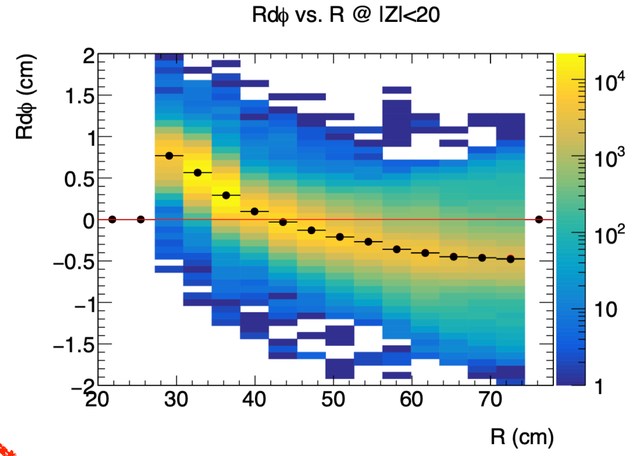

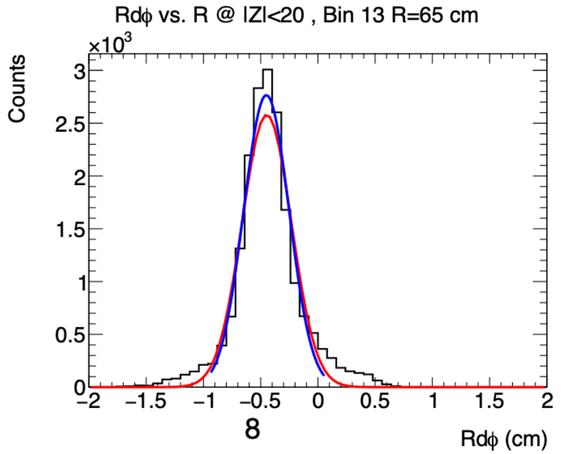

Track-based distortion correction — example 2

Old TPOT alignment

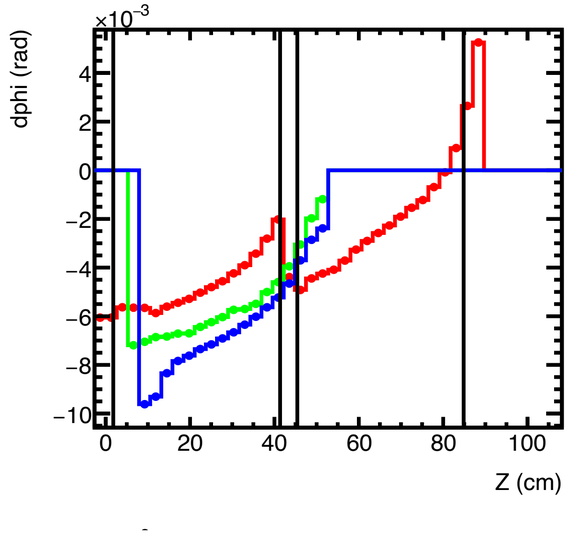

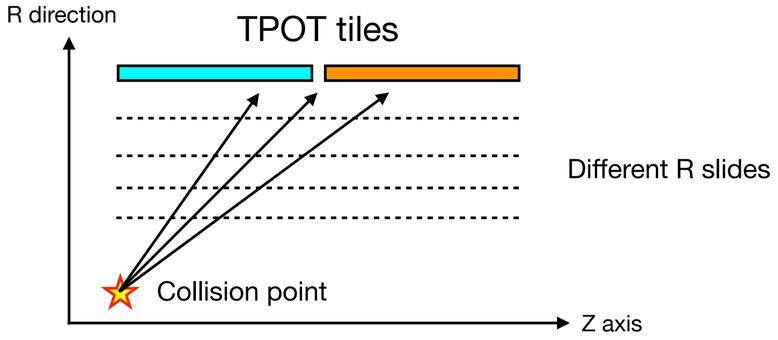

Relative phi misalignment between NCI and NCO tiles

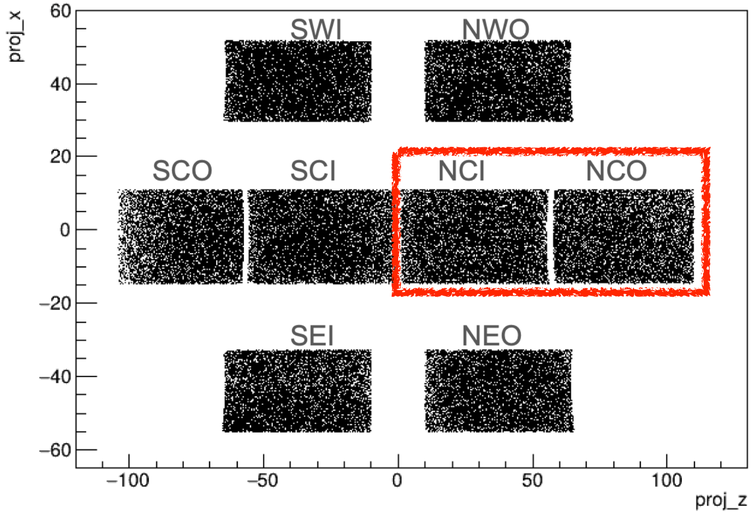

New TPOT alignment

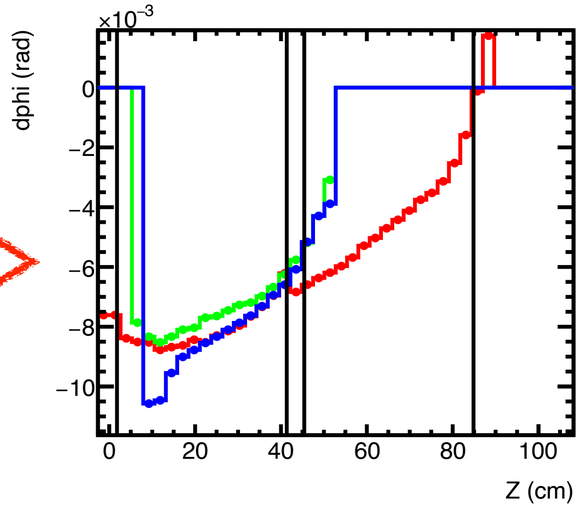

Run 53877, R = 65 cm

Central tiles

West tiles

East tiles

Track-based distortion correction — status

Closure test

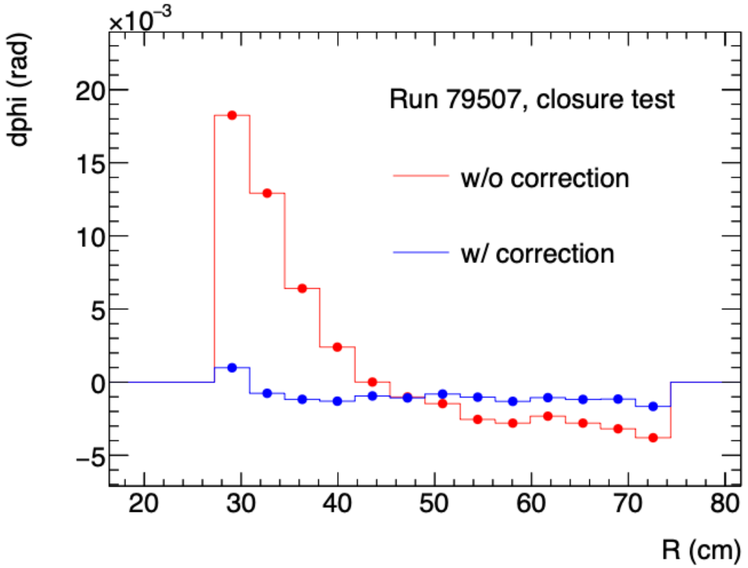

Luminosity dependent

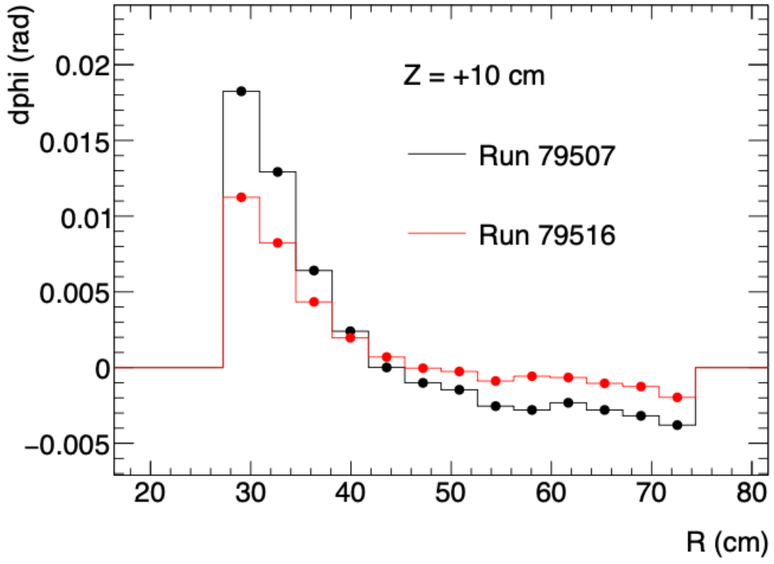

Improvement on track quality

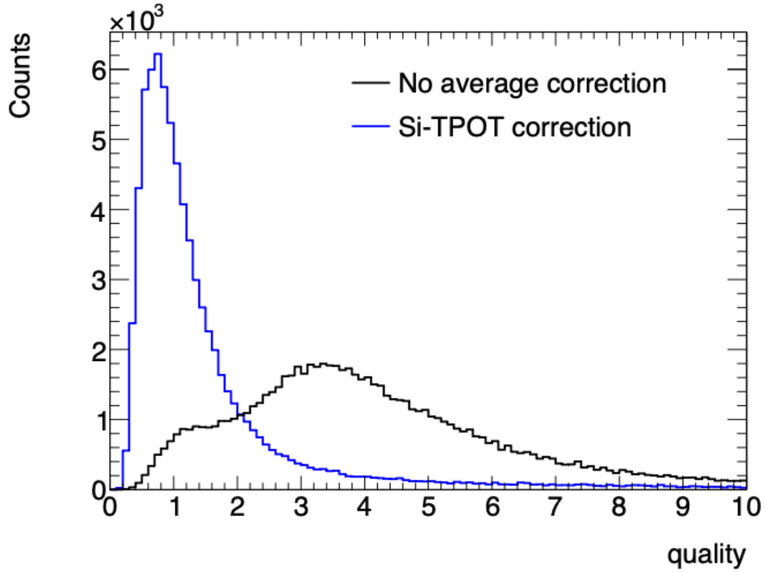

Track-based distortion correction — crossing point method

➔ **New method for sPHENIX!**

- ❖ Learnt from sPHENIX-ALICE Frankfult meeting

➔ The difference between cluster position and crossing point position is the real distortion!

- ❖ In an ideal case, if two tracks cross at the same point (in space not time), at that point, the distortion effect to the electron generated at that crossing point, the corresponding measured cluster positions will be the same
- ❖ Advantage compared to matrix inversion: decorrelate $\delta\phi$ and δr / δz and δr

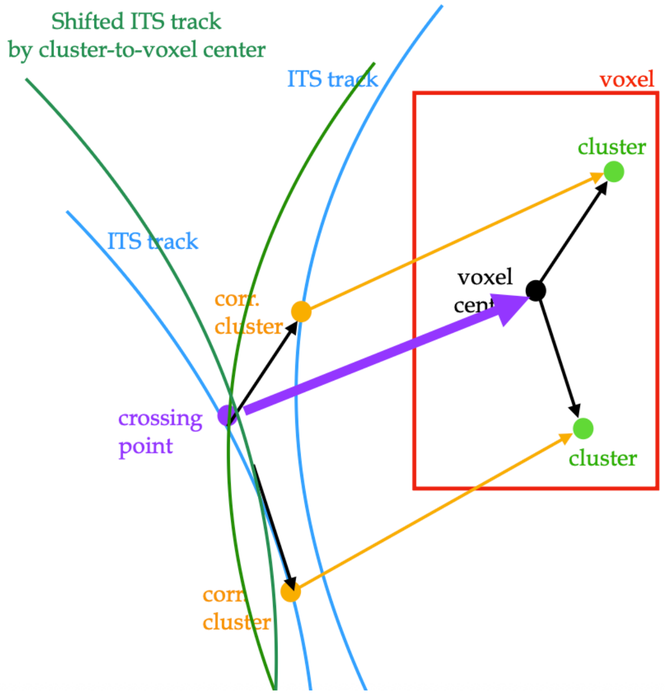

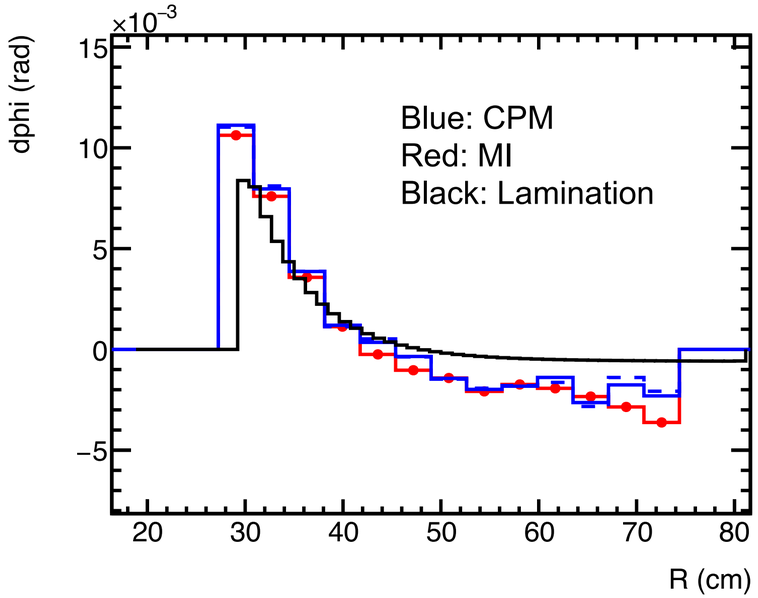

My sPHENIX Contributions

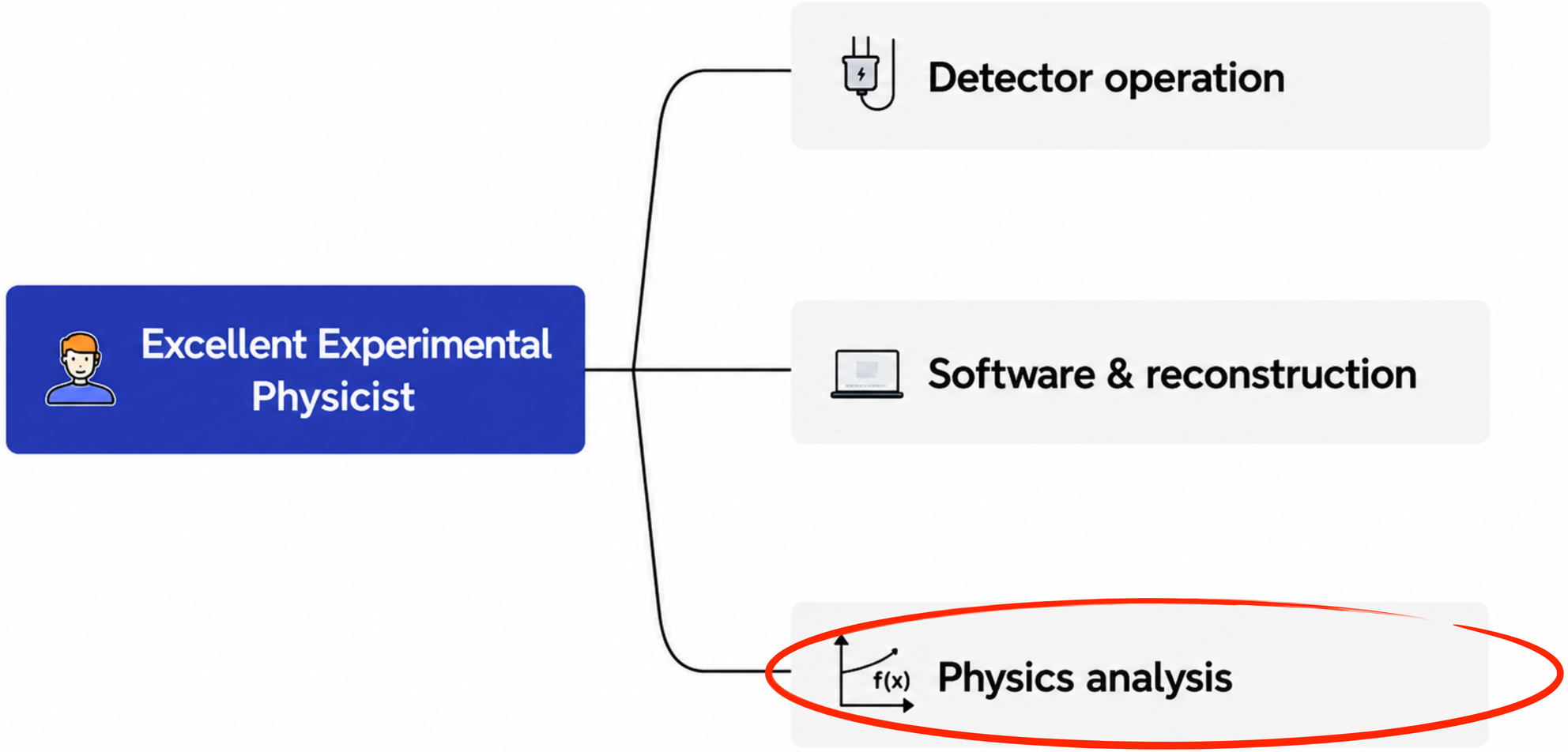

1.Conversion photon
2.Light/heavy flavor

sPHENIX Physics Program

Jet

Vary momentum and angular scale of probe

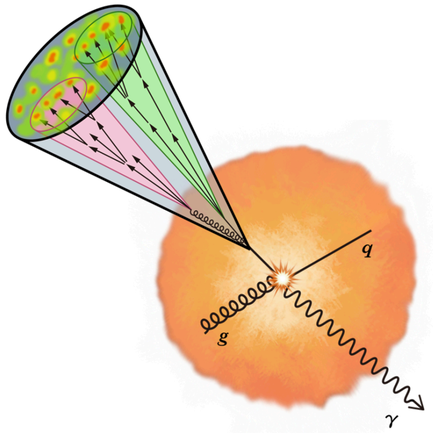

Open Heavy Flavor

Vary mass and momentum of probe

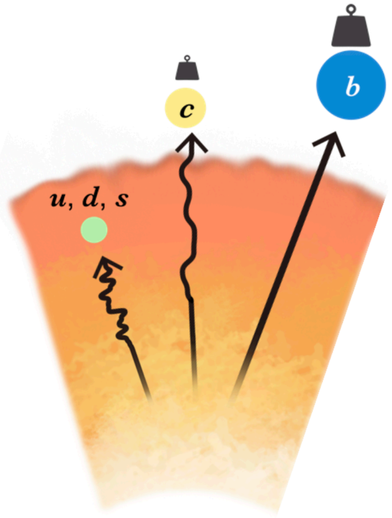

Quarkonia

Vary size of probe

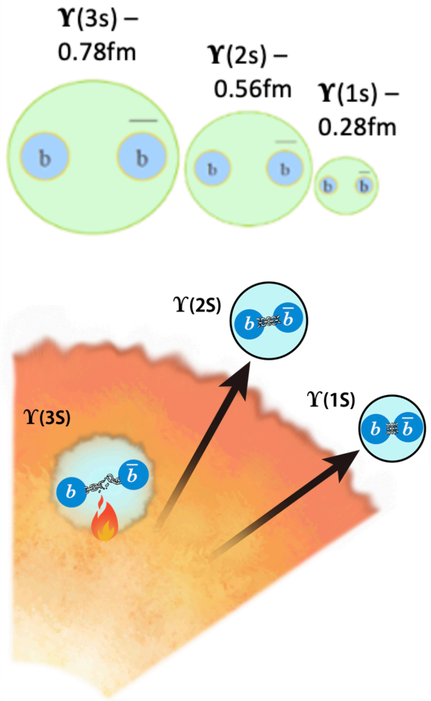

Cold QCD

Vary temperature of QCD matter
Study proton spin, dynamics, and cold nuclear effects

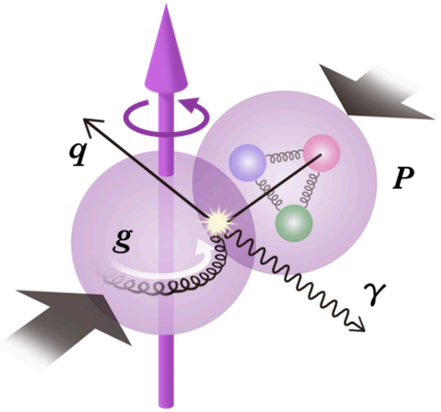

Bulk

Global and collective properties of medium

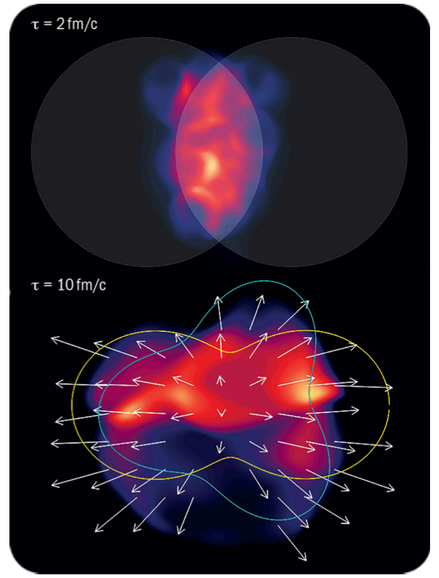

Heavy flavor probe

- Heavy quarks (charm and bottom) are ideal probes for Quark Gluon Plasma (QGP)
  - $m_{\mathrm{b,c}} \gg \Lambda_{\mathrm{QCD}}, T_{\mathrm{QCD}}$
  - Heavy quarks are produced via hard scattering in the initial stage of the collisions (~0.1 fm/c)
  - Nearly no thermal production, experience the whole evolution of QGP
  - Production rate can be calculated by pQCD
- Heavy quarks interact with QGP
  - Energy loss:
    - Radiative: Loss of energy via inelastic $Q \rightarrow Qg$ process. (Higher energy)
    - Collisional: Transfer energy via elastic $Qq \rightarrow Qq$ process. (Lower energy)
    - Observables: Nuclear modification factor R_{AA}
  - Flow development:
    - Interaction with the flowing QGP, heavy quarks can partially thermalize and exhibit collective motion.
    - Sensitive to initial state geometry and its fluctuations
    - Observables: Elliptic flow v_2

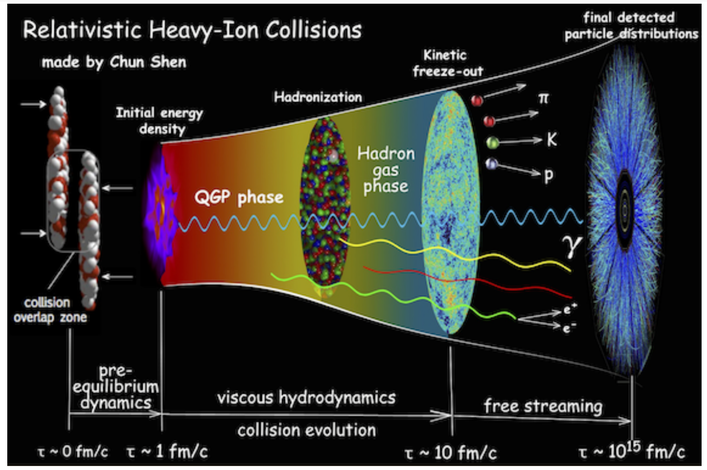

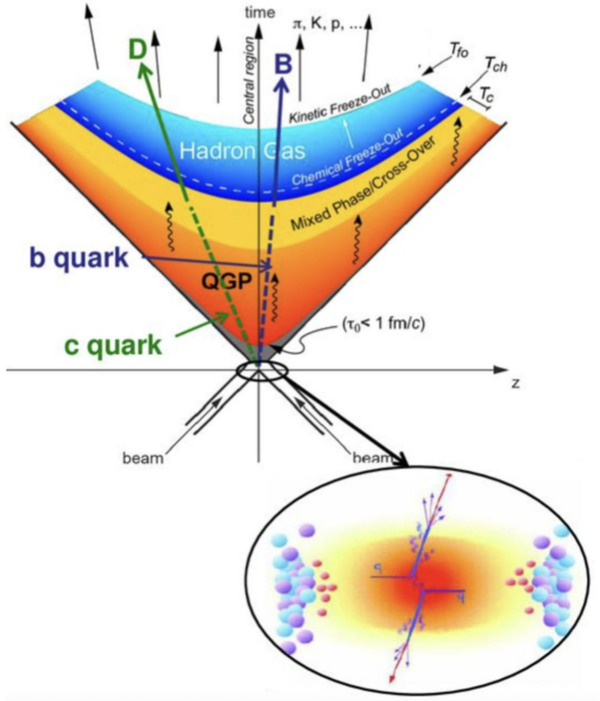

Heavy quark hadronization

- ➔ How quarks combine to form hadrons is a non-perturbative process
- ➔ In simpler collision systems (e^+e^-, ep), hadronization is described by fragmentation functions
  - ❖ Fragmentation functions are assumed to be universal, independent of the collision system and energy
- ➔ Universality break down?
  - ❖ In p+p, and A+A collisions at LHC and RHIC, the measured Λ_c/D^0 ratio is significantly higher than prediction based on fragmentation functions extracted from e^+e^- data
- ➔ New hadronization mechanisms are proposed to explain the enhancement
  - ❖ Color reconnection, Statistical hadronization, Coalescence
- ➔ New measurements will be delivered by sPHENIX in p+p and Au+Au

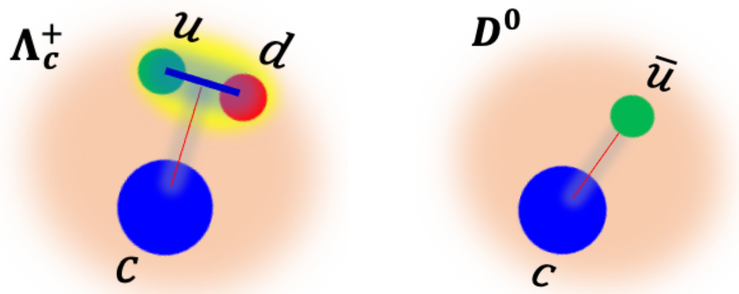

STAR, PRL 124, (2020) 172301

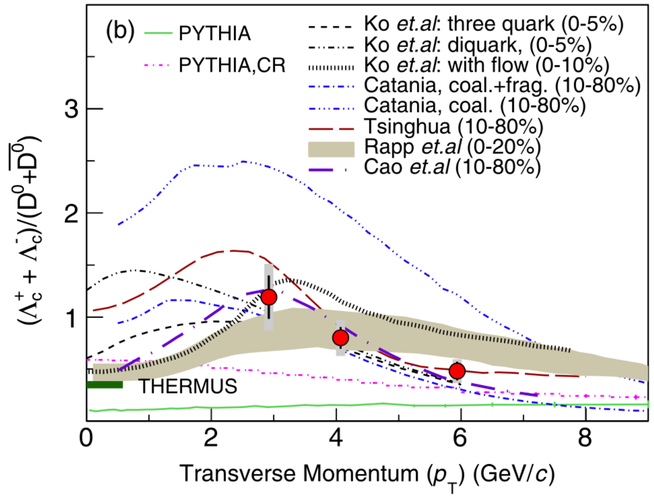

Physics analysis — conversion photon analysis

➔ Motivation for conversion photon analysis

- ❖ Lightest di-electron and with highest cross section.
- ❖ Start point for quarkonia analysis.
- ❖ Check for electron tracking, and use whole EMCal acceptance to cross check TPC distoration correction to mm level precision
- ❖ Validating KFParticle with data
- ❖ High purity electron track to study EMCal, such as position dependent non-uniformity
- ❖ Material thickness scan in sPHENIX

➔ Track-calo matching

- ❖ $-0.02 < \Delta\phi < 0.05\,\mathrm{rad}$ for electron
  $0 < \Delta\phi < 0.07\,\mathrm{rad}$ for positron
- ❖ $-5 < \Delta z < 5\,\mathrm{cm}$
- ❖ Require $\Delta\eta \in (-0.02, 0.02)$ & $\Delta\phi \in (-0.02, 0.02)\,\mathrm{rad}$ to suppress background for dielectron

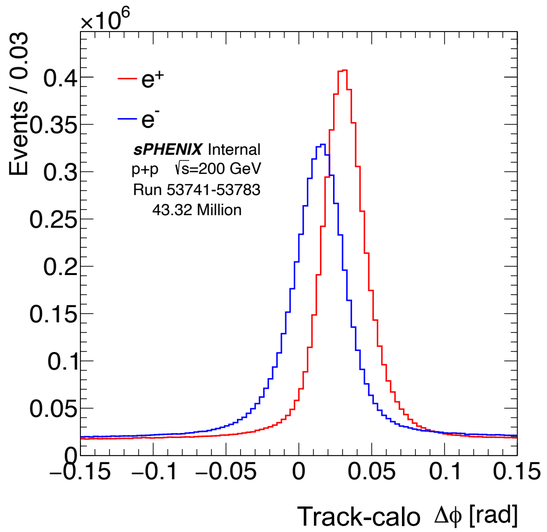

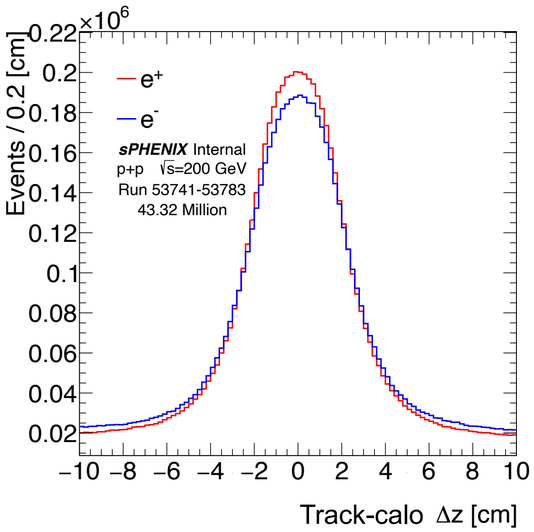

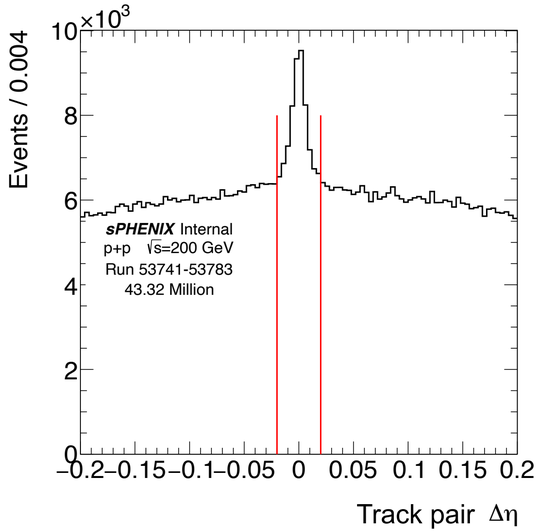

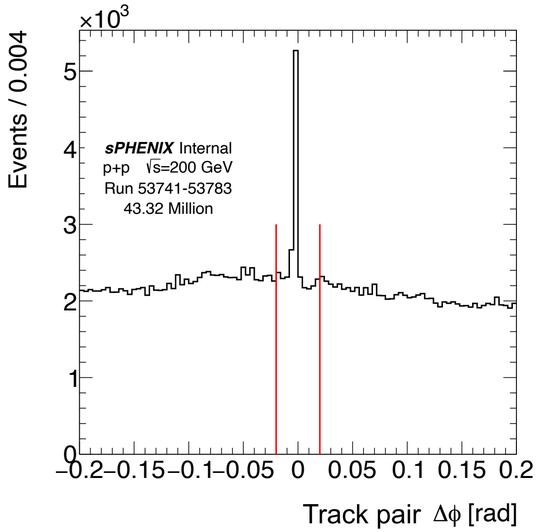

Physics analysis — conversion photon analysis

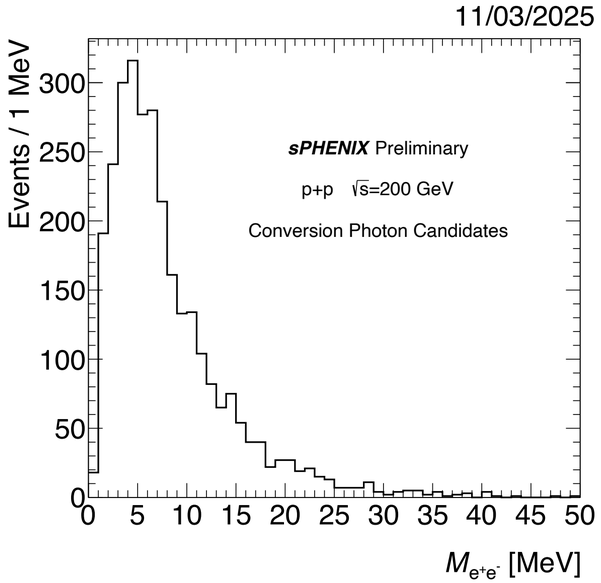

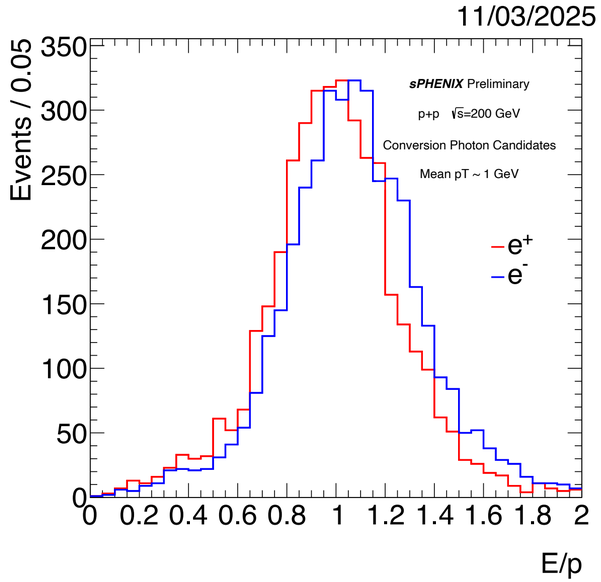

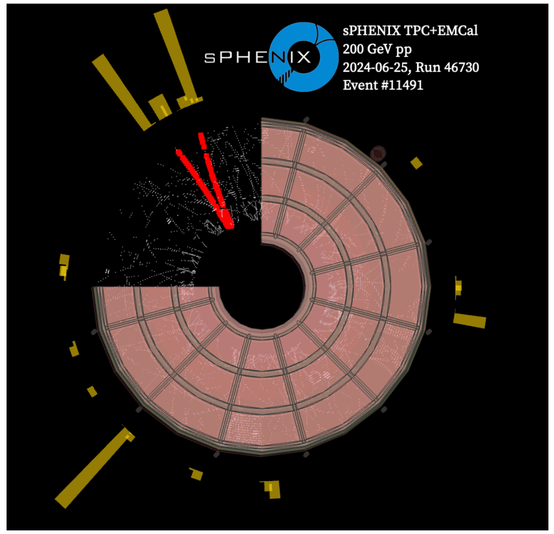

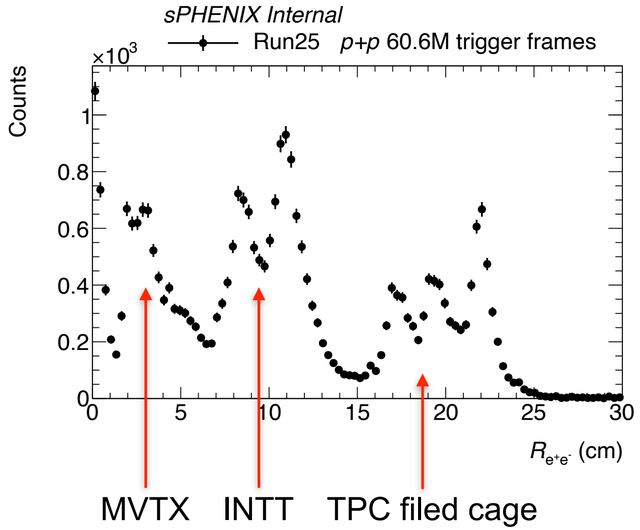

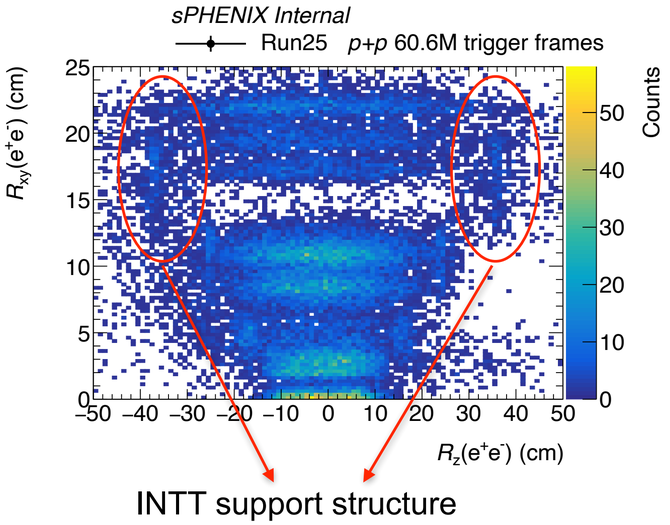

Physics analysis — conversion photon analysis

Negative E/p mean

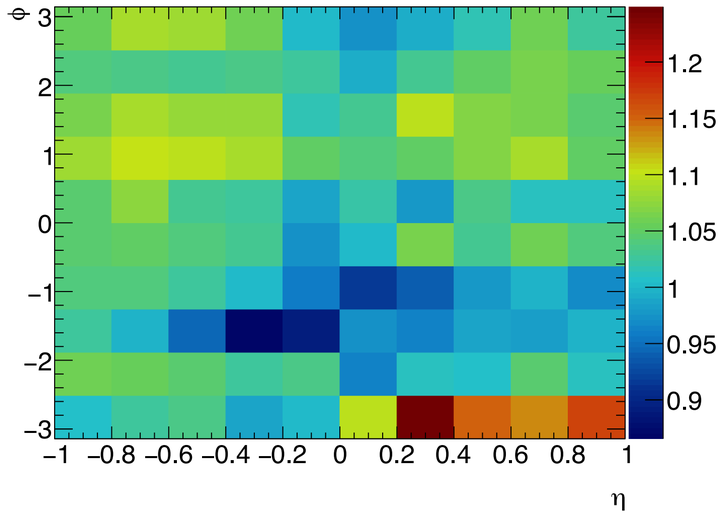

Positive E/p mean

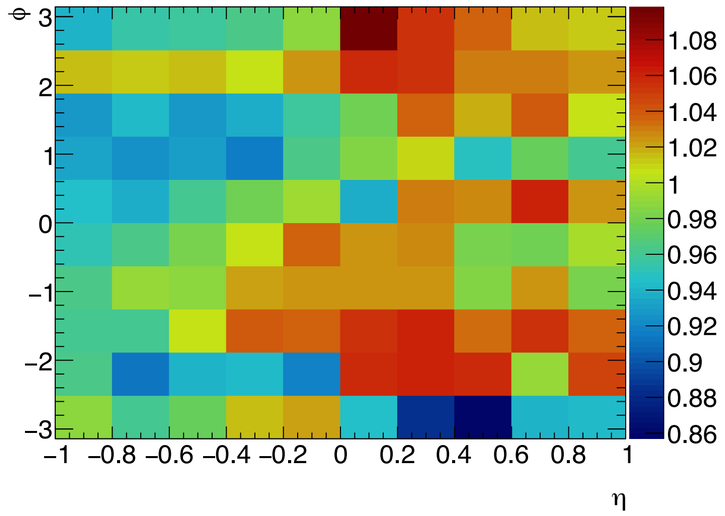

Negative/Positive E/p

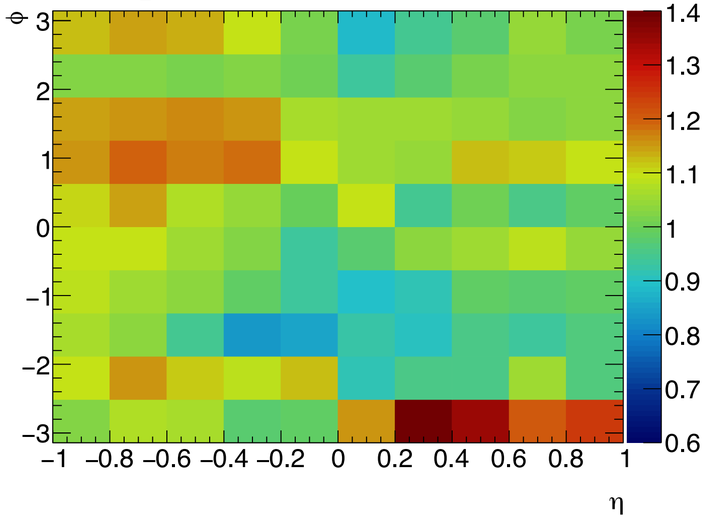

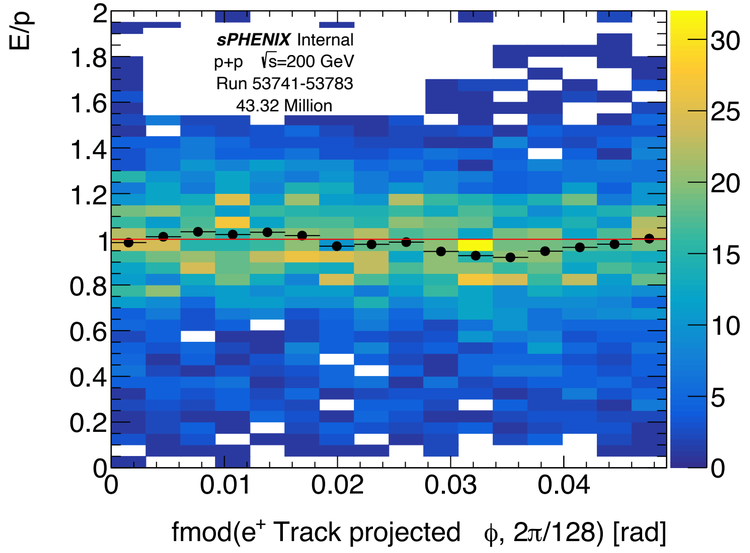

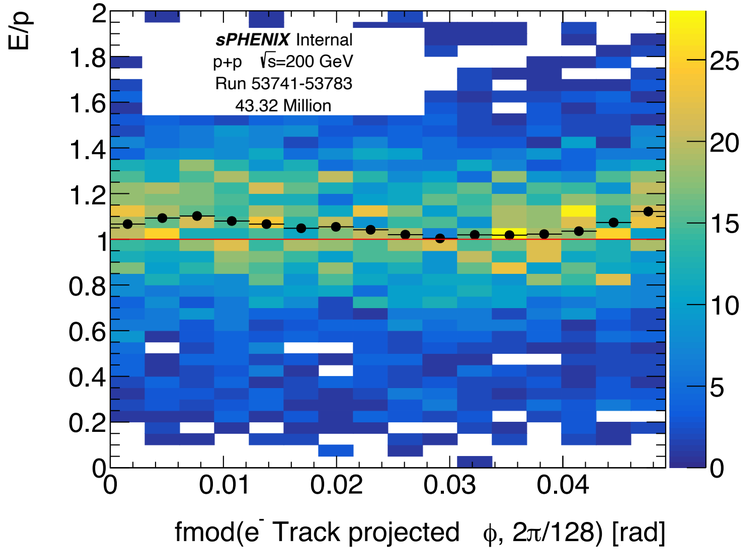

- Very useful calibration candle analysis
- First look at EMCal positional dependent non-uniformity

Top: Momentum scale study
Bottom: EMCal positional dependent non-uniformity

Physics analysis — light/heavy flavor reconstruction

- ➔ **First** D^0 invariant mass peak in sPHENIX!
- ➔ **First** measurement of Λ_c^+ at ~ 3σ confidence level in p+p at RHIC!
- ➔ Deeply involved in Heavy flavor/Quarkonium TG
  - ❖ Serve as TG production coordinator for QM2025 and IS2025 campaign
  - ❖ Contribute on first Λ_c^+/D^0 invariant mass plot and some other light flavor reconstructions
- ➔ Familiar with ***KFParticle*** tools, made some PRs to improve it

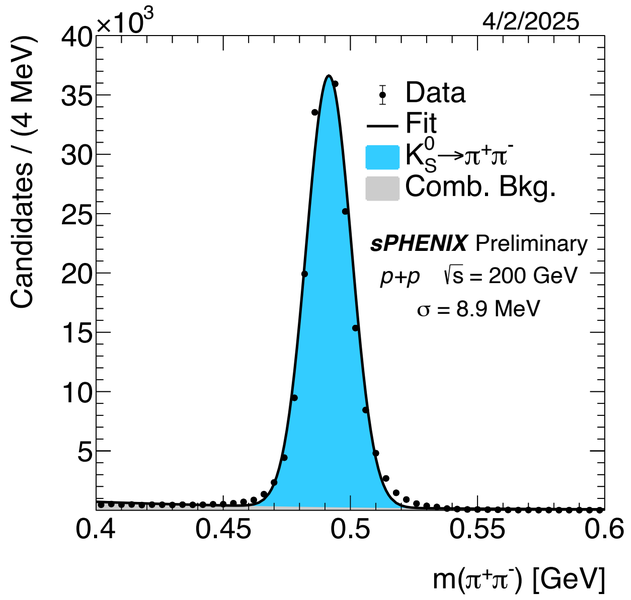

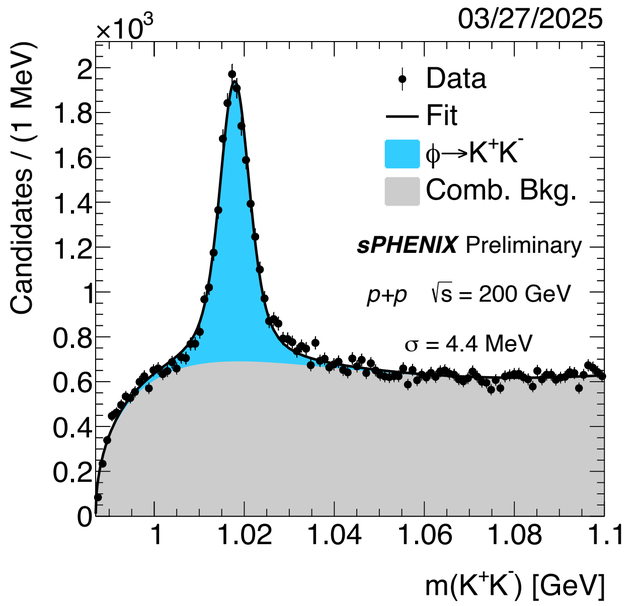

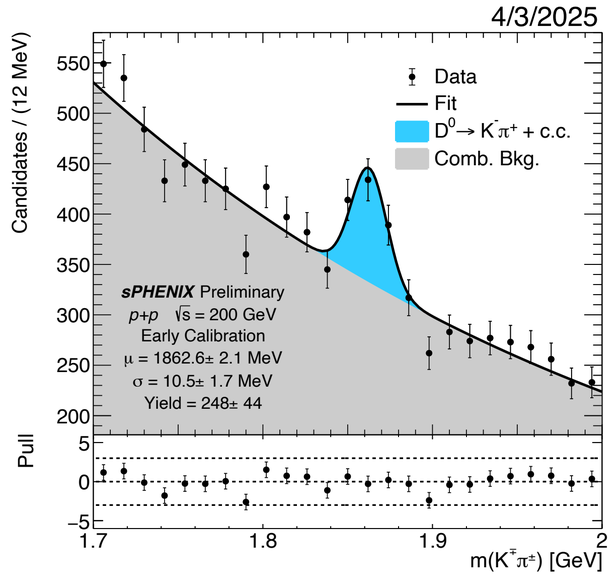

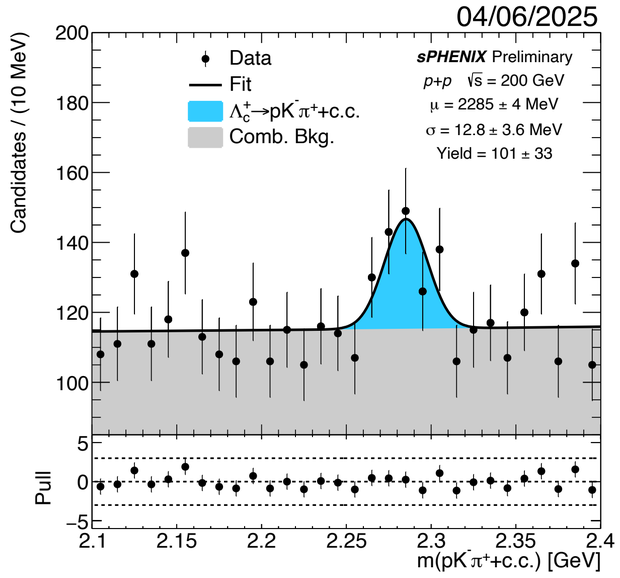

Summary

Summary & Future Plan

Stony Brook University

➔ Explore charm hadronic physics from BESIII to sPHENIX

- ❖ BESIII: studied Λ_c^+ decays to probe decay mechanisms and intermediate resonances
- ❖ sPHENIX: contributed to detector operation, offline tracking calibration, and early heavy-flavor analyses

➔ Research interests

- ❖ Heavy-flavor probes of QCD: Λ_c^+/D^0 ratio, J/ψ, Υ, hadronization, QGP, …
- ❖ AI/ML applications in high-energy and nuclear physics: generative, classification, foundation model, …

➔ Future plan

	Near term	Mid term	Long term
Phys-driven	Continue sPHENIX tracking calibration	Perform heavy-flavor analyses with sPHENIX data	Connect sPHENIX measurements with results from other experiments
Tech-driven	Validate AI methods with simulation	Apply AI models to real experimental data	Explore a cross-experiment general-purpose AI model for HEP/NP

Thanks for your attention!

Backup

Publication list

- ➔ Observation of $\Lambda_c^+ \to \Lambda a_0(980)^+$ and Evidence for $\Sigma(1380)^+$ in $\Lambda_c^+ \to \Lambda\pi^+\eta$
  - ❖ Published in *Phys. Rev. Lett.* ***134*** *(2025) 021901.*
- ➔ Observation of $\Lambda_c^+ \to n\pi^+\eta$ and search for $\Lambda_c^+ \to n a_0(980)^+$
  - ❖ arXiv: 2603.28232, submitted to JHEP
- ➔ Measurement of branching fractions of singly Cabibbo-suppressed decays $\Lambda_c^+ \to \Sigma^0 K^+$ and $\Lambda_c^+ \to \Sigma^+ K_S^0$
  - ❖ Published in *Phys. Rev. D* ***106*** *(2022) 052003.*
- ➔ Proposed Peking University muon experiment for muon tomography and dark matter search
  - ❖ Published in *Phys. Rev. D* ***110*** *(2024) 016017.*
- ➔ Search for the semi-leptonic decays $\Lambda_c^+ \to \Lambda\pi^+\pi^- e^+\nu_e$ and $\Lambda_c^+ \to p K_S^0 \pi^- e^+\nu_e$
  - ❖ Published in *Phys. Lett. B* ***843*** *(2023) 137993.*

Partial Wave Analysis — Helicity amplitude formula

➔ Isobar assumption：multi-body decay is described by cascade two-body decays

$$A^{0\to1+2}_{\lambda_0,\lambda_1,\lambda_2} = H^{0\to1+2}_{\lambda_1,\lambda_2} D^{J_0*}_{\lambda_0,\lambda_1-\lambda_2}(\phi,\theta,0) \qquad H^{0\to1+2}_{\lambda_1,\lambda_2} = \sum_{ls} g_{ls} \sqrt{\frac{2l+1}{2J_0+1}} \langle l,0;s,\delta|J_0,\delta\rangle \langle J_1,\lambda_1;J_2,-\lambda_2|s,\delta\rangle \left(\frac{q}{q_0}\right)^l B'_l(q,q_0,d)$$

Helicity coupling　Wigner-D matrix　　Partial wave amplitude　　CG coefficient　　Blatt-Weiskopf barrier factor

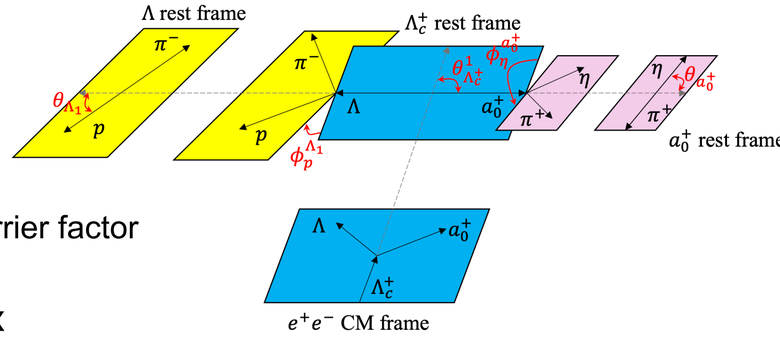

➔ Amplitude is constructed from e^+e^- collisions，Λ_c^+ polarization is considered by spin density matrix

❖ Fixed to measured α_0 and Δ_0 of $e^+e^- \to \Lambda_c^+\bar{\Lambda}_c^-$ process

$$\rho = \frac{1}{2}(\mathbb{I} + \boldsymbol{P}\cdot\boldsymbol{\sigma}) = \frac{1}{2}\begin{pmatrix} 1+P_z & P_x - iP_y \\ P_x + iP_y & 1-P_z \end{pmatrix}$$

$$\alpha_0 = \frac{|H^{e^+e^-\to\Lambda_c^+\bar{\Lambda}_c^-}_{\frac{1}{2},-\frac{1}{2}}|^2 - 2|H^{e^+e^-\to\Lambda_c^+\bar{\Lambda}_c^-}_{\frac{1}{2},\frac{1}{2}}|^2}{|H^{e^+e^-\to\Lambda_c^+\bar{\Lambda}_c^-}_{\frac{1}{2},-\frac{1}{2}}|^2 + 2|H^{e^+e^-\to\Lambda_c^+\bar{\Lambda}_c^-}_{\frac{1}{2},\frac{1}{2}}|^2},$$

$$P_z = P_x = 0, P_y(\theta_{ee},\alpha_0,\Delta_0) \propto \sqrt{1-\alpha_0^2}\sin\theta_{ee}\cos\theta_{ee}\sin\Delta_0 \qquad \Delta_0 = \arg(H^{e^+e^-\to\Lambda_c^+\bar{\Lambda}_c^-}_{\frac{1}{2},-\frac{1}{2}}) - \arg(H^{e^+e^-\to\Lambda_c^+\bar{\Lambda}_c^-}_{\frac{1}{2},\frac{1}{2}})$$

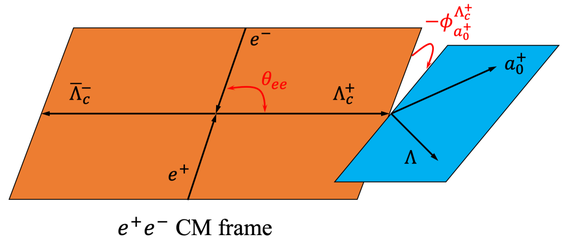

➔ Intermediate propagator

❖ $a_0(980)^+$: Flatté

❖ Λ^*/Σ^*: Breit-Wigner

❖ Non-resonant: 1

$$A^{a_0^+}_{\lambda_{\Lambda_c^+},\lambda_p} = \sum_{\lambda_\Lambda} A^{\Lambda_c^+\to a_0^+\Lambda}_{\lambda_{\Lambda_c^+},0,\lambda_\Lambda} R_{a_0^+}(M_{\pi^+\eta}) A^{a_0^+\to\pi^+\eta}_{0,0,0} A^{\Lambda\to p\pi^-}_{\lambda_\Lambda,\lambda_p,0}$$

$$\mathscr{A}_{\lambda_{\Lambda_c^+},\lambda_p} = \left(A^{a_0^+}_{\lambda_{\Lambda_c^+},\lambda_p} + A^{NR}_{\lambda_{\Lambda_c^+},\lambda_p}\right) + \sum_{\lambda'_p} A^{\Sigma^{*+}}_{\lambda_{\Lambda_c^+},\lambda'_p} D^{1/2}_{\lambda'_p,\lambda_p}(\alpha_p,\beta_p,\gamma_p) + \sum_{\lambda'_p} A^{\Lambda^*}_{\lambda_{\Lambda_c^+},\lambda'_p} D^{1/2}_{\lambda'_p,\lambda_p}(\alpha'_p,\beta'_p,\gamma'_p)$$

➔ Total amplitude is the superposition of different intermediate state amplitude (considering alignment angle)

➔ Redundant degree of freedom in $\Lambda \to p\pi^-$ decay, fix amplitude according to input α_Λ

$$\alpha_\Lambda = \frac{\left|H^{\Lambda\to\pi^-p}_{0,\frac{1}{2}}\right|^2 - \left|H^{\Lambda\to\pi^-p}_{0,-\frac{1}{2}}\right|^2}{\left|H^{\Lambda\to\pi^-p}_{0,\frac{1}{2}}\right|^2 + \left|H^{\Lambda\to\pi^-p}_{0,-\frac{1}{2}}\right|^2} = \frac{2\Re\left(g^{\Lambda\to\pi^-p}_{0,\frac{1}{2}} \cdot g^{\Lambda\to\pi^-p*}_{1,\frac{1}{2}}\right)}{\left|g^{\Lambda\to\pi^-p}_{0,\frac{1}{2}}\right|^2 + \left|g^{\Lambda\to\pi^-p}_{1,\frac{1}{2}}\right|^2}$$

Partial Wave Analysis — fitting method and physical quantities

➔ Construct Probability Density Function (PDF) according to amplitue

$$P(p_j) = \frac{\varepsilon(p_j)|\mathscr{A}(p_j)|^2 R_5(p_j)}{\int \varepsilon(p_j)|\mathscr{A}(p_j)|^2 R_5(p_j)\mathrm{d}p_j}$$

❖ Normalization using PHSP MC with detection efficiency effect

➔ Background is considered by sWeight factor in the Negative Log Likelihood (NLL)

$$-\ln L = -\alpha \sum_{i\in\text{data}} w_i \ln P(p^i) \qquad \alpha = \frac{\sum_{i\in\text{data}} w_i}{\sum_{i\in\text{data}} w_i^2}$$

$$P(p) = \frac{|\mathscr{A}(p)|^2}{\sum_{i\in\text{PHSP}} |\mathscr{A}(p^i)|^2}$$

➔ **Fit Fraction** (FF) is calculated by using PHSP MC without detection efficiency effect

$$\mathrm{FF}_i = \frac{\int |\mathscr{A}_i|^2 R_5(p)\mathrm{d}p}{\int |\sum_k \mathscr{A}_k|^2 R_5(p)\mathrm{d}p} \approx \frac{\sum_{j\in\text{PHSP}} |\mathscr{A}_i(p^j)|^2}{\sum_{j\in\text{PHSP}} |\sum_k \mathscr{A}_k(p^j)|^2} \qquad \mathrm{FF}_{i,j} = \frac{\int |\mathscr{A}_i + \mathscr{A}_j|^2 R_5(p)\mathrm{d}p}{\int |\sum_k \mathscr{A}_k|^2 R_5(p)\mathrm{d}p} - \mathrm{FF}_i - \mathrm{FF}_j$$

➔ **Decay asymmetry parameter** (α) is derived from amplitudes

$$\alpha_{\Lambda a_0(980)^+} = -\frac{2\Re\left(g^{\Lambda_c^+\to\Lambda a_0(980)^+}_{0,\frac{1}{2}} \cdot g^{\Lambda_c^+\to\Lambda a_0(980)^+ *}_{1,\frac{1}{2}}\right)}{\left|g^{\Lambda_c^+\to\Lambda a_0(980)^+}_{0,\frac{1}{2}}\right|^2 + \left|g^{\Lambda_c^+\to\Lambda a_0(980)^+}_{1,\frac{1}{2}}\right|^2}$$

$$\alpha_{\Sigma(1385)^+\eta} = \frac{2\Re\left(g^{\Lambda_c^+\to\eta\Sigma(1385)^+}_{1,\frac{3}{2}} \cdot g^{\Lambda_c^+\to\eta\Sigma(1385)^+ *}_{2,\frac{3}{2}}\right)}{\left|g^{\Lambda_c^+\to\eta\Sigma(1385)^+}_{1,\frac{3}{2}}\right|^2 + \left|g^{\Lambda_c^+\to\eta\Sigma(1385)^+}_{2,\frac{3}{2}}\right|^2}$$

$$\alpha_{\Lambda(1670)\pi^+} = \frac{2\Re\left(g^{\Lambda_c^+\to\pi^+\Lambda(1670)}_{0,\frac{1}{2}} \cdot g^{\Lambda_c^+\to\pi^+\Lambda(1670)*}_{1,\frac{1}{2}}\right)}{\left|g^{\Lambda_c^+\to\pi^+\Lambda(1670)}_{0,\frac{1}{2}}\right|^2 + \left|g^{\Lambda_c^+\to\pi^+\Lambda(1670)}_{1,\frac{1}{2}}\right|^2}$$

➔ Uncertainty estimation of physical quantity

❖ Direct fitted parameters: Inversion of Hessian matrix

❖ Indirect fitted parameters: error propagation

$$V_{ij} = -\left(\frac{\partial^2 \ln L}{\partial\theta_i \partial\theta_j}\right)^{-1}_{\theta=\hat{\theta}} \qquad V_f = \left[\left(\frac{\partial f(\theta)}{\partial\theta}\right)^T V \left(\frac{\partial f(\theta)}{\partial\theta}\right)\right]_{\theta=\hat{\theta}}$$

Measurement of BFs of $\Lambda_c^+ \to \Sigma^0 K^+$ and $\Sigma^+ K_S^0$

Phys. Rev. D ***106*** *(2022), 052003*

➔ Singly Cabibbo-suppressed (SCS) decays $\Lambda_c^+ \to \Sigma^0 K^+$ and $\Sigma^+ K_S^0$

$N(\Sigma^0 K^+) = 43.3 \pm 4.2$

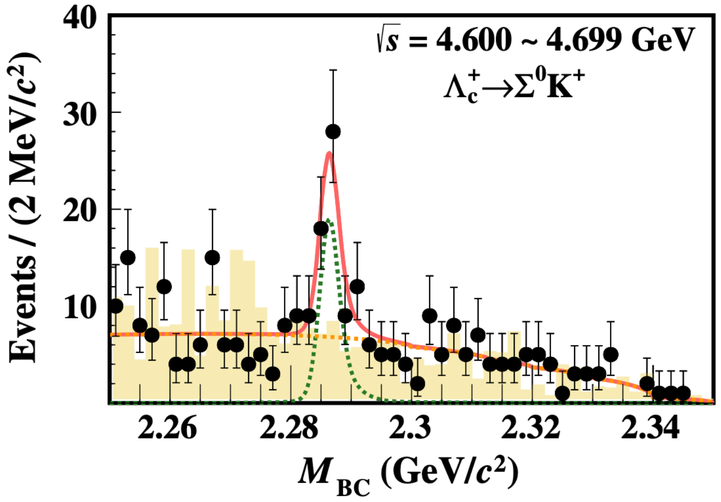

$N(\Sigma^+ K_S^0) = 43.6 \pm 6.0$

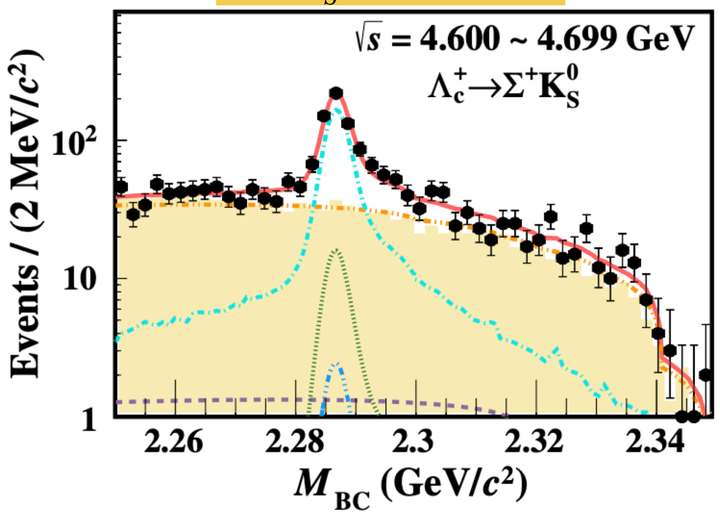

- Phenomenological model
- Model independent method — $SU(3)_F$ + global fit
- Early experimental measurements — Belle & BaBar
- ⭐ Significantly deviate from KPW theorem & $SU(3)_F$ symmetry

	$\mathcal{B}(\Lambda_c^+ \to \Sigma^0 K^+)$	$\mathcal{B}(\Lambda_c^+ \to \Sigma^+ K_S^0)$
QCD corrections [2]	2(8)	2(4)
MIT bag model [3]	7.2 ± 1.8	7.2 ± 1.8
Diagrammatic analysis [4]	5.5 ± 1.6	⭐ 9.6 ± 2.4
$SU(3)_F$ flavor symmetry [5]	5.4 ± 0.7	5.4 ± 0.7
IRA method [6]	5.0 ± 0.6	⭐ 1.0 ± 0.4
PDG 2020 [28]	5.2 ± 0.8	···

- $R = \dfrac{\mathcal{B}(\Lambda_c^+ \to \Sigma^0 K^+)}{\mathcal{B}(\Lambda_c^+ \to \Sigma^0 \pi^+)} = 0.0361 \pm 0.0073_{\text{stat.}} \pm 0.0005_{\text{syst.}}$
- $\mathcal{B}(\Lambda_c^+ \to \Sigma^0 K^+) = (4.7 \pm 0.9_{\text{stat.}} \pm 0.1_{\text{syst.}} \pm 0.3_{\text{ref.}}) \times 10^{-4}$
- Consistent and comparable with Belle and BaBar
- Consistent with $SU(3)$ flavor symmetry

- $R = \dfrac{\mathcal{B}(\Lambda_c^+ \to \Sigma^+ K_S^0)}{\mathcal{B}(\Lambda_c^+ \to \Sigma^+ \pi^+ \pi^-)} = 0.0106 \pm 0.0031_{\text{stat.}} \pm 0.0004_{\text{syst.}}$
- $\mathcal{B}(\Lambda_c^+ \to \Sigma^+ K_S^0) = (4.8 \pm 1.4_{\text{stat.}} \pm 0.2_{\text{syst.}} \pm 0.3_{\text{ref.}}) \times 10^{-4}$
- First measurement for $\Sigma^+ K_S^0$

Λ_c^+ SL decays

Phys. Lett. B ***843***, *(2023), 137993*

- Semi-leptonic (SL) decays: good platform to study weak/strong interaction and probe new physics beyond the Standard Model
- Compare meausred inclusive SL decay BF and exclusive decay BFs
  $\sim 1.4 \times 10^{-3}$ BF room for $\Lambda_c^+ \to \Lambda^*(c \to s)$ and $\Lambda_c^+ \to N^*(c \to d)$
- Search for Λ^* in $\Lambda\pi^+\pi^-$ and $pK_S^0\pi^-$ channels
  - Upper limits are reported based on profile likelihood method
  - $\mathcal{B}(\Lambda_c^+ \to \Lambda\pi^+\pi^- e^+\nu_e) < 3.9 \times 10^{-4} @ 90\%\,\mathrm{C.L.}$
  - $\mathcal{B}(\Lambda_c^+ \to pK_S^0\pi^- e^+\nu_e) < 3.3 \times 10^{-4} @ 90\%\,\mathrm{C.L.}$
- Search for N^* in $p\pi^-$ channel
  - Evidence is found in $\Lambda_c^+ \to p\pi^- e^+\nu_e$
  - Due to statistical limit, no obvious intermediate states found

$$\mathscr{H}_{\text{eff}} = \frac{G_F}{\sqrt{2}} V_{cs}^* [\bar{\nu}_e \gamma_\mu (1-\gamma_5) e][\bar{s}\gamma^\mu (1-\gamma_5) c]$$

Lepton current L_μ

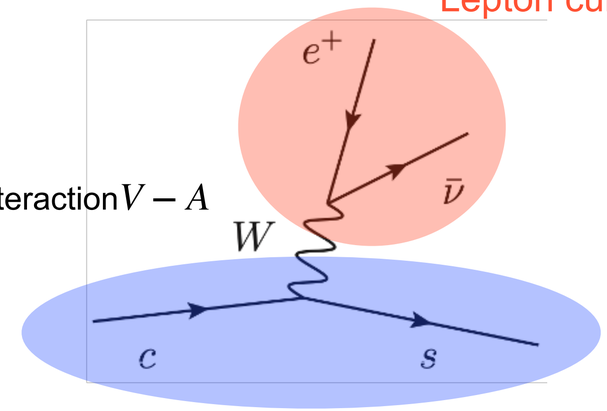

Weak interaction $V-A$

Hadronic current H^μ

$\Lambda_c^+ \to \Lambda\pi^+\pi^- e^+\nu_e$

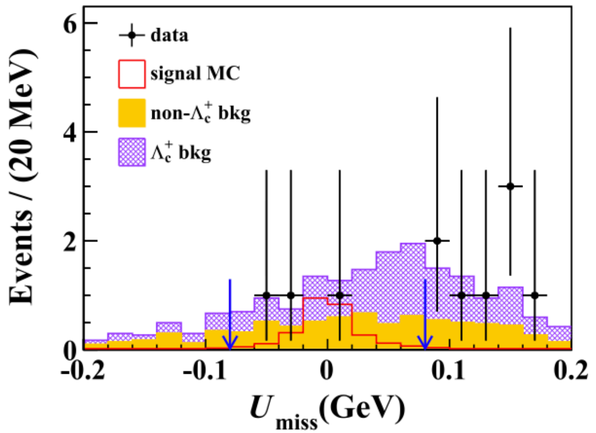

$\Lambda_c^+ \to pK_S^0\pi^- e^+\nu_e$

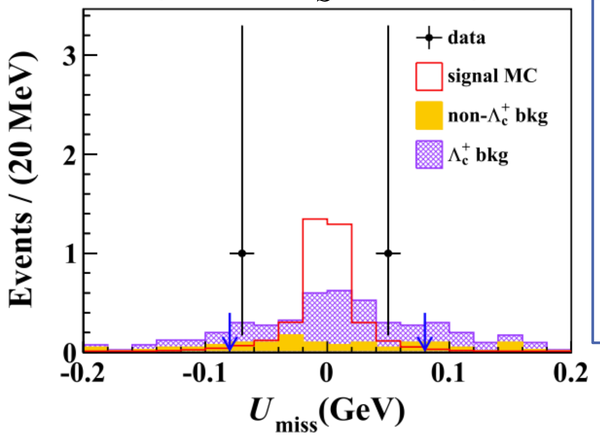

$\Lambda_c^+ \to p\pi^- e^+\nu_e$

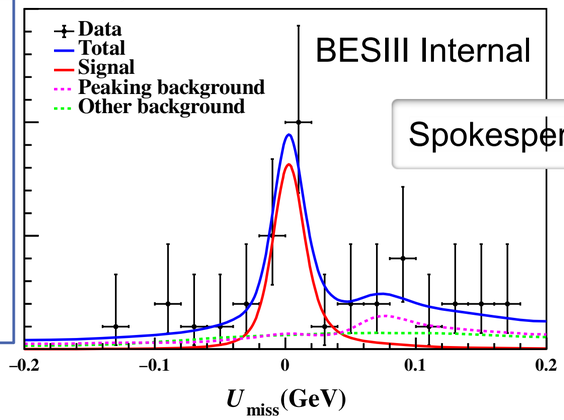

Spokesperson review stage

Jpsi QEC

Dandan Shen (SDU) @ Hot Quarks 2025

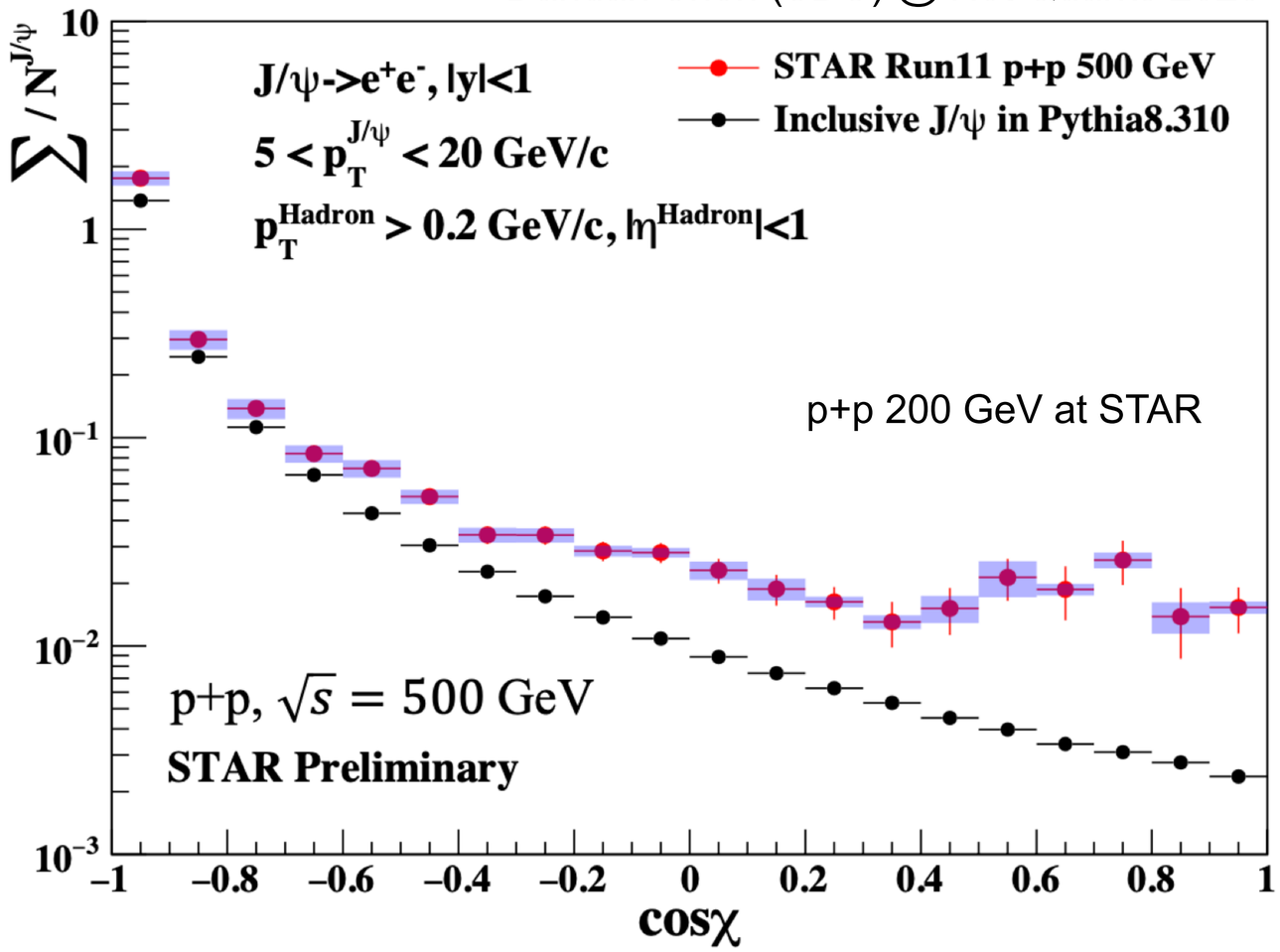

Pair production near threshold & tag method

➔ $e^+e^- \to \gamma^* \to \Lambda_c^+\bar{\Lambda}_c^-$: production without accompanying hadrons at 4.6~4.7 GeV

➔ Clean backgrounds and well constrained kinematics

- $\Delta E = E_{\Lambda_c} - E_{\rm beam}$
- $M_{\rm BC} = \sqrt{E_{\rm beam}^2/c^4 - p^2c^2}$

➔ **Single Tag (ST) method**: detect one of the $\Lambda_c^+\bar{\Lambda}_c^-$

- Relative higher background with higher efficiencies
- Full reconstruction only

➔ **Double Tag (DT) Method**: detect both of the $\Lambda_c^+\bar{\Lambda}_c^-$

- Lower background with lower efficiency
- Full or partial reconstruction (technique for missing particle: ν, n, K_L^0)
  - Reconstruct $\bar{\Lambda}_c^-$ by dominant and clean decay modes, e.g., $\bar{\Lambda}_c^- \to \bar{p}K_S^0, \bar{p}K^+\pi^-, \ldots$ with $\mathcal{B}^{\rm ST}\cdot\varepsilon^{\rm ST} \approx 8\,\%$
  - Search for Λ_c^+ signal decay in the recoiling side
- Systematic in tag side are mostly cancelled

DT BF formula

$$\mathcal{B}_{\rm sig} = \frac{\sum_{i,j} N_{\rm DT}^{i,j}}{\sum_{i,j}\left(\frac{N_{\rm ST}^{i,j}}{\epsilon_{\rm ST}^{i,j}}\cdot\epsilon_{\rm DT}^{i,j}\right)} = \frac{N_{\rm DT}}{\sum_{i,j}\left(\frac{N_{\rm ST}^{i,j}}{\epsilon_{\rm ST}^{i,j}}\cdot\epsilon_{\rm DT}^{i,j}\right)} = \frac{N_{\rm DT}}{N_{\rm ST}\cdot\epsilon^{\rm sig}},$$

$$N_{\rm ST}^{i,j} = 2N_{\Lambda_c^+\bar{\Lambda}_c^-}^{j}\mathcal{B}_{\rm tag}^{i}\epsilon_{\rm ST}^{i,j}, \qquad \epsilon^{\rm sig} = \sum_{i,j}\left(\frac{N_{\rm ST}^{i,j}}{\epsilon_{\rm ST}^{i,j}}\cdot\epsilon_{\rm DT}^{i,j}\right)\Big/\sum_{i,j}N_{\rm ST}^{i,j},$$

$$N_{\rm DT}^{i,j} = 2N_{\Lambda_c^+\bar{\Lambda}_c^-}^{j}\mathcal{B}_{\rm tag}^{i}\mathcal{B}_{\rm sig}\epsilon_{\rm DT}^{i,j}, \qquad N_{\rm ST} = \sum_{i,j}N_{\rm ST}^{i,j}$$

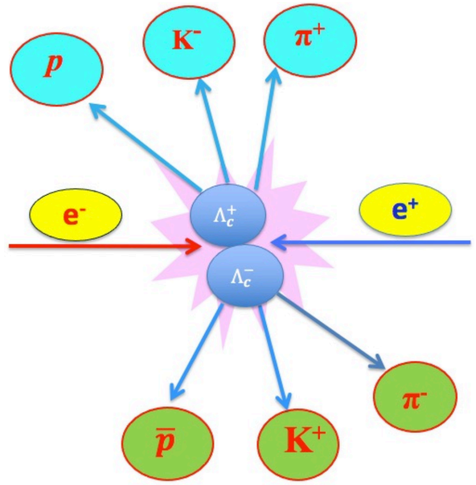

Follow-up stories…

Chia-Wei Liu highlighted our results at HFCPV2022

Chia-Wei Liu (SJTU) @ HFCPV2022

Research Motivation - Nonleptonic decays

channel	data	$SU(3)_F$	Current Algebra
$10^4\mathcal{B}(\Lambda_c^+ \to \Sigma^0 K^+)^a$	$4.7 \pm 0.9 \pm 0.1 \pm 0.3$	5.4 ± 0.7	7.2
$10^4\mathcal{B}(\Lambda_c^+ \to \Sigma^+ K_S^0)^a$	$4.8 \pm 1.4 \pm 0.2 \pm 0.3$	5.4 ± 0.7	7.2
$10^4\mathcal{B}(\Lambda_c^+ \to n\pi^+)^b$	$6.6 \pm 1.2 \pm 0.4$	8.5 ± 2.0	2.7
$\alpha(\Lambda_c^+ \to pK_S^0)^c$	$0.18 \pm 0.43 \pm 0.14$	$-0.89^{+0.26}_{-0.11}$	−0.90
$\alpha(\Lambda_c^+ \to \Lambda K^+)^d$	$-0.585 \pm 0.049 \pm 0.018$	0.32 ± 0.32	−0.96
$\alpha(\Lambda_c^+ \to \Sigma^0 K^+)^d$	$-0.55 \pm 0.18 \pm 0.09$,	~ -1	−0.73
$100\mathcal{B}(\Xi_c^0 \to \Xi^-\pi^+)^e$	1.43 ± 0.32	2.21 ± 0.11	6.47
$100\mathcal{R}(\Xi_c^0 \to \Xi^- K^+)$	$2.75 \pm 0.51 \pm 0.25$	4.4	6.0
$100\mathcal{R}(\Xi_c^0 \to \Sigma^0 K_S^0)^f$	$3.8 \pm 0.6 \pm 0.4$	2.3 ± 1.8	< 0.4
$10\mathcal{R}(\Xi_c^0 \to \Sigma^+ K^-)^f$	$1.23 \pm 0.07 \pm 0.10$	2.7 ± 0.5	0.71
$100\mathcal{B}(\Xi_c^+ \to \Xi^0\pi^+)$	1.6 ± 0.8	0.38 ± 0.20	1.72
$\mathcal{R}(\Xi_c^+ \to \Xi^0\pi^+)$	1.1 ± 0.6	0.17 ± 0.09	0.27

PRD **101** 014011 (2020); PRD **97** 074028 (2018)

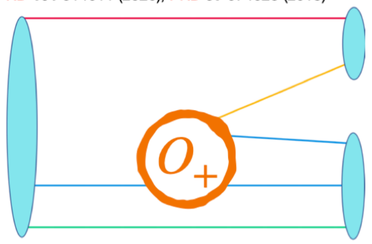

$= 0$

$O_+ = \frac{1}{2} \sum_{q,q'=d,s} V_{uq} V_{cq'}^* \left((\bar{u}q)(\bar{q}'c) + (\bar{q}'q)(\bar{u}c)\right)$

Körner-Pati-Woo theorem

	$\mathcal{B}(\Lambda_c^+ \to \Sigma^0 K^+)$	$\mathcal{B}(\Lambda_c^+ \to \Sigma^+ K_S^0)$
QCD corrections [2]	2(8)	2(4)
MIT bag model [3]	7.2 ± 1.8	7.2 ± 1.8
Diagrammatic analysis [4]	5.5 ± 1.6	9.6 ± 2.4
$SU(3)_F$ flavor symmetry [5]	5.4 ± 0.7	5.4 ± 0.7
IRA method [6]	5.0 ± 0.6	1.0 ± 0.4
PDG 2020 [28]	5.2 ± 0.8	/

[2]Phys. Rev. D **106**, 052003 (2022).
[3]Phys. Rev. Lett. **128**, 142001 (2022).
[4]Phys. Rev. D **100**, 072004 (2019).
[5]arXiv:2208.08695 [hep-ex].
[6]Phys. Rev. Lett. **122**, 082001 (2019).
[f]Phys. Rev. D **105**, L011102 (2022).

$\mathcal{R}(X) := \frac{\mathcal{B}(X)}{\mathcal{B}(\Xi_c^0 \to \Xi^-\pi^+)}$

Input:
$10^4\mathcal{B}(\Lambda_c^+ \to \Sigma^0 K^+) = 5.2 \pm 0.8$
$100\mathcal{B}(\Xi_c^0 \to \Xi^-\pi^+) = 1.80 \pm 0.52$

$\frac{\mathcal{B}(\Lambda_c^+ \to \Sigma^0 K^+)}{\mathcal{B}(\Lambda_c^+ \to \Sigma^+ K_S^0)} \sim 1$ comfirms Körner-Pati-Woo theorem

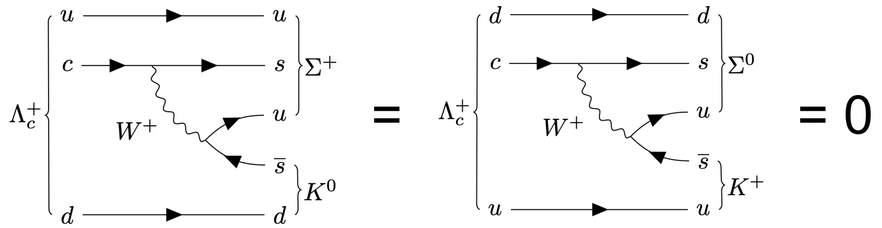

$= 0$

Our measurement helped theorists to find out numerical error in their calculations

JHEP ***09*** *(2022) 087*

There was a numerical error in 15th line of table 1. for the decay channel $\Lambda_c^+ \to \Sigma^+ K_S^0/K_L^0$ due to misuse of a normalization factor $1/2\sqrt{3}$ for the amplitude instead of the correct one $1/\sqrt{2}$, and obtained a branching ratio of $(0.0103 \pm 0.0042) \times 10^{-2}$. We have now corrected this mistake and the result in table 1 should be changed to

channel	SU(3) amplitude	branching ratio(10^{-2})	α
$\Lambda_c^+ \to \Sigma^+ K_S^0/K_L^0$	$\sin\theta\,(-b_6 + b_{15} + d_6 - d_{15})$	0.062 ± 0.025	-0.13 ± 0.98

Table 1. SU(3) amplitudes and predicted branching fractions (the third column) and polarization parameters (the fourth column) of anti-triplet charmed baryons decays into an octet baryon and an octet meson.

All other the conclusions presented in the paper remain unchanged. The new result is in agreement with BESIII recent data [1].

Impact on theoretical calculation

Hyperparameters

- Four particle attention block and two class attention block.
- Particle feature embedding: 3 MLP (64, 256, 64) encoding
- Interaction pairwise feature embedding: 4 layers pointwise 1D convolution (32, 64, 32, 8) encoding
- Dropout rate = 0.05 to prevent overtraining
- Lookahead optimizer, cross entropy, k=6, alpha=0.5
- Radam, beta1=0.95, beta2=0.99, epsilon=10^{-5}
- Total number of hyperparameters: 380 thousand
- 100 epoches, batch size 512
- Initial learning rate 0.001, keep constant in the first 70% epoches; in the last 30% epoches, learning rate decays exponentially to 1% of the initial learning rate
- **Model ensemble**: train for more than one time, randomize the initial values of hyperparameters(network initialization, batch processing order, dropout layer, …) to make model more robust and generalized.

Tracking calibration — Silicon-TPC seed matching

- ➔ In sPHENIX tracking reconstruction, silicon seed and TPC seed are reconstructed separately
  - ❖ Silicon seed: good vertex resolution, timing information
  - ❖ TPC seed: good momentum resolution, no timing information
- ➔ Silicon seed and TPC seed are matched geometrically
- ➔ Improve Silicon-TPC seed matching module
  - ❖ Match seeds in eta/phi/x/y firstly
  - ❖ Match seeds in z with/without crossing correction
  - ❖ Store matched/unmatched seeds into separate containers
- ➔ Tuning matching window w.r.t. Q/pT

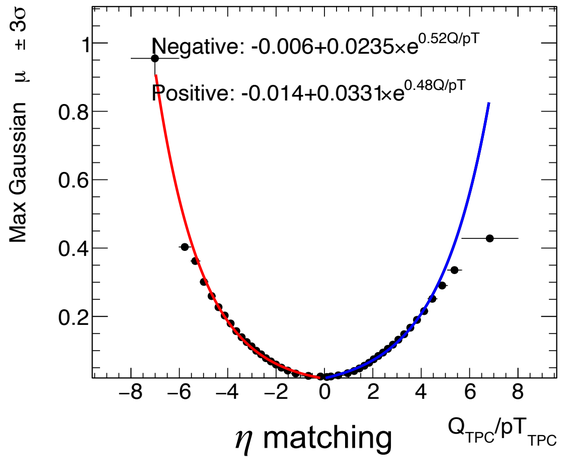

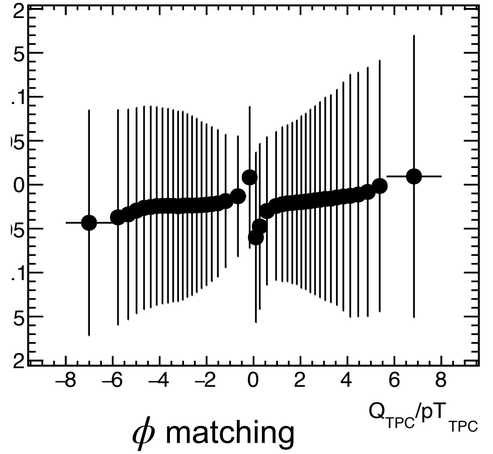

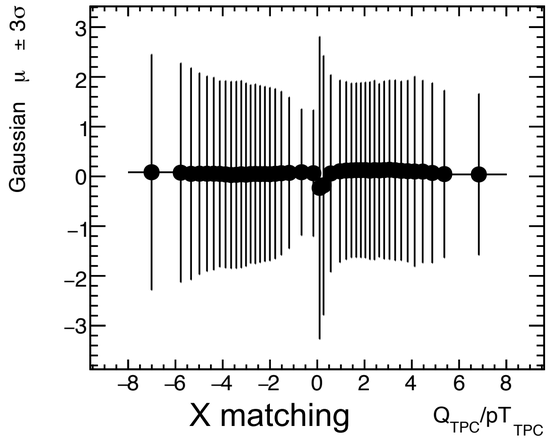

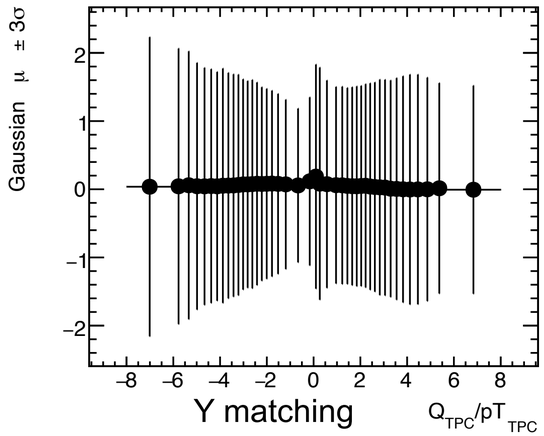

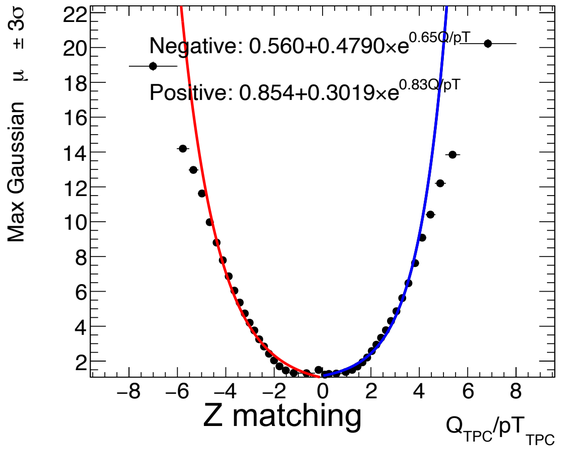

Λ_c^+ SL

The BFs for $\Lambda_c^+ \to \Lambda^* e^+ \nu_e$ predicted by different theoretical models, in units of 10^{-4}.

Λ^* state	CQM [8]	NRQM [9]	LFQM [10]	LQCD [11]
$\Lambda(1520)$	10.00	5.94	––	5.12 ± 0.82
$\Lambda(1600)$	4.00	1.26	(0.7 ± 0.2)	––
$\Lambda(1890)$	––	3.16×10^{-2}	––	––
$\Lambda(1820)$	––	1.32×10^{-2}	––	––

AI/ML Experience and Future Applications

➔ Current experience

- ❖ DNN/Transformer-based event selection in BESIII
- ❖ Low-level detector information as particle features
- ❖ Control-channel validation and domain-shift studies
- ❖ Model uncertainty evaluation

➔ Future directions in sPHENIX

- ❖ ML-assisted heavy-flavor signal extraction
- ❖ Detector QA and anomaly detection
- ❖ Simulation acceleration and generative models
- ❖ Cross-experiment foundation models for HEP/NP